

MANA Progress Report

Research Digest 2010



World Premier International (WPI) Research Center
International Center for
Materials Nanoarchitectonics (MANA)



National Institute for Materials Science (NIMS)

Preface

Masakazu Aono
MANA Director-General
NIMS



More than three years have passed since our International Center for Materials Nanoarchitectonics (MANA) was launched in the National Institute for Materials Science (NIMS) in October 2007 as one of six research centers approved/supported by the World Premier International Research Initiative (WPI Program) of the Ministry of Education, Culture, Science and Technology (MEXT). The aim of MANA is to carry out world topnotch research for the creation of novel materials necessary for the development of innovative technologies that are inevitable for the realization of the sustainable society in the 21st century.

Thankfully, in the year 2010 so many outcomes of MANA have materialized; several scientists young and senior won prestigious awards and a number of research outcomes were published in high impact journals. Consequently, MANA activities and research achievements have been highlighted in many TV programs and news, and appeared in a number of articles in newspapers and magazines.

This booklet, which is the part “Research Digest 2010” of the MANA Progress Report, summarizes the research activities of *MANA Principal Investigators*, *MANA Independent Scientists* and *ICYS-MANA Researchers* in the calendar year 2010. A *MANA Principal Investigator* is a world-top class scientist, who takes the main role to achieve the *MANA* research targets and serves as a mentor for younger scientists. A *MANA Independent Scientist* is a younger researcher at NIMS, who works full-time for MANA and can perform his own research independently. *ICYS-MANA Researcher* is a position for postdoctoral fellows selected from all over the world by open recruitment. *ICYS-MANA Researchers* perform their own research independently by receiving advice from *MANA Principal Investigators* and other mentors. Other information on *MANA* research achievements (e.g., the lists of publications and patents) is given in the part “Facts and Achievements 2010” of the *MANA Progress Report*.

Lastly, on behalf of MANA, I would like to ask you for your continued understanding and support to MANA.

MANA Research Digest 2010

MANA Principal Investigators (28)

Nano-Materials Field

Takayoshi SASAKI (Field Coordinator)	6
Inorganic Nanosheets	
Katsuhiko ARIGA	7
Supramolecular Materials	
Yoshio BANDO (MANA Chief Operating Officer)	8
Inorganic Nanostructured Materials	
Dmitri GOLBERG	9
Nanotube Properties	
Kazuhiro HONO	10
Nanostructured Metallic Materials	
Kenji KITAMURA	11
Photo-Ferroelectric Materials	
Naoki OHASHI	12
Optoelectronic Materials	
Yoshio SAKKA	13
Structure Controlled Ceramics	
Zhong Lin WANG (Satellite)	14
Nanogenerators for Self-Powering Nanosystem	

Nano-System Field

Masakazu AONO (MANA Director-General, Field Coordinator)	15
Nano-System Architectonics	
Daisuke FUJITA	16
Extreme-Field Nanofunctionality	
James K. GIMZEWSKI (Satellite)	17
MANA Brain: Atomic Neural Networks	
Tsuyoshi HASEGAWA	18
Atomic Electronics for Future Computing	
Xiao HU	19
Nano Superconductivity and Terahertz Emission	
Christian JOACHIM (Satellite)	20
Surface Atomic Scale Logic Gate	
Kazuo KADOWAKI (Satellite)	21
Superconducting Quantum Nanoarchitectonics	

Tomonobu NAKAYAMA	22
Integration of Nano Functionality for Novel Nanosystems	
Hideaki TAKAYANAGI (Satellite)	23
Mesoscopic Superconductivity and Quantum Information Physics	
Kazuhito TSUKAGOSHI	24
Solution-Processable Organic Single Crystals with Bandlike Transport in Field-Effect Transistors	
Mark WELLAND (Satellite)	25
Bio-Inspired Materials for Sustainable Energy	

Nano-Green Field

Kohei UOSAKI (Field Coordinator)	26
Construction of Interphases with Atomic/Molecular Order for Efficient Conversion of Energy/Materials	
Liyuan HAN	27
Dye Sensitized Solar Cells	
Kazunori TAKADA	28
Solid State Batteries	
Enrico TRAVERSA	29
Nanostructured Materials for Solid Oxide Fuel Cells and Sustainable Development	
Omar YAGHI	30
Reticular Materials	
Jinhua YE	31
Nanoarchitectonics of Hybrid Artificial Photosynthetic System	

Nano-Bio Field

Takao AOYAGI (Field Coordinator)	32
Smart Nano-Biomaterials	
Yukio NAGASAKI (Satellite)	33
PEGylated Polymer Micelle-Based Nitric Oxide (NO) Photodonor with NO-Mediated Antitumor Activity	

MANA Independent Scientists (14)

Ryuichi ARAFUNE	34
Laser-Based Inelastic Photoemission Spectroscopy	
Alexei A. BELIK	35
Search for New Ferroelectric, Magnetic and Multiferroic Materials using High-Pressure Technique	
Naoki FUKATA	36
Next-Generation Semiconductor Nanomaterials and Nanodevices	
Masayoshi HIGUCHI	37
Fluorescent Metallo-Supramolecular Polymers	
Satoshi MORIYAMA	38
Graphene-Based Quantum-Dot Devices	
Tadaaki NAGAO	39
Controlling the Electromagnetic Waves on the Nano-Scale and Atomic-Scale	
Jun NAKANISHI	40
Development of Photoresponsive Biointerfaces	
Yoshitaka TATEYAMA	41
Computational Physical Chemistry	
Shunsuke TSUDA	42
Photoluminescence and Raman Study on Boron Doped Diamond	
Lionel VAYSSIERES	43
Aqueous Design, Electronic Structure and Size Dependence Effect of Metal Oxide Quantum-Confined Structures	
Ajayan VINU	44
Gold Nanoparticles in Nanoporous CN for Catalysis	
Katsunori WAKABAYASHI	45
Theory Design and Physical Properties Forecast of Nano-Carbon Systems	
Yusuke YAMAUCHI	46
Rational Design of Mesoporous Metals	
Chiaki YOSHIKAWA	47
Precise Structural Control of Polymer Materials toward Novel Biomaterials	

ICYS-MANA Researchers (15)

Xiaosheng FANG	48
Enhanced Photocurrent and Stability from Microscale ZnS Nanobelts-based Ultraviolet (UV)-Light Sensors	
Ujjal K. GAUTAM	49
Natural Selection of Unipolarity in Zinc Oxide Nanorod Assemblies and Collective Luminescence	
Fatin HAJJAJ	50
Magnetic-Field-Guided Self Assembly	
Ryoma HAYAKAWA	51
Single-Electron Tunneling through Molecular Quantum Dots in a Metal-Insulator-Semiconductor Structure	
Masataka IMURA	52
Development of Diamond Field Effect Transistors by AlN/Diamond Heterostructure	
Tatsuo SHIBATA	53
Orientation Controlled Film Growth by Nanosheet Seed Layer Method	
Lok Kumar SHRESTHA	54
Synthesis and Characterization of C ₆₀ Microcrystal at Liquid-Liquid Interface: Effects of Mixing Solvents	
Pavuluri SRINIVASU	55
Fabrication of Novel Nanostructured Bioceramics	
Yoshihiro TSUJIMOTO	56
High-Pressure Synthesis of New Layered Cobalt Oxyfluoride	
Hisanori UEKI	57
Bottom-Up Synthetic Strategy to Highly Organized Multi-Functional System	
Jung-Sub WI	58
Direct Fabrication of Raman-Active Nanoparticles by Top-Down Physical Routes	
Jesse WILLIAMS	59
Photovoltaic CIGS Thin-Films from Nanoparticle Powders using Aerosol Deposition	
Genki YOSHIKAWA	60
Nanomechanical Membrane-Type Surface Stress Sensor (MSS): Opening a New Era of Sensors	
Tianyou ZHAI	61
One-Dimensional Inorganic Nanostructures for High-Performance Photodetectors	
Yuanjian ZHANG	62
Nano-Carbon Materials for Green Energy	

Inorganic Nanosheets

MANA Principal Investigator

(Field Coordinator)

MANA Scientist

MANA Research Associate

Graduate Student

Takayoshi SASAKI

Minoru Osada, Yasuo Ebina, Tadashi Ozawa, Renzhi Ma

Jianbo Liang, Jia Baoping, Shibata Tatsuo,

Xiaohe Liu, Fengxia Geng

Baowen Li, Linfeng Hu



1. Outline of Research

We aim at developing a new nanofabrication process involving organization of inorganic nanosheets through wet-processes, which allows architectural design of materials from a nanoscale level. New innovative materials will be created by utilizing advantages of the wet-process nanofabrication approach (soft-chemical materials nanoarchitecture).

We will develop wet-process techniques for organizing the functional nanosheets into multilayer or superlattice assemblies with a finely controlled nanostructure. Based on the exotic approach with nanosheets, we will establish the tailoring ability and controllability over nanostructures with a precision down to 1 nm, which is comparable to that of modern vapor-phase deposition techniques.

In the second stage, we will take challenges to develop exotic nanostructured materials comparable to artificial lattice systems through nanoscale assembly of nanosheets and a range of foreign species, based on the new nanofabrication processes. We plan to create novel nanostructured materials or nanodevices with a sophisticated function. Followings are some of selected targets.

- (1) High- k nanofilms, which work at a thickness down to several nanometers.
- (2) Transparent magnetic films, which act in response to UV or short-wavelength visible light.
- (3) A new technique, which promotes the growth of high-quality films of functional crystals.

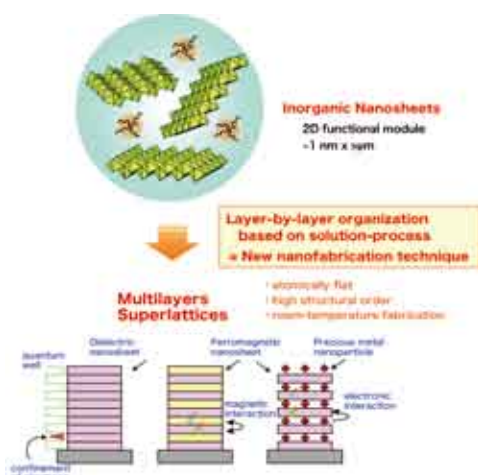


Fig. 1. Conceptual explanation of the research plan.

2. Research Activities

(1) Construction of Multilayer Films of Perovskite-type Oxide Nanosheets and Their Dielectric Properties.¹⁾

We have applied Langmuir-Blodgett method for layer-by-layer assembly of perovskite-type nanosheets, $A_2M_3O_{10}$

($A=Ca, Sr; M=Nb, Ta$). Optimizing deposition parameters led to well-organized multilayer nanostructures, which are clearly confirmed by various characterizations including TEM observation (Fig. 2). The films showed superior dielectric properties. A specific dielectric constant of 210 to 230 for $Ca_2Nb_3O_{10}$ and $Sr_2Nb_3O_{10}$, respectively, is the top performance for ultrathin films of various materials. Furthermore, the films were found to be highly insulating, giving a leakage current density of $<10^{-7} A cm^{-2}$. These characteristics suggest promising potential of these nanosheets as next generation high- k materials workable at a nanoscale thickness.

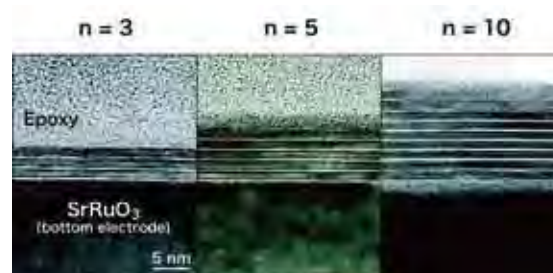


Fig. 2. Cross-sectional TEM images for multilayer films of $Ca_2Nb_3O_{10}$ nanosheets with the repeating deposition number of $n = 3, 5, 10$.

(2) Delamination of Layered Rare-Earth Hydroxides.²⁾

Layered rare-earth hydroxides, which we discovered in 2008, were successfully delaminated by applying a soft-chemical process involving intercalation of dodecylsulfate ions and subsequent treatment with formamide. The obtained nanosheet, $Eu(OH)_{2.5}xH_2O$, had a thickness of ~ 1.6 nm versus a lateral size of submicrometers (Fig. 3). The nanosheet suspension showed photoluminescence upon exposure to UV light. The nanosheet can be taken as a new member of functional 2D nanomaterials.

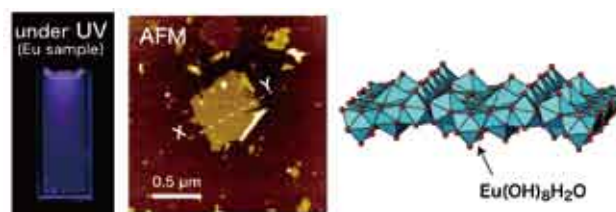


Fig. 3. A colloidal suspension of Eu-hydroxide nanosheet, its AFM image and structure.

References

- 1) M. Osada, K. Akatsuka, Y. Ebina, H. Funakubo, K. Ono, T. Sasaki, *ACS Nano* **4**, 5225 (2010).
- 2) L. Hu, R. Ma, T. C. Ozawa, and T. Sasaki, *Chem. Asian J.* **248** (2010).

Supramolecular Materials

MANA Principal Investigator

MANA Scientist
MANA Research Associate

Katsuhiko ARIGA

Jonathan P. Hill
Gary J. Richards, Venkata Krishnan, Jan Labuta
Dattatray Sadashiv Dhawale



1. Outline of Research

Functional materials have been wisely constructed via bottom-up approaches as seen in preparation of molecular and nano patterns, complexes, and nanomaterials¹⁻⁴⁾ organized nano- and microstructures,⁵⁻⁷⁾ and function materials.^{8,9)} In addition, novel concepts to bridge nano (molecular) structures and bulk systems now becomes crucial in order to control real nano and molecular functions from our visible worlds. We have proposed a novel methodology “hand-operating nanotechnology” where molecular orientation, organization and even functions in nanometer-scale can be operated by our bulk (hand) operation.^{10,11)} Selected examples of research results on supramolecular materials are shown below.

2. Research Activities

(1) Mechanical Molecular Recognition.¹²⁾

Construction of enzyme-like artificial cavities is a complex and challenging subject. Rather than synthesizing complicated host molecules, we have proposed mechanical adaptation of relatively simple hosts within dynamic media to determine the optimum conformation for molecular recognition. We synthesized the novel cholesterol-armed triazacyclononane as a host molecule, and subjected it to structural tuning by compression of its Langmuir monolayers in the absence and presence of Li⁺ cations in the sub-phase. Experimental results confirm that the monolayer of triazacyclononane host selectively recognizes uracil over adenine (ca. 7 times based on the binding constant) and thymine (ca. 64 times) under optimized conditions (Fig. 1).



Fig. 1. Mechanical molecular recognition at the air-water interface.

(2) Graphene Sensor.¹³⁾

Graphene-sheet/ionic-liquid (GS-IL) layered films been prepared by direct reduction of graphene oxide sheet in the presence of ionic liquids, followed by re-assembling through electrostatic layer-by-layer (LbL) adsorption on a quartz crystal microbalance. Layer spacings of graphene sheets are regularly expanded upon insertion of ionic liquid

molecules. Selective sensing of aromatic compounds using the GS-IL LbL films have been demonstrated (Fig. 2).

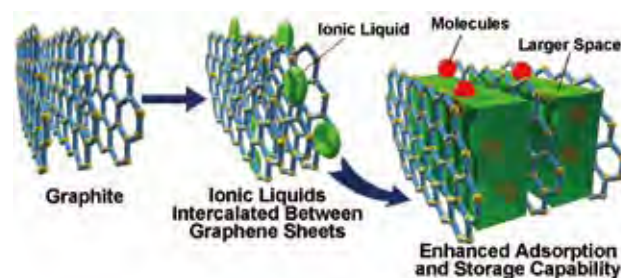


Fig. 2. Layer-by-layer film of graphene and ionic liquid.

(3) Open-Mouth Capsule.¹⁴⁾

We fabricated metallic (platinum) microcapsules with sufficient accessibility and electroactivity at both interior and exterior surfaces (open-mouthed platinum microcapsules). The open-mouthed platinum microcapsules exhibit a substantial increase of their electrode capability for methanol oxidation and catalytic activities for carbon monoxide (CO) oxidation (Fig. 3). Notably, activity-loss during CO oxidation due to undesirable particle agglomeration can be drastically suppressed using the open-mouthed microcapsules. This strategy is highly useful in reduced use of important resources such as rare-metals and rare earth materials.

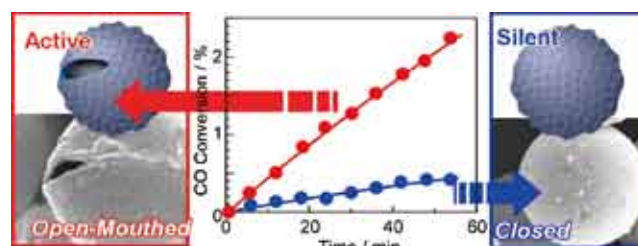


Fig. 3. Enhanced catalytic capability of open-mouthed capsule.

References

- 1) *J. Am. Chem. Soc.* **131**, 9494 (2009).
- 2) *J. Am. Chem. Soc.* **131**, 11282 (2009).
- 3) *J. Am. Chem. Soc.* **131**, 16138 (2009).
- 4) *J. Am. Chem. Soc.* **132**, 1212 (2010).
- 5) *J. Am. Chem. Soc.* **131**, 4220 (2009).
- 6) *J. Am. Chem. Soc.* **131**, 6372 (2009).
- 7) *J. Am. Chem. Soc.* **131**, 18030 (2009).
- 8) *Angew. Chem. Int. Ed.* **48**, 7358 (2009).
- 9) *Angew. Chem. Int. Ed.* **49**, 5961 (2010).
- 10) *Adv. Colloid Interface Sci.* **154**, 20 (2010).
- 11) *Chem. Sci.*, in press. DOI: 10.1039/c0sc00300j
- 12) *J. Am. Chem. Soc.* **132**, 12868 (2010).
- 13) *J. Am. Chem. Soc.* **132**, 14415 (2010).
- 14) *Angew. Chem. Int. Ed.*, in press. (DOI: 10.1002/anie.201004929).

Inorganic Nanostructured Materials

MANA Principal Investigator **Yoshio BANDO**

(MANA Chief Operating Officer)
MANA Scientist

MANA Research Associate
Graduate Student (Waseda Univ.)

Ryutaro Souda, Takao Mori, Chengchun Tang,
Chunyi Zhi
Lang Li, Jing Lin, Chun Li, Haibo Zeng
Xuebin Wang



1. Outline of Research

Our ultimate goal is to explore various applications of one-dimensional nanomaterials, including their optoelectronic applications, composites materials fabrication etc. At current stage, we are developing controllable methods for synthesis of nanomaterials, investigating their properties, developing novel nanofillers for polymeric composites, and fabricating photodetectors using semiconductor nanowires etc.

In order to accomplish this purpose, we set up a full set of instruments for synthesis and characterization of nanomaterials, including induction furnace, transmission electron microscope etc, which enable us to effectively control synthesis of various nanotubes and nanowires. Various semiconductor nanowires /nanotubes with good quality can be fabricated in our group, and we have started their property and device studies. In addition, We had years' research experience on boron nitride nanotubes (BNNTs). Now we can synthesize large quantities of highly pure BNNTs. Very recently, we are successful to fabricate new 2D BN nanocrystals. Based on the ultimate goal and our current researches, we set up following three sub-themes (Fig.1).

- (i) Developing highly effective synthesis method for various semiconductor nanomaterials;
- (ii) Systematic property investigation to fabricated nanomaterials;
- (iii) Application studies, including device fabrication, performance test and composite materials studies etc.

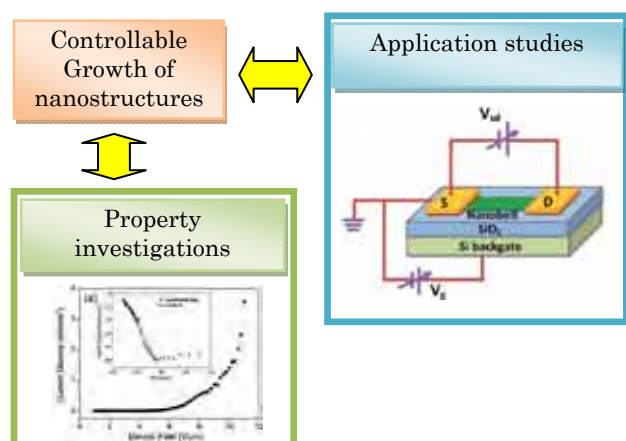


Fig. 1. Three sub-themes and their organic coordination.

2. Research Activity

(1) White Graphene – 2D boron nitride nanocrystal.¹⁾

Two-dimensional Boron Nitride (BN) graphene analogues, i.e. few- and single-layer nanoribbons and nanosheets, so called “white graphenes”, were fabricated through

unwrapping multi-walled BN nanotubes under plasma etching (Fig. 2). The plane structures become conducting in a sharp contrast with electrically insulating nature of the starting tubes.

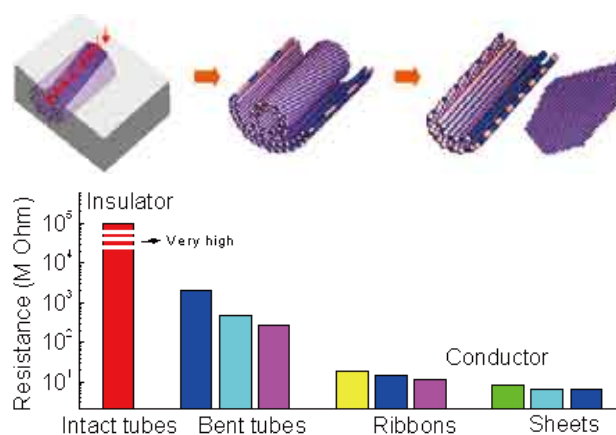


Fig. 2. Schematic of fabrication BN nanoribbon and electrical conductivity variation induced by morphology.

(2) Photodetectors by semiconductor nanostructures.^{2,3)}

Methods were developed to synthesize CdS nanobelts and ZrS₂ nanobelts, followed by property investigation and photodetector fabrication. Excellent performance was revealed. For example, nanoscale visible light photodetectors by CdS nanobelts showed good sensitivity and wavelength selectivity (Fig. 3). Ultrafast response time (20 μ s) and ultrahigh quantum efficiency (1.9×10^7 %). The performance rivals that of detectors made of other 1D semiconductors.

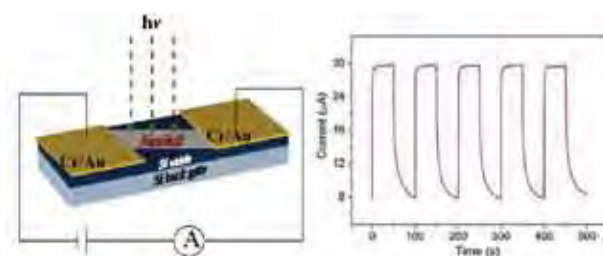


Fig. 3. A photodetector device by CdS nanobelt and reproducible on/off switching upon 490-nm light illumination.

References

- 1) H.B. Zheng, C. Zhi, Z. Zhang, X. Wei, X. Wang, W. Guo, Y. Bando, D. Golberg, *Nano Lett.* **10**, 5049 (2010).
- 2) L. Li, P. Wu, X. Fang, T. Zhai, L. Dai, M. Liao, Y. Koida, H. Wang, Y. Bando, D. Golberg, *Adv. Mater.* **22**, 3161 (2010).
- 3) L. Li, X. Fang, T. Zhai, M. Liao, U. Gautam, X. Wu, Y. Koida, Y. Bando, D. Golberg, *Adv. Mater.* **22**, 4151 (2010).

Nanotube Properties

MANA Principal Investigator
MANA Research Associate

Dmitri GOLBERG
Mingsheng Wang, Xianlong Wei, Daiming Tang



1. Outline of Research

Nowadays major synthetic routes and atomic structures of nanotubes, one of the most prospective materials of the 21st century, have well been established. By contrast, their physical properties, in particular, the mechanical response to an external tensile load (especially at the individual structure level) have remained questionable. The advanced technique utilized by the Nanotubes Group, *i.e.* atomic force microscope (AFM) setup integrated into a high-resolution transmission electron microscope (HRTEM), allow us to accurately *in situ* measure tensile properties of the two most promising nanotube types, namely, C nanotubes (CNTs) and BN nanotubes (BNNTs), while paying a special attention to peculiar deformation kinetics under various experimental conditions, and the effects of intrinsic tube defects on resultant mechanics.

2. Research Activities

(1) Ultimate tensile strength of single-walled carbon nanotubes.

CNTs have theoretically been predicted to be the toughest materials on Earth. However, so far, clear experimental verifications of such claims have been lacking. Our pioneering experiments in regard of true yield strength measurements of single-walled carbon nanotubes (SWNTs)¹ are shown in Fig. 1. The SWNTs were prepared *in situ* through gradual peeling of multi-walled C nanotubes (MWNTs) under a moderate current flow ($\sim 2 \mu\text{A}$) through them. Before testing, reliable clamping of a nanotube to the metal leads was achieved by in-tandem electron beam irradiation and minor Joule-induced tube heating. Defect-free single-layered C nanotubes revealed the yield strength of $\sim 100 \text{ GPa}$, thus being more than 100 times stronger than a standard steel, just in accord with the bright theoretical estimates. Direct observations of the tube defect structures (before testing) under high spatial resolution of 1.7 \AA allowed us to link the measured strengths with CNT defects. We found that if the pentagon-heptagon pair defects pre-existed within a single-shell honeycomb lattice they served



Fig. 1. (left) Experimental setup inside a high-resolution transmission electron microscope designed for Joule-heating-induced step-wise peeling of a multi-walled C nanotube (MWNT) down to the single-layer-thick structure of only $\sim 2 \text{ nm}$ in diameter, its direct tensile testing, and recording a breaking force (right) by a MEMS sensor of the AFM cantilever.

as stress concentrators which dramatically reduced the tensile strength (nearly twice).

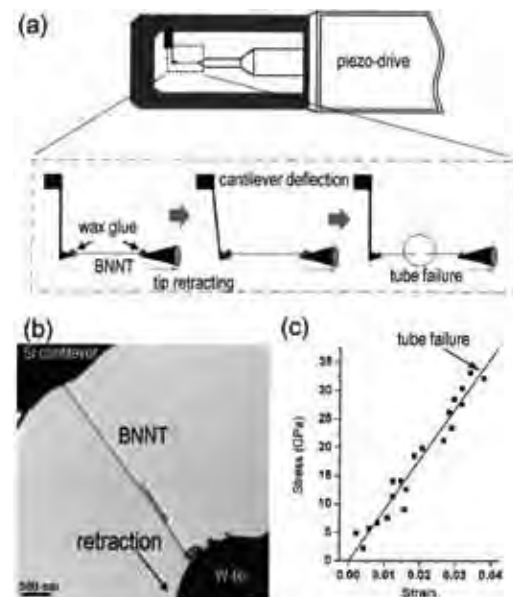


Fig. 2. (top) Experimental setup inside a high-resolution transmission electron microscope developed for tensile testing of individual multi-walled BN nanotubes; (low-left) TEM view of a BNNT stretched between a silicon cantilever and a movable tungsten tip; (low-right) A true stress-strain curve obtained under BNNT tension until it breaks.

(2) Tensile properties of multi-walled boron nitride nanotubes.

BNNTs are structural analogs of CNTs, but they possess much higher chemical, thermal and oxidation stabilities.²⁾ Thus BNNT utilization in structural components working at elevated temperatures and/or hazardous environments may be envisioned. However, to date, their strength data, even at room temperature, has never been acquired. Herein, we performed first tensile tests on multi-walled BNNTs inside TEM (Fig. 2).³⁾ The nanotubes displayed exceptionally high Young modulus, up to $\sim 1.3 \text{ TPa}$, a value that rivals diamond. The tensile strength of multi-layered BN structures reached $\sim 30 \text{ GPa}$, thus being lower than that of CNTs. However, the specific feature of a partially ionic layered BN system to exhibit strong intra-layer coupling, and thus common breakage in multi-shelled packages, allows BN nanotubes to withstand a tensile force that $\sim 4\text{-}5$ times exceeds that of their C counterparts.

References

- 1) M.S. Wang, D. Golberg, Y. Bando, *Adv. Mater.* **22**, 4071 (2010).
- 2) D. Golberg, Y. Bando, Y. Huang, T. Terao, M. Mitome, C.C. Tang, C.Y. Zhi, *ACS Nano* **4**, 2979 (2010).
- 3) X.L. Wei, M.S. Wang, Y. Bando, D. Golberg, *Adv. Mater.* **22**, 4895 (2010).

Nanostructured Metallic Materials

MANA Principal Investigator

Magnetic Materials Center
MANA Research Associate
Graduate Student (Univ. Tsukuba)

Kazuhiro HONO

T. Furubayashi, Y. K. Takahashi, T. Ohkubo
L. Zhang, C. L. Mendis
B. Varaprasad, T. M. Nakatani, N. Hase



1. Outline of Research

We are developing critical materials for ultrahigh density magnetic recording exceeding the areal density of 2 Tbit/in². The current perpendicular magnetic recording system for hard disk drives (HDD) is expected to reach a limit in a recording density of less than 1 Tbit/in², and the thermally assisted magnetic recording (TAR) system is considered to be most promising for the next generation system. Here we report our effort on the development of L1₀-FePt nanogranular perpendicular films for thermally assisted magnetic recording media and current-perpendicular-to plane giant magnetoresistive (CPP-GMR) devices for potential read head applications.

2. Research Activities

(1) FePt recording media.

FePt granular thin films are considered to be one of the most promising candidates for ultrahigh density magnetic recording media beyond 1 Tbits/in² because of the high magnetocrystalline anisotropy of the L1₀-FePt (~7×10⁷ erg/cc). In order to apply this material to TAR, it is required to control grain size to 4-5 nm with narrow size distribution, aligning the c-axis perpendicular to the film plane. We recently succeeded in fabricating a (FePt)_{0.9}Ag_{0.1}-50vol.%C (t=6.4nm) film on a thermally oxidized silicon substrate with a 10 nm thick MgO interlayer using an ultrahigh vacuum cosputtering machine (Fig. 1). The M-H loops show that this film has a perpendicular coercivity of 35 kOe. It indicates that the c-axis of this film is predominantly normal to the film plane. By fitting time dependent coercivity by Sharrock equation, we obtained $E_b \sim 200k_B T$. The recording pattern tracks written at varying bit lengths from 15 to 50 nm at a fixed track width of 92 nm tested at HGST using a TAR static tester. Taking the narrow-band amplitude full width half maximum (FWHM) of the tracks as an estimation of the achievable track pitch and 15 nm as

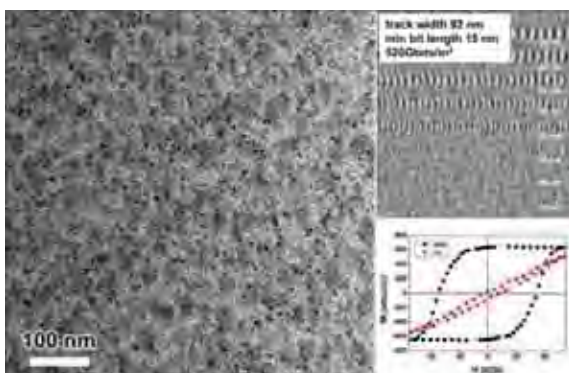


Fig. 1. FePtAg-C nanogranular thin film with perpendicular anisotropy. Static test results demonstrate 520 Gbit/in² recording density using thermally assisted recording head.

the smallest achievable bit length, we calculate the achievable maximum areal density as 520 Gbits/in². Through the above investigation, we demonstrate that the (FePt)Ag-C granular thin film is a promising candidate for high-density TAR media.

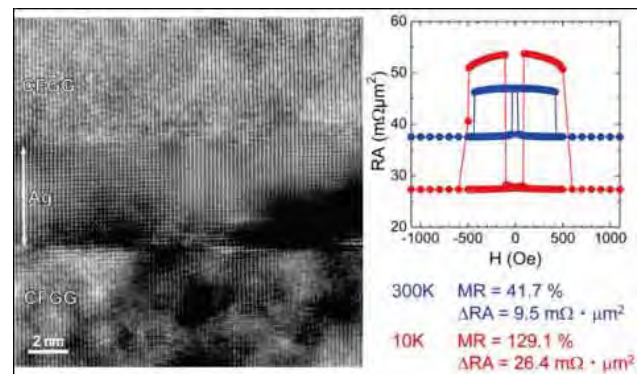


Fig. 2. Cross sectional HREM image of the CFGG/Ag/CFGG pseudo spin valve and its magnetoresistive curve.

(2) Heusler alloy CPP-GMR.

Using Andreev reflection measurements, we have been searching for a new Co-based Heusler alloys with high spin polarization and high Curie temperature. We found the Co₂Fe(Ga_{0.5}Ge_{0.5}) (CFGG) alloy exhibits relatively high spin polarization with the L2₁ ordered structure. Using the newly developed Heusler alloy as ferromagnetic layers, we have fabricated a current-perpendicular-to-plane (CPP) pseudo spin valve (PSV). High resolution TEM observation of the optimally annealed pseudo spin valve (Fig. 2) showed that all the layers were epitaxially grown on the MgO substrate and the interfaces between the CFGG layers and the Ag layers were atomically flat. Nano-beam electron diffraction pattern showed that both of the CFGG layers had the B2 ordered structure, not the L2₁ structure. The resistance change of the CPP-GMR device as a function of magnetic field. Blue and red lines represent the MR curves at 300 K and 10 K, respectively. ΔRA and MR ratio were 9.5 m $\Omega \cdot \mu\text{m}^2$ and 41.7 % at 300 K. This ΔRA value is more than 4 times larger than that reported for CoFe/Cu/CoFe CPP-GMR. At 10 K, the values were enhanced to 26.4 m $\Omega \cdot \mu\text{m}^2$ and 129.1%. Such large temperature dependence of ΔRA considered to be due to the temperature dependence of P of the CFGG alloy. Note that the chemical composition of the Heusler layers deviated from the stoichiometric value and its structure was B2. If the composition of the film is tuned to the stoichiometric value and the L2₁ ordering is improved, higher MR values can be expected. Thus, we conclude that the Co₂Fe(Ga_{0.5}Ge_{0.5}) alloy is promising candidate for a spin polarized current source.

Photo-Ferroelectric Materials

MANA Principal Investigator **Kenji KITAMURA**



1. Outline of Research

Lithium niobate (LiNbO₃) and tantalate (LiTaO₃) are typical ferroelectric materials possessing excellent piezoelectric, pyroelectric, opto-electric, photovoltaic and non-linear optical properties. There is no material except them which has been studied and applied in so wide fields. As a nature of ferroelectric material, such effects depend on the direction of spontaneous polarization. When anti-parallel domains are created in a single crystal by locally inverting polarization, the patterned domain structures enable various new applications to be developed.

2. Research Subjects and Activities

(1) Tunable IR-THz Wavelength Conversion Materials.

This project is to develop a new capability with potentially wide application of tunable THz wavelength conversion devices using a quasi-phase-matched optical parametric (QPM) generation. In this research, APRI (Korea), as a collaboration partner, plays a role in developing and testing proposed tunable THz wavelength conversion modules.

Femtosecond optical pulse was used to generate narrow-band terahertz pulses depending on a quasi-phase-matched condition in periodically poled lithium niobate (PPLN) and stoichiometric lithium tantalate (PPLT) crystals by difference frequency generation (Fig. 1). The origin of narrow-band THz generation proved that the two frequency components of the fs pulse contribute to the frequency mixing. By cryogenic cooling, the absorption of THz waves in the crystal was significantly reduced which resulted in efficient THz generation. Simultaneously generated forward and backward THz pulses were 1.38 and 0.65 THz with as narrow as the bandwidth of 32 GHz in the PPSLT sample. Temperature dependence of the generated THz waveforms had good agreement with the simulation result using one dimensional plane-wave propagation model.¹⁾

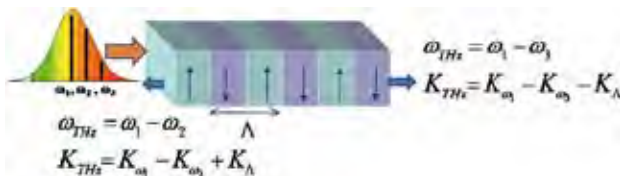


Fig. 1. Schematic diagram of forward and backward THz generation via different frequency components within the broad bandwidth of ultra-short laser pulses.

(2) Light induced pyroelectric effects for miniaturized X-ray generator.

As the pyroelectric effect relies on a change in temperature, simplified models suggest that the pyroelectric current depends on how quickly heating and cooling cycles are performed. The time scales for temperature change are typically much longer than for electronic interactions. Heat conduction through the crystal is the limiting step in the thermal exchange process, so in this study, we are focusing on the pyroelectric effect induced by the irradiation of a short pulse laser.

We demonstrated the pyroelectric effect induced by a short pulse laser with an intensity up to 6 MW/cm² which was used to heat the Fe-doped LiNbO₃ crystal. 0.2 °C temperature rise induced by a 10 ns green laser pulse caused a very large current peak up to 25 mA since the rate of temperature rise was extremely large comparing with that induced by using an ordinary heater. On the other hand, the pyroelectric current during the cooling is much smaller because of the slow cooling rate by thermal conduction (Fig. 2).²⁾

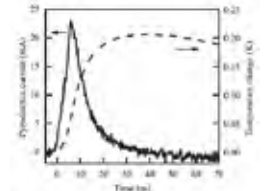


Fig. 2. Time dependence of pyroelectric current and calculated temperature change.

(3) Molecule Manipulation on Nano-Domain Patterned Ferroelectric Templates.

Surface polarization has a strong effect on reactivity on surfaces, combining domain patterning with domain-specific reaction have been made to fabricate metallic nanostructures and nanoparticles specifically on the patterned-polar surfaces.

We selected inorganic specific peptides using bio-combinatorial techniques, and functional nano-entities such as proteins, nano-particles as well as organic dyes, were immobilized onto metallic nanoparticle patterned LiNbO₃ surfaces using the peptides as linkers.³⁾ Once these peptides, which have conjugated with functional proteins and enzymes, anchored onto specific ferroelectric substrates that consequently developed platforms would provide ways for monitoring specific targets such as cell receptors or indicator biological molecules from medicine to environmental monitoring.



Fig. 3. Controlled binding of MBP-GFP-AgBP on LiNbO₃ surfaces.

Engineered peptides hybridized with functional synthetic molecules named MBP(Mentose Binding Peptide)-GFP(Green Fluorescent Peptide)-AgBP*(Ag Binding Peptide) was used for controlled binding on the LiNbO₃ substrate. After incubation for 2 hrs at RT, MBP-GFP-AgBP molecules were specifically bound onto Ag nanoparticles pattern on LiNbO₃ substrate as expected (Fig. 3), which can be visualized by a fluorescence image. The fluorescence contrast can be adjusted by the size and intensity of Ag nanoparticles. (under the collaboration with GEM-SEC/University of Washington).

References

- 1) N-E. Yu et al., *Optics Communications* **284**, 1395 (2011).
- 2) K. Kitamura et al., *Appl. Phys. Lett.* **97**, 082903 (2010).
- 3) M. Sarikaya et al., *Nature Materials* **2**, 577 (2003).

Optoelectronic Materials

MANA Principal Investigator
MANA Research Associate

Naoki OHASHI
Baoye Li, Yuhua Zhen, Jianyong Li



1. Outline of Research

Consumption of mine resources, particularly rare-metals, is one of critical issues on sustainable development of human life. For example, indium (In), one of the focused rare-metal elements, is quite useful element for semiconductor solar cells and display device. For solar cells, tin-doped indium oxide shows very high performance as transparent conducting oxide (TCO), and Cu(In,Ga)Se₂ (CIGS) and its related alloys are also useful as sunlight absorber for high efficiency solar-cell: In is main component of them. It is also said that the usage of light emitting diodes (LEDs) may reduce energy consumption for lighting in comparison to conventional lighting devices, production of (In,Ga)N based white light LEDs are also increasing. Thus, In is necessary for high efficiency of human life but its resource is quite limited.

At this situation, we have to develop materials and process to achieve high efficiency devices with less rare-metal consumption. In this context, we devote ourselves to find appropriate high performance materials with less rare-metal concentration to save natural resources for our future. In our project in MANA, we paid attention to Cu(In,Ga)Se₂ based sunlight absorber material for solar cell applications and (2) TCO used in solar cells, lighting devices and display panels.

2. Research Activities

(1) Sunlight absorbers.^{1,2)}

Our strategies for the reduction of In consumption in absorber materials in solar cells are (1) achieving high yield of Cu(In,Ga)Se₂ production and (2) utilizing sunlight absorbers not containing In.

Fig. 1 shows a conventional setup for thermal reflux synthesis of sunlight absorbers such as CIGS using organic solvent. In contrast to so-called solvothermal method, this thermal reflux method never require high pressure ambient

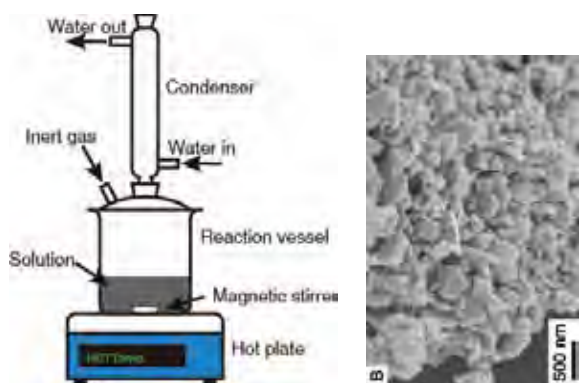


Fig. 1. Conventional setup for thermal reflux synthesis of CIGS and its related alloys and SEM image of the CIGS powder produced by the thermal reflux method.

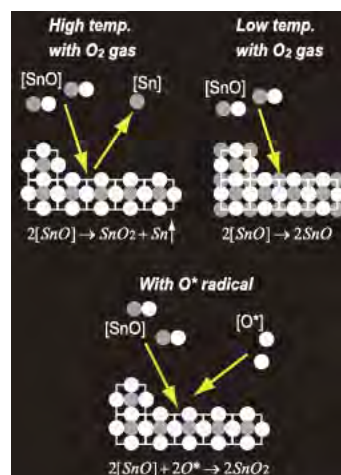


Fig. 2. Asymmetric *I-V* behavior observed at SIS structure interface composed of polar ZnO crystals as also shown.

and, actually, all process can be performed under ambient pressure and high yield ($\approx 100\%$) of CIGS can be achieved with this technique after optimization of the choice of precursors. We are currently developing CIGS film deposition using the obtained CIGS powders as precursors.

(2) Management of defects in oxide films.^{3,5)}

The most crucial issue in search for high performance TCO is management of defects, such as oxygen vacancy, because those defects cause lowering of conductivity as well as the lifetime of the devices. In order to optimize the film deposition process for TCO, we investigated kinetics in film deposition process for TCO.

In particular we focus on the effect of oxygen partial pressure in the deposition environment and we employed isotope tracer technique^{6,7)} for analyses of reaction kinetics in film deposition process. As a result, we found a tradeoff relationship between defect concentration and crystallinity of the films. For example for tin oxide film deposition by pulsed laser deposition, high crystallinity film could be obtained under conditions of significant tin evaporation but it simultaneously means that defects causing shallow donor states are stable under this condition (Fig. 2). We are still working to design appropriate film deposition process to achieve both low defect concentration and high film quality simultaneously.

References

- 1) J. Williams, Japanese patent applied.
- 2) J. Williams, N. Ohashi, in preparation.
- 3) Y. Zhen et al., *J. Appl. Phys.* **108**, 104901 (2010).
- 4) I. Sakaguchi et al., *J. Ceram. Soc. Jpn.* **118**, 362 (2010).
- 5) K. Matsumoto et al., *J. Euro. Ceram. Soc.* **30**, 423 (2010).
- 6) H. Haneda et al., *Appl. Surf. Sci.* **252**, 7265 (2006).
- 7) H. Ryoken et al., *J. Mater. Res.* **20**, 2866 (2005).

Structure Controlled Ceramics

MANA Principal Investigator
 MANA Research Associate
 Graduate Student

Yoshio SAKKA
 Chunfen Hu, Weihua Di, Mamiko Kawakita,
 Salvatore Grasso, Wang Lin



1. Outline of Research

We plan to fabricate highly structure controlled ceramics that show novel properties through the development of nanoparticle processing. Especially the broad objective of the research is to develop novel colloidal processing techniques for preparation of advanced ceramic materials. One is for deposition of 2-D and 3-D patterned/ ordered array of functional inorganic nanoparticles.

An important aspect of the study will consist of novel colloidal processing by external stimulation such as strong magnetic field, electric current, etc. to obtain textured/laminated ceramics to be able to tune and enhance the desired functional properties. Recently pulsed electrophoretic deposition (EPD) has been demonstrated to produce bubble-free deposits from aqueous suspension. Also the alignment of feeble magnetic ceramics by EPD in a strong magnetic field is developed at NIMS. Both techniques are expected to be a powerful method to produce highly structure controlled ceramics resulting in excellent functional ceramics.

Another important aspect will consist of novel sintering techniques such as milliwave sintering and spark plasma sintering (SPS). Both are relatively new materials processing technologies and extremely short heat processing time and are expected to be powerful methods for obtaining nanostructure materials. The temperature measurement of the sample during sintering is the most severe limiting factor. Computer modeling is generally considered an effective means to solve above problems provided that the models are designed to capture the essential multiphysics of actual SPS apparatus and are reliably tested against experiments. This self-consistent experimental/numerical methodology is expected to develop a novel sintering techniques.

We set following three sub-themes and are conducting the materials exploration research effectively (Fig. 1).

- (i) Tailor-made nanoparticle preparation,
- (ii) Fabrication and application of textured and laminate ceramics,
- (iii) Development of novel sintering technology.

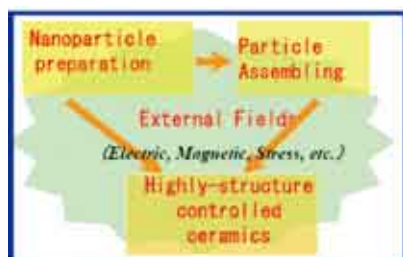


Fig. 1. Three sub-themes and their organic coordination for conducting effective materials exploration research.

2. Research Activities

(1) Textured nanolayered Nb₄AlC₃ ceramic.

Textured Nb₄AlC₃ ceramic was fabricated by slip cast-

ing in a strong magnetic field followed by spark plasma sintering.¹⁾ It possesses a shell-like microstructure configuration from the nanoscale to the milliscale. It has a high flexural strength to the c-axis direction and a high fracture toughness parallel to the c-axis direction. Also, this ceramic showed excellent machinability and could be easily machined by a high-speed steel cutter. The tailored Nb₄AlC₃ ceramic possesses the highest bending strength and fracture toughness (Fig. 2).

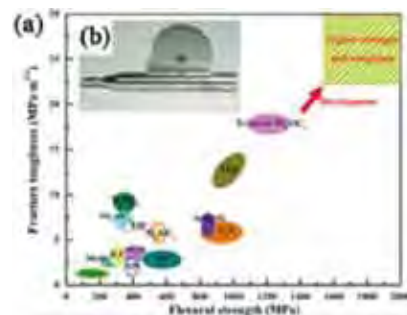


Fig. 2. Flexural strength and fracture toughness of textured Nb₄AlC₃ ceramic compared with those of other advanced ceramics (a), as well as its machinability (b).

(2) Development of Spark Plasma Sintering (SPS).

The developed SPS model used a moving-mesh technique to account for the electrothermal contact resistance change during both shrinkage and punch sliding follow-up (Fig. 3). The experimental and numerical results showed the effects of pressure on grain growth, residual porosity, and hardness observed along the sample radius. Upon increasing sintering pressure, complete densification was obtained by reducing the peak temperature measured at the die surface. The application of high pressure allowed to obtain highly transparent full dense alumina at low temperatures with no considerable grain growth.²⁾



Fig. 3. Scheme of the proposed methodology based on SPS current control mode (CCm) experiments and simulations.

References

- 1) C. Hu, Y. Sakka, et al., *Scripta Materialia*, (doi: 10.1016/j.scriptamat).
- 2) S. Grasso, B.N. Kim, C. Hu, G. Maizza, Y. Sakka, *J. Am. Ceram. Soc.* **93**, 2460 (2010).

Nanogenerators for Self-Powering Nanosystem

MANA Principal Investigator

(Satellite at Georgia Tech, USA)
 Research Scientist
 Graduate Student

Zhong Lin WANG

Youfan Hu
 Chen Xu, Guang Zhu, Sheng Xu



1. Outline of Research

Developing novel technologies for wireless nanodevices and nanosystems are of critical importance for sensing, medical science, defense technology and even personal electronics. It is highly desired for wireless devices and even required for nanodevices to be self-powered without using battery. It is essential to explore innovative nanotechnologies for converting mechanical energy, vibration energy, and hydraulic energy into electric energy, aiming at building self-powered nanosystems (Fig. 1). We have invented a nanogenerator for converting such random energy into electric energy using piezoelectric zinc oxide nanowire arrays. The mechanism of the nanogenerator relies on the piezoelectric potential created in the nanowires by an external strain: a dynamic straining of the nanowire results in a transient flow of the electrons in the external load because of the driving force of the piezopotential. The advantage of using nanowires is that they can be triggered by tiny physical motions and the excitation frequency can be one Hz to thousands of Hz, which is ideal for harvesting random energy in the environment.

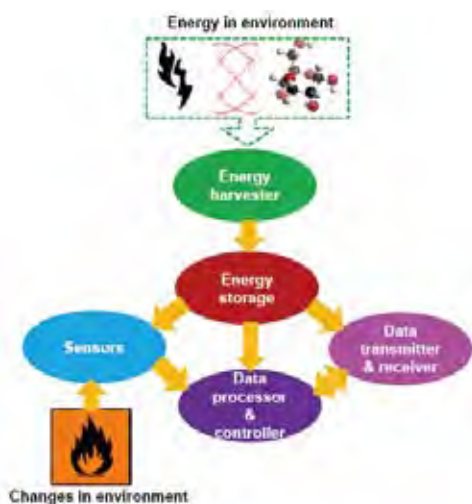


Fig. 1. Design of a self-powering nanosensor system for independent and sustainable operation.

2. Research Activities

We have developed a simple and effective approach, named scalable sweeping-printing-method, for fabricating flexible high-output nanogenerator (HONG) that can effectively harvesting mechanical energy for driving a small commercial electronic component (Fig. 2). The HONG consists of two main steps. In the first step, the vertically-aligned ZnO nanowires (NWs) are transferred to a receiving substrate to form horizontally-aligned arrays. Then, parallel stripe type of electrodes are deposited to connect



Fig. 2. SEM image of ZnO nanowire arrays bonded by Au electrodes. Inset: demonstration of an as-fabricated nanogenerator. The arrowhead indicates the effective working area of the nanogenerator.

all of the NWs together. Using a single layer of HONG structure, an open-circuit voltage of up to 2.03 V and a peak output power density of $\sim 11 \text{ mW/cm}^2$ have been achieved (Fig. 3). The generated electric energy was effectively stored by utilizing capacitors, and it was successfully used to light up a commercial light-emitting diode (LED), which is a landmark progress toward building self-powered devices by harvesting energy from the environment. Furthermore, by optimizing the density of the NWs on the substrate and with the use of multi-layer integration, a peak output power density of $\sim 0.44 \text{ mW/cm}^2$ and volume density of 1.1 W/cm^3 are predicted. This research opens up the path for practical applications of nanowire based piezoelectric nanogenerators for self-powered nanosystems.

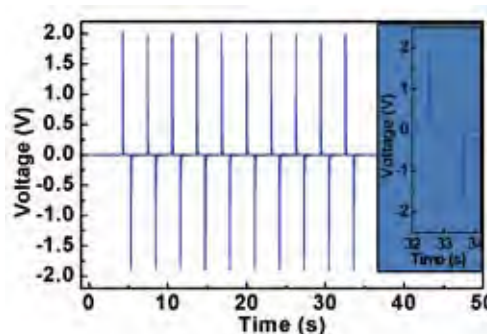


Fig. 3. Open circuit voltage measurement of the nanogenerator. The output charges have been stored by a capacitor, and later be used for driving a LED.

Nano-System Architectonics

MANA Principal Investigator Masakazu AONO

(MANA Director-General, Field Coordinator)

MANA Scientist
MANA Research Associate

Yuji Okawa, Makoto Sakurai, Hideo Arakawa
Hiromi Kuramochi, Hiroyuki Tomimoto, Liu Kewei,
Swapan K. Mandal, Keita Mitsui



1. Outline of Research

The goal of our Nano-System Construction Group is to create new nano-systems with novel functionality by the use of various key technologies for “materials nano-architectonics” and put the created nano-systems to practical use to contribute to our society in such forms as next-generation information processing and communication, environmental and energy sustainability, and regenerative medicine.

To achieve this interdisciplinary research, we make close collaboration with other groups in MANA as shown in Fig.1. We are also making collaboration with MANA’s satellite labs headed by Prof. Jim Gimzewski (UCLA, USA), Prof. Mark Welland (Univ. of Cambridge, UK), Prof. Christian Joachim (CNRS, France).

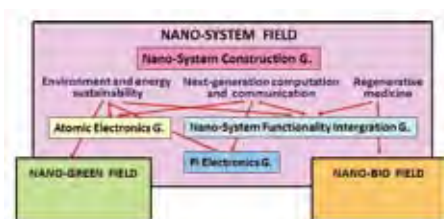


Fig. 1. Collaboration of the Nano-System Construction Group with other groups in MANA.

2. Research Activities

Our recent research activities are classified into the following five subjects:

- 1) Electrically wiring a single molecule by conductive polymer chains through chemical soldering.¹⁻⁵⁾
- 2) Development of a novel scanning-probe method for nanoscale magnetic imaging using a non-magnetic probe and its application to nanomagnetism studies.⁶⁻⁸⁾
- 3) Atomic switch: a) Practical application of the atomic switch to programmable ICs (in collaboration with NEC Corp.)⁹⁻¹¹⁾ and b) the utilization of the learning ability of the atomic switch to realize novel neuro-morphic computational circuits.¹²⁾
- 4) Development of multiprobe scanning-probe microscopes and their application to the measurement of nanoscale electrical conductivities and the analysis of signal transmission in neural networks.¹³⁾
- 5) Exploration of various functional nanostructures.¹⁴⁾

In what follows, only 1) and 2) will be discussed in more detail.

We have developed a method¹⁻³⁾ to create a single conductive linear polymer chain (polydiacetylene)⁴⁾ at designated positions by initiating chain polymerization of monomers (diacetylene) using a scanning tunneling microscope (STM) tip. By using this method, we have tried to make

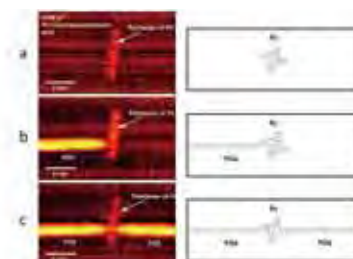


Fig. 2. Wiring a single molecule (phthalocyanine) by conductive molecular chains (polydiacetylene); STM images and schematic figures.

two-terminal nanowiring for a single phthalocyanine molecule and succeeded in making such nanowiring through chemical soldering (firm covalent bonding, see Fig.2).

We have developed a new scanning-probe method to measure nanomagnetism using no magnetip tip⁵⁾, which is based on the principle shown in Fig. 3. The method was successfully applied to measure the magnetic properties of nanometer-thick iron films on a GaAs substrate.

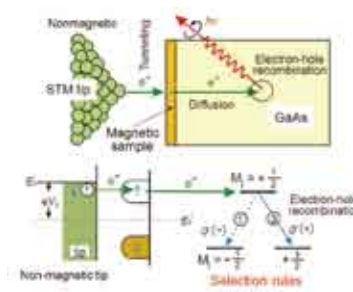


Fig. 3. Principle of a novel scanning-probe method for nanoscale magnetic imaging.

References

- 1) Y. Okawa, M. Aono, *Nature* **409**, 683 (2001).
- 2) Y. Okawa, M. Aono, *J. Chem. Phys.* **115**, 2317 (2001).
- 3) D. Takajo, Y. Okawa, T. Hasegawa, M. Aono, *Langmuir* **23**, 5247 (2007).
- 4) Y. Okawa, D. Takajo, S. Tsukamoto, T. Hasegawa, M. Aono, *Soft Matter* **4**, 1041 (2008).
- 5) Y. Okawa et al., to be published.
- 6) M. Sakurai, M. Aono, to be published (for reference, see Refs. 7-8).
- 7) M. Sakurai, C. Thirstrup, M. Aono, *Appl. Phys. A* **80**, 1153 (2005).
- 8) M. Sakurai, Y-G Wang, M. Aono, *Surf. Sci.* **602**, L45 (2008).
- 9) K. Terabe, T. Hasegawa, T. Nakayama, M. Aono, *Nature* **433**, 47 (2005).
- 10) T. Sakamoto, H. Sunamura, H. Kawaura, T. Hasegawa, M. Aono, *Appl. Phys. Lett.* **82**, 3032 (2003).
- 11) T. Tsuruoka, K. Terabe, T. Hasegawa, M. Aono, *Nanotechnology* **21**, 425205 (2010).
- 12) T. Hasegawa, T. Ohno, K. Terabe, T. Tsuruoka, T. Nakayama, J. K. Gimzewski, M. Aono, *Adv. Mater.* **22**, 1831 (2010).
- 13) See for example: S. Higuchi, H. Kuramochi, O. Laurent, T. Komatsubara, S. Machida, M. Aono, K. Obori, T. Nakayama, *Rev. Sci. Instrum.* **81**, 073706 (2010).
- 14) M. Nakaya, S. Tsukamoto, Y. Kuwahara, M. Aono, T. Nakayama, *Adv. Mater.* **22**, 1622 (2010).

Extreme-Field Nanofunctionality

MANA Principal Investigator
MANA Research Associate

Daisuke FUJITA
Jian-Hua Gao, Hongxuan Guo



1. Outline of Research

In the nanoscale world on surfaces, dimensionality is limited to two, one and zero, where low-dimensional functionality might manifest itself. The nanofunctionality may lead us to innovative nanoscale systems. Most nanofunctionality stems from quantum mechanical effects, whose appearance is expected in extreme fields such as low temperature, high magnetic field, and ultrahigh vacuum. Moreover, the combination of surfaces and extreme fields may cause low-dimensional phases through self organizations such as adsorption, segregation, reconstruction, precipitation and so on. Spontaneous phase transition is possible by giving a perturbation with nanoscale probes. Thus, the research composed of self organization, extreme fields and nano probes is our main theme. The purposes of our research are creation of low-dimensional nanoscale systems, and exploration of their novel functionality using advanced nanoprobe technology. In 2010, we have achieved various innovations in the fabrication and characterization of graphene layers.

2. Research Activities

(1) Production of Extended Single-Layer Graphene.^{1,2)}

We have developed a novel method for producing single-layer graphene fully covering an entire substrate (Fig. 1). Single-layer graphene has been synthesized on a whole 2 cm×2cm Ni film deposited on a HOPG substrate by heating in a ultrahigh vacuum. The carbon atoms forming the graphene are diffused from the HOPG substrate through the Ni template. Our results demonstrate how to control the amount of carbon atoms to yield graphene films with a controlled thickness. Our method represents a significant step toward the scalable synthesis of high-quality graphene films with predefined thickness and toward realizing the unique properties of graphene films.

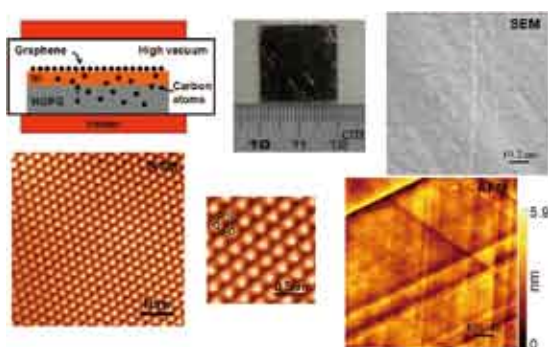


Fig. 1. Novel Ni(111)/HOPG(0001) system for the novel production of single-atomic graphene layers and their SEM, STM and AFM images.

(2) Rational Method for Determining Graphene Layer.³⁾

We have developed the novel method for graphene layer characterization by Auger electron spectroscopy (AES). AES spectra have been measured on different numbers

of graphene layers, which shows distinct spectrum shape, intensity, and energy characteristics with an increasing number of graphene layers (Fig. 2). We also have extracted electron inelastic mean free paths for graphene layers. The method allows unambiguous determination of thickness up to six graphene layers and detection of defect and dopant in graphene films on almost any substrate.

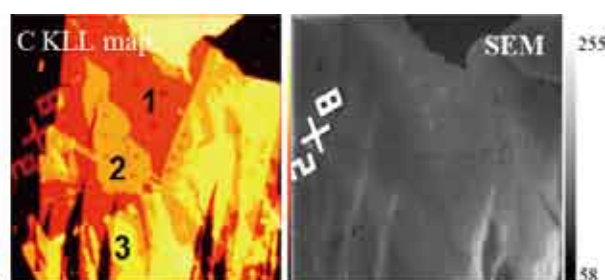


Fig. 2. C KLL Auger map and SEM of graphene layers on SiO₂.

(3) Electron-beam irradiation effects on graphenes.⁴⁾

By using AES and Raman spectroscopy, we have studied electron-beam irradiation effects on graphene damage (Fig. 3). We have shown that irradiation with an electron-beam can selectively remove graphene layers and induce chemical reactions, as well as possible structural transformations. We have also demonstrated the dependence of damage in graphene on electron-beam dose. Our work provides ideas on how to optimize the experimental conditions for graphene characterization and device fabrication. The results throw light on how energy transfer from the electron beam to graphene layers leads to the removal of carbon atoms from graphene layers and on the possibility of using electron-beam irradiation to locally induce chemical reactions in a controlled manner.

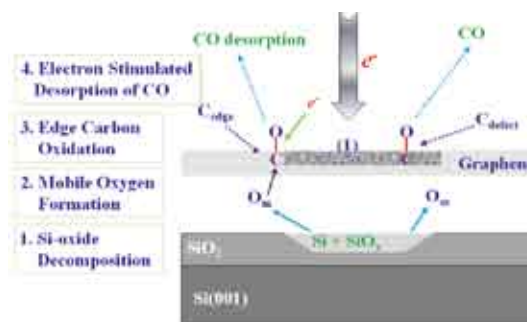


Fig. 3. Model of electron-beam irradiation effect on graphene.

References

- 1) J.-H. Gao, D. Fujita, M.-S. Xu, K. Onishi, S. Miyamoto, *ACS Nano* **4**, 1026 (2010).
- 2) M.-S. Xu, D. Fujita, K. Sagisaka, E. Watanabe, N. Hanagata, *ACS Nano*, in press (2011).
- 3) M.-S. Xu, D. Fujita, J.-H. Gao, N. Hanagata, *ACS Nano* **4**, 2937 (2010).
- 4) M.-S. Xu, D. Fujita, N. Hanagata, *Nanotechnology* **21**, 265705 (2010).

MANA Brain: Atomic Neural Networks

MANA Principal Investigator
(Satellite at UCLA, USA)

MANA Scientific Advisor
Postdoctoral Scholar
Graduate Student

James K. GIMZEWSKI

Adam Z. Stieg
Greg Pawin, Cristina Martin-Olmos
Henry Sillin



1. Outline of Research

Interest in the fundamental correlations between neural activity, cognition, associative memory and intelligence has motivated the creation of bio-mimetic neural network-based computing devices. Neuromorphic computation involving analog-VLSI circuits has been explored in quantum dots as well as molecular, CMOS and CMOL devices. They apply models of neural network systems, by implementing innovative software algorithms on high-density device architectures. In contrast, biological neural networks are intrinsically complex, and utilize self-configuring architectures capable of dynamic topological alteration.

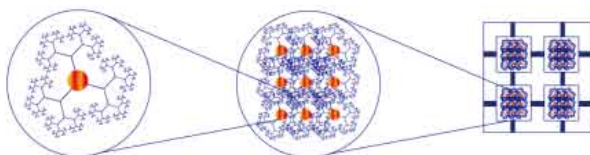


Fig. 1. Hierarchical model of the multi-scale fractal network architecture embedded in a electrically addressable device for multiplexed stimulation and interrogation.

We are working on hardware-based, physically intelligent neural network through a synergy of biological inspiration and advanced nano-electronics using the exciting properties of atomic-switch technology. Our approach involves the development of a complex, asymmetric hierarchical network based on dynamic local rewiring and Hebbian type activity-dependent interfaces fabricated through self-assembly (Fig. 1). This multi-scale approach will involve the combination of fractal architectures and solid-state nanoelectronics to generate a strongly coupled ‘small world’ (nano) network of dense electrical interconnects within a weakly coupled long range (micro) network embedded in a global (macro) device.

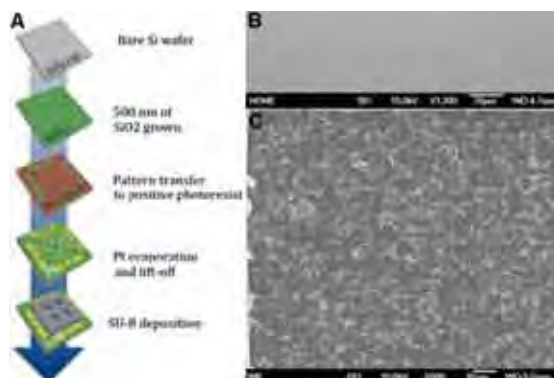


Fig. 2. Fabrication scheme for device architecture (A) and SEM micrographs of an ordered array of copper nucleation sites prepared by electron beam lithography (B) and dendritic silver wiring architectures (C) for multiplexed electrical characterization.

2. Research Activities

Current work at the UCLA-CNSI Satellite involves:

- Ongoing development of a functional theoretical model of intelligence based on self-organized criticality
- Fabrication of dendritic electronic circuits embedded with highly dense ($\sim 10^9/\text{cm}^2$) interfacial atomic switches (Fig. 2)
- Examination of memristive device characteristics
- Multiplexed electrical stimulus/response measurements to examine emergent spatiotemporal correlations (Fig. 3)

Future research includes: stabilization of 2D fractal networks within sol-gel matrices; extension of the networks towards 3D topologies; and development of device teaching/learning strategies.

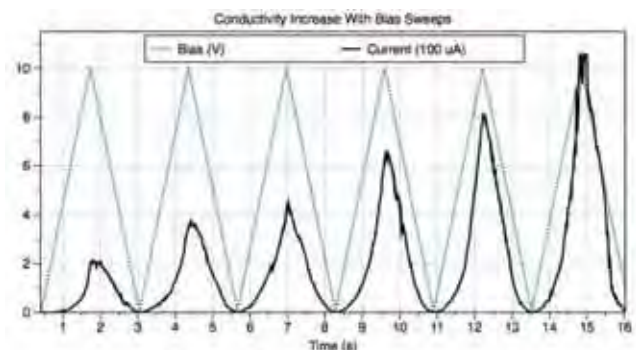


Fig. 3. Evolution of non-linear current-voltage (I-V) device characteristics during sequential bias sweeps.

Recent Publications with MANA recognition:

- 1) H. Rasool, E. Song, M. Allen, J. Wassei, R. Kaner, K. Wang, B. Weiller, J.K. Gimzewski, *Nano Lett.* **11**, 251 (2011).
- 2) S. Sharma, E. Grintsevich, M. Phillips, E. Reisler, J.K. Gimzewski, *Nano Lett.*, published online (2010).
- 3) A.Z. Stieg, J.K. Gimzewski, *Handbook of Nanophysics: Principles and Methods*, CRC Press, (2010).
- 4) C. Hsueh, H. Chen, J.K. Gimzewski, J. Reed, T. M. Abdel-Fattah, *ACS Applied Materials and Interfaces* **2**, 3249 (2010).
- 5) H.I. Rasool, P.R. Wilkinson, A.Z. Stieg, J.K. Gimzewski, *Review of Scientific Instruments* **81**, 023703 (2010).
- 6) S. Sharma, H.I. Rasool, V. Palanisamy, C. Mathisen, M. Schmidt, D. Wong, J.K. Gimzewski, *ACS Nano* **4**, 1921 (2010).
- 7) S. Sharma, S.E. Cross, C. Hsueh, R.P. Wali, A.Z. Stieg, J.K. Gimzewski, *International Journal of Molecular Sciences* **11**, 2523 (2010).
- 8) N. Yokoi, H. Inaba, M. Terauchi, A.Z. Stieg, N.J.M. Sanghamitra, T. Koshiyama, K. Yutani, S. Kanamaru, F. Arisaka, T. Hikage, A. Suzuki, T. Yamane, J.K. Gimzewski, Y. Watanabe, S. Kitagawa, T. Ueno, *Small* **6**, 1873 (2010).
- 9) R.P. Wali, P.R. Wilkinson, S. Eaimkhong, J. Hernando-Garcia, J.L. Sánchez-Rojas, A. Ababneh, J.K. Gimzewski, *Sensors and Actuators B* **147**, 508 (2010).

Atomic Electronics for Future Computing

MANA Principal Investigator

MANA Scientist
MANA Research Associate

Tsuyoshi HASEGAWA

Kazuya Terabe, Tohru Tsuruoka
Alpana Nayak, Takami Hino, Soumya R. Mohapatra



1. Outline of Research

We aim to explore new nanosystems showing novel functions based on atomic electronics. The new nanosystems are expected to realize new computing systems such as by achieving fault tolerant logic circuits, nonvolatile logic circuits, optical and chemical sensors, and so on. Since the present-day semiconductor systems based on CMOS devices is approaching to their maximum performance due to the ultimate downsizing, new types of logic systems using beyond-CMOS devices should be developed for further progress in information technology.

In this study, we will use the atomic electronic device, which has been developed by ourselves, for making new nanosystems. The atomic electronic device, such as atomic switch, is operated by controlling movements of cations and/or atoms in a nano-scale using nanoionics phenomena. The atomic electronic device has a possibility for configuring new computing systems, such as non-Boolean logic systems. For instance, the atomic electronic device is non-volatile, which enables simultaneous logical operation and memorization by a single device. The characteristic could enable for configuring conceptually new logic systems, which changes by itself according to the logical operation. We believe that neural computing systems are ultimate style of the non-volatile logic systems.

In order to accomplish the purpose, we will conduct 1) basic research on nanoionic phenomena, 2) developing new atomic electronics devices showing the novel functions based on the basic research, 3) developing nanofabrication technique for making the atomic electronics devices, 4) demonstration of novel operation of the atomic electronics devices and basic circuits using them.

2. Research Activities

(1) Development of Photoassisted Atomic Switch.¹⁾

Electronic devices which operate by sensing photo-signals and memorize the information are required to develop electronic systems such as artificial eyes. In the project, we developed a new type of atomic switch in collaboration with a group of Osaka Univ. The new atomic switch includes a photoconductive organic layer between the two electrodes of a conventional atomic switch. The photoconductive organic layer allows for a light-controlled operation of the atomic switch. Namely, a weak photocurrent induced in the photoconductive organic layer by irradiation with light is used in control of the solid electrochemical reaction that grows a metal filament between the two electrodes. Because the metal filament exists stably after irradiation with light, the photoassisted atomic switch operates as a nonvolatile device, and the device “remembers” whether an optical signal has been received or not.

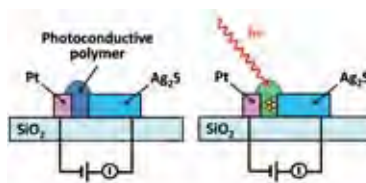


Fig. 1. Schematic of photoassisted atomic switch.

(2) Late-limiting Processes of Gap-type Atomic Switches.^{2,3)}

We have revealed the late-limiting processes of gap-type atomic switches made of Ag_2S and Cu_2S . Two different activation energies were measured in the switching time measurements depending on the switching bias ranges as shown in Fig. 2a, suggesting that different processes determine the switching time in the ranges. That is, the solid electrochemical reaction is a rate-limiting process in the lower bias range, and the diffusion of metal cations in the materials is a rate-limiting process in the higher bias region (Fig. 2b).

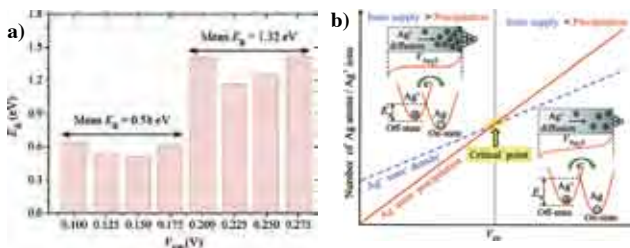


Fig. 2. a) Activation energy values extracted from the switching time measurements as a function of temperature and a bias. b) Schematic of the operating mechanism and late-limiting processes.

(3) Atom Transistor.⁴⁾

We have developed a new type of three-terminal atomic switch, ‘Atom Transistor’, which has novel characteristics such as extremely low power consumption and volatile/nonvolatile dual-functionality.

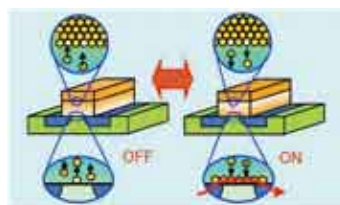


Fig. 3. Schematic of atom transistor. Diffusion and Redox-reactions of metal atoms are controlled.

References

- 1) T. Hino, H. Tanaka, T. Hasegawa, M. Aono and T. Ogawa, *Small* **6**, 1745 (2010).
- 2) A. Nayak, T. Tamura, T. Tsuruoka, K. Terabe, S. Hosaka, T. Hasegawa, and M. Aono, *J. Phys. Chem. Lett.* **1**, 604 (2010).
- 3) A. Nayak, T. Tamura, T. Tsuruoka, K. Terabe, S. Hosaka, T. Hasegawa, and M. Aono, submitted.
- 4) T. Hasegawa, Y. Itoh, H. Tanaka, T. Hino, T. Tsuruoka, K. Terabe, H. Miyazaki, K. Tsukagoshi, T. Ogawa, S. Yamaguchi and M. Aono, *Appl. Phys. Exp.*, in press.

Nano Superconductivity and Terahertz Emission

MANA Principal Investigator

MANA Scientist
MANA Research Associate
Graduate Student

Xiao HU

Masanori Kohno
Shu-Jun Hu, Shi-Zeng Lin, Zhi Wang
Feng Liu



1. Outline of Research

Terahertz (10^{12} Hertz, THz) electromagnetic (EM) waves are useful in many applications such as DNA diagnosis, observation on ultrafast dynamics of electrons in materials, telecommunication, and so on. However, development of strong and compact source of THz waves is still very challenging.

Josephson effects are associated with the quantum tunneling of Cooper pairs across the superconductor/insulator/superconductor structure, called Josephson junction, which induce Josephson plasma, a composite wave of superconductivity phase and EM oscillation. Based on this principle, a research team of Argonne National Lab of US and University of Tsukuba of Japan succeeded in stimulating strong monochromatic EM wave from a mesa structure of single crystal of $\text{Bi}_2\text{Sr}_2\text{CaCu}_2\text{O}_8$, a typical cuprate high- T_c superconductor.

This layered superconductor behaves in many aspects like a sequence of Josephson junctions stacked along its c axis with huge inductive coupling between neighboring junctions, since the stacking period is as small as 1.5 nanometers. Analyzing the coupled sine-Gordon equations as the mathematical model of the material, we have discovered a novel state for the superconductivity phase dynamics. Under the dc voltage bias, the system develops a π phase twist inside each junction when superconductivity phases are rotating overall, which provides a strong coupling between the standing wave of Josephson plasma and the driving current. When the bias voltage is tuned appropriately, a cavity resonance in the mesa of single crystal takes place with the amplitude of Josephson plasma enhanced greatly, which results in large dc current injection into the system and strong radiation of THz waves from the edge.

In order to reduce the energy cost of the π phase twist, the system piles up $+$ and $-\pi$ phase kinks alternatively in the stacking direction, which corresponds to one of the eigenvectors of the coupling matrix of the coupled sine-Gordon equations. The attractive interaction between the opposite π kinks makes the π kink state stable.

Our theory provides a consistent explanation on the experimental observations, and predicts that the optimal radiation power is larger than the observed value by orders of magnitude. These results reveal the possibility of a novel quantum source of EM wave based on a principle totally different from the conventional laser.

2. Research Activities

(1) Optimal condition for strong THz radiation.¹⁾

In order to increase the radiation power, we propose to use a BSCCO sample with its thickness much larger than

the EM wavelength (Fig. 1L). It is found that for the optimal dielectric surrounding material the radiation energy equals the plasma dissipation inside the sample (Fig. 2R). This result will serve as the design principle for THz generator.

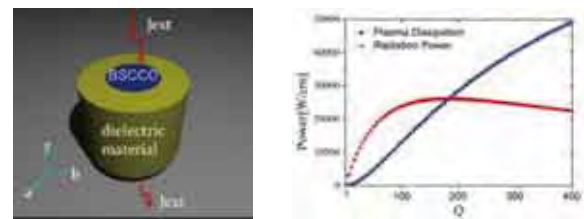


Fig. 1. Left: schematic diagram of the device; Right: radiation power and dissipation as functions of Q factor, which is monotonic to the dielectric constant of the surrounding material.

(2) Mott transition of electron systems.²⁾

By using exact solutions and numerical simulations, single-particle spectral properties near the Mott transition are investigated in the one-dimensional Hubbard model. (Fig. 2). The results show pseudogap, hole-pocket behaviors, anomalous spectral-weight transfer, and the upper Hubbard band, which are reminiscent of anomalous features observed in cuprate high- T_c superconductors. In contrast with conventional metal-to-band-insulator transitions, the Mott transition turned out to be characterized as a loss of charge character from the mode having both spin and charge characters, while the spin part remains almost unchanged. Or, from the insulating side, the Mott transition is characterized by the emergence of a gapless mode whose dispersion relation extends up to the order of hopping integral t [spin exchange J] in the weak [strong] interaction regime.

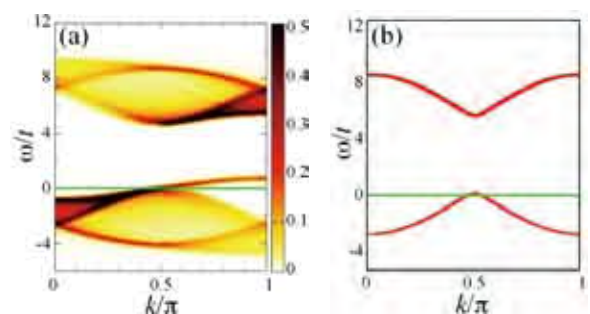


Fig. 2. Single-particle spectral function $A(k, \omega)$ near (a) the Mott transition and (b) the metal-to-band-insulator transition.

References

- 1) X. Hu, S.-Z. Lin, *Supercond. Sci Technol.* **23**, 253001 (2010) (Review Article).
- 2) M. Kohno, *Phys. Rev. Lett.* **105**, 106402 (2010).

Surface Atomic Scale Logic Gate

MANA Principal Investigator
(Satellite at CNRS Toulouse, France)

Toulouse Scientist
MANA Research Associate
Graduate Student

Christian JOACHIM

Jacques Bonvoisin
Mohamed Hliwa, Maricarmen Grisolia
Nicolas Renaud, Sabrina Munery



1. Outline of Research

The fundamental question for the design and construction of an atomic scale calculator is to determine the required minimum number of atoms. Then, the assembled nano-system must be able to perform alone a complex computation. Answering this question requires the exploration of:

- The quantum design of a molecule (or atom surface circuit) able to perform alone a logical operation,
- The molecule synthesis (respectively atom by atom UHV-STM construction on a surface) of the molecule logic gate (respectively the atom surface circuit logic gate),
- The development of a surface multi-pad interconnection technology with a picometer precision respecting the atomic order of the surface nano-system assemblage.
- The improvement of specific quantum chemistry software like N-ESQC able to simulate the full logic gate nano-system functionalities with its interconnections and its supportive surface.

The CNRS Toulouse MANA satellite is working on 2 specific areas of this broad academic problem: the molecule synthesis of quantum logic gate with or without qubits (SWAP, NOR, AND gates) and the theory of surface electronics interconnects using surface atomic interconnections. We expect to understand the physics of surface interconnection of simple single molecule logic gate (or surface atomic circuit logic gate) using atomic wire, to certify logic gate design and pursue the exploration of the molecule logic gate complexity roadmap to embed the maximum possible computing power inside a single molecule or a single surface atomic scale circuit.

2. Research Activities

(1) Surface atomic scale logic gate.

Finite length surface atomic wires are constructed using atom by atom vertical manipulation on a passivated semi-conducting surface. Two surfaces are of interest for the Toulouse MANA Satellite: MoS₂ and Si(100)H. For

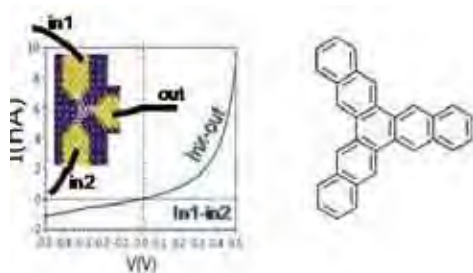


Fig. 1. The I-V Characteristics of a starphene OR gate calculated with N-ESQC taking into account the full 3 electrodes molecular junction and the detail Si(100)H surface electronic structure.²⁾

MoS₂, single S atom surface extraction is studied in NIMS in collaboration with Toulouse.¹⁾ For Si(100)H, we study theoretically classical surface atomic scale logic circuits comparing their performances with classical mono-molecular logic gate (Fig. 1). Taking the realistic surface implantation of an OR gate in both cases and for a surface gap semi-conductor, we have demonstrated how to abandon the construction of hybrid classical circuits using surface atomic wires combined with molecules.²⁾

(2) Molecule logic gate.

The synthesis and surface compatibility of our controlled SWAP molecule logic gate (a 4 center mixed valence organometallic molecule³⁾) was started in 2010. We have now trouble checked that our “Ru” qubit can be deposited intact on a Ag(111) surface and LT-UHV-STM imaged (see Fig. 2).

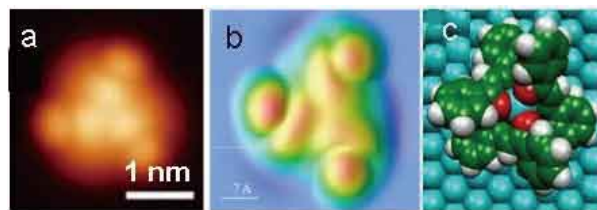


Fig. 2. (a) LT-UHV-STM of a Ru(dbm)₃ precursor of the Ru(dbm)₂(acac-Br) qubit on Ag(111) for I = 15 pA and V = 1.5 V. (b) the ESQC calculated image for the optimized (c) conformation of chemisorbed on Ag(111). Molecule synthesized in the Toulouse MANA satellite.⁷⁾

The theory of light controlled SWAP molecule was extended to include multi-configurational states through a full density matrix approach.⁴⁾

For the Quantum Hamiltonian Computing (QHC) molecule logic gate approach,⁵⁾ the MANA Satellite symbolic analysis leads to the design and synthesis of the starphene molecule (Fig.1). This molecule was first calculated in a planar atomic scale 3 terminals junction (Fig. 1), showing a nice OR truth table. Then, it was studied experimentally as physisorbed on an Au(111) surface using an LT-UHV-STM.⁶⁾ Single manipulated Au atoms contacting one at a time the starphene are like single classical digital input. A QHC NOR logical truth table results as a function of the number of coordinated Au atoms.⁶⁾ Extension of this concept towards surface atomic circuit on Si(100)H is underway.

References

- 1) N. Kodoma, T. Hasegawa, T. Tsuruoka, C. Joachim, M. Aono, *Jap. J. App. Phys.* **49**, 08LB01 (2010).
- 2) F. Ample et al., *J. Phys. CM*, submitted (2010).
- 3) J. Bonvoisin et al., *Inorg. Chem. Acta* **363**, 1409 (2010).
- 4) M. Hliwa et al., *Chem. Phys. Lett.*, submitted (2010).
- 5) N. Renaud, C. Joachim, *J. Phys. A*, submitted (2010).
- 6) W.H. Soe et al., *Phys. Rev. B*, submitted (2010).
- 7) S. Munery et al., *Inorg. Chem.*, submitted (2010).

Superconducting Quantum Nanoarchitectonics

MANA Principal Investigator
(Satellite at Univ. Tsukuba, Japan)
Graduate Student

Kazuo Kadowaki

Shota Fukuya, Shinya Hashimoto, Manabu Tsujimoto,
Tomoki Goya, Hisato Yamaguchi, Kota Deguchi,
Takashi Koike, Naoki Orita, Yohei Jono, Ryo Nakayama,
Krsto Ivanovic, Kaveh Delfanzari



1. Outline of Research

Our objective in this research is to develop a new concept of materials science, which is referred to as Nanoarchitectonics, especially in the field of superconductivity by making use of highly developed modern nanotechnology in the ultimate quantum regime of materials. The challenge to accomplish this has been set forth on the nature of the intrinsic Josephson junctions (IJJ's) with and without magnetic field using high- T_c superconductor (HTSC) $\text{Bi}_2\text{Sr}_2\text{CaCu}_2\text{O}_{8+\delta}$, which can be grown by us in the highest quality of single crystal form available in the world. June in 2007, a remarkable phenomenon, which has never been observed before, was discovered in the mesa structure of this material: strong, continuous and coherent electromagnetic waves at THz frequencies were observed. The very sharp spectrum of this radiation is considered as LASER emission from stacked intrinsic Josephson junctions in the mesa. This achievement has attracted much attention because this device may bring us the first full solid state THz sources, which will be ideal and desired for a variety of important applications in the 21st century.

Furthermore, in order to break through the potential research barriers it is of necessity to discover new materials with a higher superconducting transition temperature. As for this line of research we have been developing new iron based-superconductors, AFe_2X_2 compounds, where A=alkaline, alkali-earth, Tl, etc., and X=As, P, Se. Remarkable development has been achieved.

2. Research Activities

(1) THz radiation from HTSC IJJ's.

The research has been focused on two directions: one is the development of devices with high power, and another is to develop frequency variable devices in wide range frequencies. For the former we have developed a stand-alone mesa structure without the large superconducting substrate. Although this has still been in progress, the output power of 30-50 μW has been achieved. This can be improved further by exploring better fabrication technique of the stand-

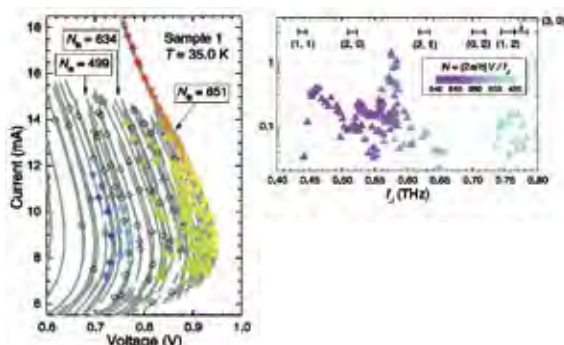


Fig. 1. Branch structure of the I - V curve in a rectangular mesa ($137 \mu\text{m} \times 99.2 \mu\text{m} \times 1.3 \mu\text{m}$) (left), and the frequency spectrum of the radiation from all branches (right). The colored points corresponds to the points where the spectrum was measured.



Fig. 2. Photos of single crystal of $\text{BaFe}_2(\text{As}_{1-x}\text{P}_x)_2$ (left) and $\text{K}_{0.8}\text{Fe}_2\text{Se}_2$ (right).

alone mesa structure and by constructing an array structure. Concerning the wide tunability, we discovered a phenomenon that the radiation frequency goes higher and higher as the branch of the I - V curve goes deeper and deeper inside and as long as the emission occurs on it. This peculiar behavior is still not fully understood but it offers an excellent performance as oscillator devices. In Fig. 1, an example of this behavior is given together with the radiation spectrum. (2) Search for novel superconductors.

Development of the novel superconducting materials is essential for developing the new research field of superconducting quantum nanoarchitectonics. Here, we show an example of a successful growth of high quality single crystal of $\text{BaFe}_2(\text{As}_{1-x}\text{P}_x)_2$ and $\text{K}_{0.8}\text{Fe}_2\text{Se}_2$ compounds as shown in Fig. 2. To reveal the physical properties, we have measured specific heat of some of them as shown in Fig. 3 as an example using of $\text{BaFe}_2(\text{As}_{1.62}\text{P}_{0.38})_2$ single crystal. A clear and sharp jump of the specific heat at $T_c = 30 \text{ K}$ ($\Delta C_p/T_c = 46 \text{ mJ/molK}^2$, where the specific heat of BaFe_2As_2 was subtracted). Furthermore, the specific heat at low temperature did not show exponential behavior but had a T^3 dependence, indicating a polar type of gap opening at the Fermi surface.

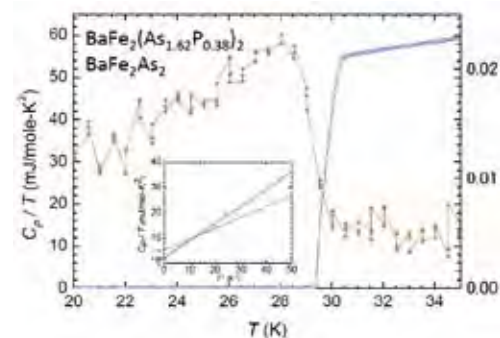


Fig. 3. The Specific heat around T_c and at low temperatures (inset). The resistive transition is also shown.

References

- 1) M. Tsujimoto et al., *Phys. Rev. Lett.* **105**, 037005 (2010).
- 2) R. A. Klemm et al., *J. Phys.: Condens. Matter* **22**, 975701 (2010).

Integration of Nano Functionality for Novel Nanosystems

MANA Principal Investigator

MANA Scientist

MANA Research Associate

Tomonobu NAKAYAMA

Takashi Uchihashi, Yoshitaka Shingaya,
Osamu Kubo, Katsumi Nagaoka
Shin Yaginuma, Masato Nakaya,
Puneet Mishra, Jianxun Xu



1. Outline of Research

We develop novel techniques and methodologies toward the realization of novel nanosystems for future information technology. Development and application of multiple-scanning-probe microscopes (MSPM), manipulation of individual atoms and molecules, and measurements of signal transfer through living cell systems, are explored for a common purpose; creation and characterization of elemental nanostructures and functional nanosystems which transmit and transduce electrical, optical, mechanical, ionic and magnetic signals.

MSPM is an instrument which has simultaneously and independently controlled 2 to 4 scanning probes.¹⁻⁶ Those probes are brought into electrical contact to a single nanostructure and reveal its electrical property.⁵ We have measured electrical resistances of films of fullerene C₆₀ molecules, single rare-earth metal silicide nanowires self-organized on Si(001), single-walled carbon nanotubes, nanostructured graphenes and so on.

Fabrication of nanostructures by means of self-organization,^{7,8} atom/molecule manipulation⁹⁻¹¹ and dynamic shadow mask deposition is pursued because such these methodologies are keys to realize functional nanosystems.

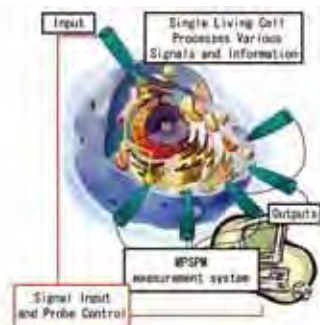


Fig. 1. Schematic illustration of a “cell odyssey” using the MSPM which works in liquid environment.

A nerve cell and a network of the cells are sophisticated hierarchical materials systems which are known to ultimately device a human brain. We believe that the understanding working principle of such a cell system changes the present computing technology. Investigation of signal transmission and transduction through single and conjugated living cells (see Fig. 1) are promoted in collaboration with the Biomaterials Center of NIMS. Here, we use our MSPM and related techniques to understand the signal transfer from nanoscopic viewpoints.

2. Research Activities

(1) Multiple-scanning-probe Microscope.¹⁻⁶

We added atomic force microscope functions to our MSPM systems¹⁻³ using newly developed tuning fork probes.⁶ This development provided us a new method to

investigate electrical properties of various nanostructures and nanomaterials placed on insulating substrates. In addition to nanowires grown on Si substrates,³ electrical properties of nanostructured graphenes on SiO₂ substrates are studied using our multiple-scanning-probe force microscope (MSPFM).

(2) Controlling reversible intermolecular reaction for data storage.^{9,11}

We found that the transformation between monomers and a dimer (or trimer) of C₆₀ can be surprisingly well-controlled by a sharp probe of SPM at room temperature.^{8,9} As an application of this method, we have demonstrated data storage with a bit density of 190 Tbits/in². Furthermore, we found that it is possible to control the degree of polymerization to form dimer, trimer, tetramer and so on (Fig. 2).¹¹

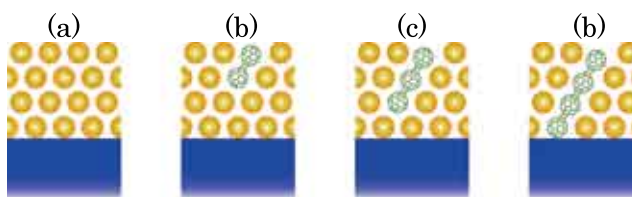


Fig. 2. Using a probe of a scanning tunneling microscope, it is possible to control the degree of local polymerization to form (a) monomer, (b) dimer, (c) trimer, (d) tetramer and so on.

(3) Application of MSPM to living nerve cells.¹²

To understand the signal processing scheme used by the brain, we have been developing various nanoprobes which can be used in liquid and/or inserted into living cells: Local measurements of pH values, ionic conductivity, mechanical stiffness¹² and single molecule recognition in physiological environment have been studied. Combination of such nanoprobes and MSPM enables “cell odyssey” using MSPM.

References

- 1) M. Aono, C.-S. Jiang, T. Nakayama, T. Okuda, S. Qiao, M. Sakurai, C. Thirstrup, Z.H. Wu, *Oyoh Butsuri* **67**, 1361 (1998).
- 2) T. Nakayama, C.-S. Jiang, T. Okukda, M. Aono, *SICE J. Control, Measurement, and System Integration* **38**, 742 (1999).
- 3) S. Higuchi, H. Kuramochi, O. Laurent, T. Komatsubara, S. Machida, M. Aono, K. Obori and T. Nakayama, *Rev. Sci. Instrum.* **81**, 073706 (2010).
- 4) O. Kubo, Y. Shingaya, M. Nakaya, M. Aono, T. Nakayama, *Appl. Phys. Lett.* **88**, 254101 (2006).
- 5) D.-K. Lim, O. Kubo, Y. Shingaya, T. Nakayama, Y.-H. Kim, J.-Y. Lee, M. Aono, H. Lee, D. Lee, S. Kim, *Appl. Phys. Lett.* **92**, 203114 (2008).
- 6) S. Higuchi, H. Kuramochi, O. Kubo, S. Masuda, Y. Shingaya, M. Aono, T. Nakayama, *Rev. Sci. Instrum.*, submitted.
- 7) P. Mishra, T. Uchihashi, T. Nakayama, *Phys. Rev. B* **81**, 115430 (2010).
- 8) T. Uchihashi, K. Kobayashi, T. Nakayama, *Phys. Rev. B* **82**, 113413 (2010).
- 9) M. Nakaya, S. Tsukamoto, Y. Kuwahara, M. Aono, T. Nakayama, *Adv. Mater.* **22**, 1622 (2010).
- 10) M. Nakaya, Y. Kuwahara, M. Aono, T. Nakayama, *Small* **4**, 538 (2008).
- 11) M. Nakaya, M. Aono, T. Nakayama, submitted.
- 12) S. Machida, T. Watanabe-Nakayama, I. Harada, R. Afrin, T. Nakayama, A. Ikai, *Nanotechnology* **21**, 385102 (2010).

Mesoscopic Superconductivity and Quantum Information Physics

MANA Principal Investigator
 (Satellite at Tokyo Univ. Sci., Japan)
 MANA Research Associate
 Guest Researcher
 Graduate Student

Hideaki TAKAYANAGI

S. Kim, K. Tsumura
 R. Inoue, R. Ishiguro
 M. Kamio, T. Hayashi, K. Muranaga, M. Yakabe,
 K. Yokobatake



1. Outline of Research

Our research topic is so-called mesoscopic superconductivity which aims to explore new quantum phenomena in different kind of superconducting devices and to apply them to quantum information physics.

We are now developing an ultimate SQUID (Superconducting Quantum Interference Device), i.e., a nano-SQUID which can detect single or several spins. We will also clarify the quantum interaction between a nano-SQUID with embedded quantum dots and spins in dots. This leads to the implementation of an entangled state between a superconducting qubit and spin qubit. The combination of these qubits is a promising candidate for a quantum interface that will be indispensable in the future quantum information network.

We are also working on superconductor-based Light Emitting Diode. Superconductor-based LED is expected to be the key device in quantum information technology because of its promising giant oscillator strength due to the large coherence volume of the superconducting pairs together with the possibility of the *on-demand* generation of entangled photon pairs.

Our other research targets are (i) graphene SQUID and (ii) spin injection effect into superconductor.

2. Research Activities

(1) π junction transition in InAs self-assembled quantum dot coupled with SQUID.^{1,2)}

We measure the transport of the InAs self-assembled quantum dots (SAQDs) which have a unique structural ze-

ro-dimensionality, coupled to a superconducting quantum interference device (SQUID) (Fig. 1). Owing to SQUID geometry, we directly observe a π phase shift in the current phase relation and the negative supercurrent indicating π junction behavior by not only tuning the energy level of SAQD by back-gate but also controlling between SAQD and electrodes by side-gate (Fig. 1(d)). Our results support that the π junction transition was explained by the singlet-doublet transition of the spin state of the InAs SAQD due to a change of the coupling between SAQD and superconducting leads by side-gate without direct observation of π state. Employing InAs SAQD to QD-SQUID may open new possibility for a quantum information processing in a wide range of optics, spintronics.

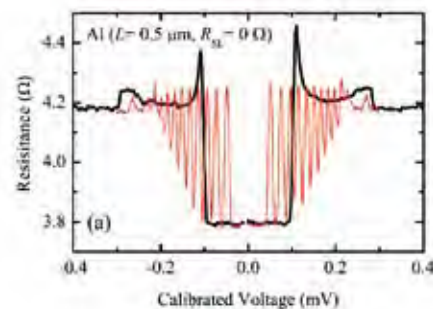


Fig. 2. Differential resistance as a function of voltage. The black and red lines represent the data without and with RF irradiation (1.77 GHz).

(2) Transport properties of Andreev polarons in superconductor-semiconductor-superconductor junction with superlattice structure.^{3,4)}

Transport properties of a superconductor-semiconductor-superconductor junction with superlattice structure are studied. Differential resistance as a function of voltage shows oscillatory behavior under the irradiation of RF waves of 1.77 GHz regardless of the junction geometry (Fig. 2). Experimental data are explained in terms of the coupling of superconducting quasiparticles with long-wavelength acoustic phonons excited by the RF waves. We propose that the strong coupling causes the formation of novel composite particles, Andreev polarons.

References

- 1) S. Kim et al., to be published in the proceedings of 30th International Conference on the Physics of Semiconductors (ICPS2010), COEX, Seoul, Korea, July 25~30, 2010.
- 2) S. Kim et al., *Appl. Phys. Lett.*, to be published.
- 3) R. Inoue et al., to be published in the proceedings of 30th International Conference on the Physics of Semiconductors (ICPS2010), COEX, Seoul, Korea, July 25~30, 2010.
- 4) R. Inoue et al., arXiv:1009.0611v1.

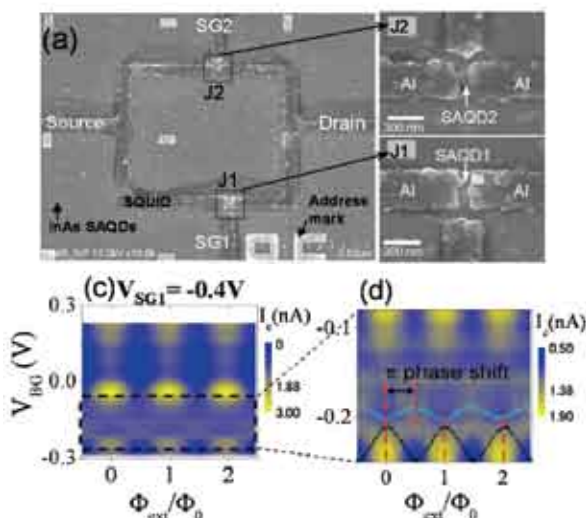


Fig. 1. (a) SEM image of the SQUID coupled with InAs SAQD. Here randomly distributed small dots are InAs SAQDs. (c) I_c oscillation as a function of external magnetic field and backgate voltage V_{BG} . Side gate voltage V_{SG1} is fixed to be -0.4 V for (c). (d) is enlarged plot of (c) in the range of V_{BG} from -0.08 V to -0.25 V.

Solution-Processable Organic Single Crystals with Bandlike Transport in Field-Effect Transistors

MANA Principal Investigator

MANA Scientist
MANA Research Associate

Kazuhito TSUKAGOSHI

Takeo Minari
Chuan Liu



1. Outline of Research

In organic field-effect transistors (OFETs), the best performance of semiconducting oligomers is usually observed in single crystalline state rather than their polycrystalline or amorphous state. As single crystals are free of grain boundaries and molecular disorders, carrier transport is not limited by hopping between localized states but featured with high mobility ($> 1 \text{ cm}^2/\text{Vs}$) and band-like transport. The single crystalline can be widely synthesized by sublimation in heated furnace. However, the field effect mobility of organic transistor fabricated by solution process has been limited in low performance because the channel is composed of many grains due to the polycrystalline. It is widely desired to improve the channel formation method and the organic molecules.

Here, we developed a method to directly make the single crystals on gate insulator by solution process. In the crystal, a band-like transport in the temperature dependence was reproducibly observed. As the highest mobility, $9.1 \text{ cm}^2/\text{Vs}$ is obtained. Although this is still in a demonstration of basic characteristic of the organic transistor, a high performance of the organic molecule can be seen even in the transistor made by solution process.

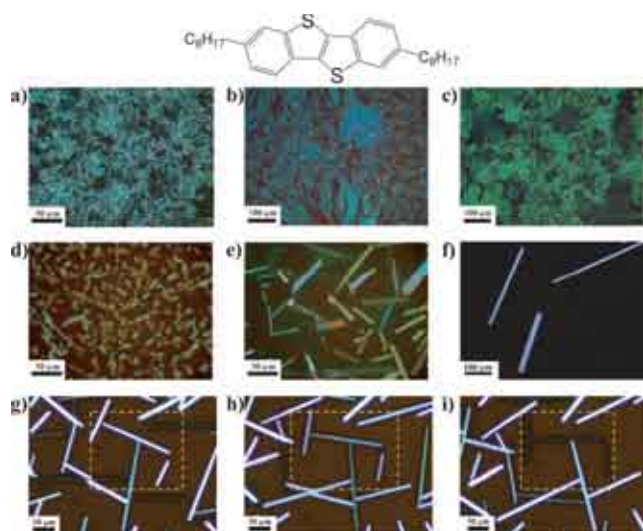


Fig. 1. Top: molecular structure of C8-BTBT. a)–f) Optical images of films taken by microscope before (a–c) and after SVA (d–f): C8-BTBT on SiO_2 (a, d); C8-BTBT on PMMA (b, e); the mixture of C8-BTBT and PMMA (c, f). Note that different scale bars are used for clarity. g)–i) Optical images of the crystals under a cross polarizer. From g) to i), the sample holder was rotated 15° per image in the anticlockwise direction. The dashed squares indicate the crystal colors which changed uniformly from visible to nearly invisible.

2. Research Activities

Single crystals of organic semiconductor are directly formed from solution by our two step formation.

The semiconductor dioctylbenzothienobenzothiophene (C8-BTBT) was used as the organic transistor channel (Fig. 1). The C8-BTBT film evaporated on the PMMA or SiO_2 surface can be reorganized into small crystals via solvent vapor annealing (SVA), but the crystals are irregular and short ($< 50 \mu\text{m}$). We used the self-organized phase separations by spin-coating the mixture of the semiconductor and insulator PMMA in order to improve the interface quality. After applying SVA to the C8-BTBT film formed by the phase separation, the top semiconductor layer was drastically changed by nucleation-governed self-assembly process, and was reorganized into 1-dimensional single crystals on PMMA surface. The crystals grow in the [100] direction and can reach over $300 \mu\text{m}$ long with a highly uniform width and smooth top surface.

Based on these crystals, we fabricated FETs and observed high mobility up to $9.1 \text{ cm}^2/\text{Vs}$, which is one of the highest mobility for transistors based on an organic single crystal produced by solution processing (Fig. 2). In temperature dependence measurements, the FET mobilities increase upon cooling from about 300 K to 80 K , indicating the band-like transport in a temperature region as wide as 200 K . Surprisingly, the threshold voltage is nearly temperature independent, implying extra low density of trap states. These results are significant for fundamental research and device application in organic FETs.

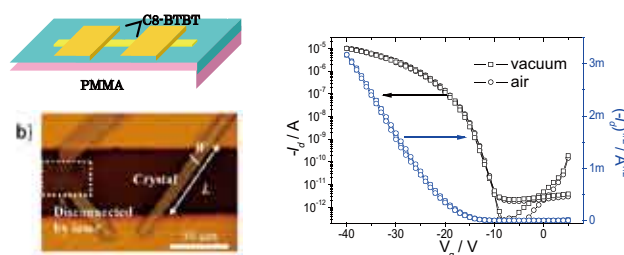


Fig. 2. a) Scheme and b) photo of the single crystal FET, in which only one crystal remains and all the others were ablated by laser. c) Transfer characteristics of a typical device with operated at -40 V drain voltage under vacuum (open squares) and in air (open circles), exhibiting $\mu\text{FET} = 5.2 \text{ cm}^2/\text{Vs}$.

Reference

- 1) C.Liu, T.Minari, X.Lu, A.Kumatani, K.Takimiya, K.Tsukagoshi, *Adv. Mater.*, in press (2010). DOI: 10.1002/adma.201002682

Bio-Inspired Materials for Sustainable Energy

MANA Principal Investigator
(Satellite at Univ. Cambridge, UK)

Research Co-Director
MANA Research Student

Mark WELLAND

David Bowler
Rami Louca, Conn O'Rourke, Umberto Terranova



1. Outline of Research

Our ultimate aim is to combine biological inspiration with electronics to give high efficiency materials and solar cells with applications to energy and sustainability. We will use a combination of self-assembly and directed assembly via lithography to create appropriate structures, taking our inspiration from biological systems. Our research combines experiment and theoretical modeling to give a detailed insight into the properties of the materials.

We have established a network of collaboration between three different institutions: MANA in NIMS, Nanoscience Centre in University of Cambridge and the London Centre for Nanotechnology in University College London. We are actively seeking to increase the collaborations between these sites and with other groups within MANA. In this year, we have arranged collaborative research visits to MANA for the co-director, as well as visits to UCL from collaborators in NIMS (Y. Tateyama).

2. Research Activities

(1) Synthesis of metal oxide nanowires for DSSCs.

We are investigating low temperature methods to grow highly crystalline titanium dioxide nanowires directly on transparent conducting substrates. These structures, to be used as DSSC electrodes, are expected to improve the electron transport properties compared to nanocrystalline electrodes, leading to better performing devices and higher conversion efficiencies. We are optimising the growth methods to achieve high uniformity of the nanowire films on a macro scale, as well as optimum nanowire morphology and dimensions.

Different nanowire morphologies have been obtained; we are investigating which morphology gives the best performance in a DSSC device. We can also apply thin inorganic shell layers covering the nanowires (including aluminium oxide, zirconium oxide and magnesium oxide), and will investigate the effect of these shells on suppressing charge recombination and passivating surface traps. Fig. 1 shows two titanium dioxide nanowire morphologies obtained.

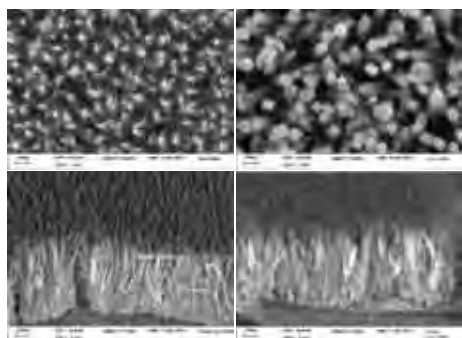


Fig. 1. Top left and top right – two titanium dioxide nanowire morphologies obtained. Bottom left and bottom right – corresponding tilted views of the same nanowires.

(2) Atomic and Electronic Structure of Dye Molecules on Substrates.

Using standard DFT, we are characterising the interaction of different dyes with TiO_2 surfaces found on nanoparticles.^{1,2} We have shown that catechol (a prototype for many dyes) will bind most strongly to defect sites will bind sites, but this may not be the ideal binding for efficient charge transfer.¹ We have also modelled the changes in electronic structure for indoline-based dyes with different functional groups in gas phase and on surfaces,² illustrated in Fig. 2. In collaboration with NIMS we have also modelled a Ru-based dye bound to anatase and considered its dynamics.³ This exchange of expertise between different centres has been extremely beneficial. We have also looked at the nucleation of Al_2O_3 on TiO_2 ,⁴ as part of a study on the mechanisms underlying the change in electronic structure and dye efficiency following growth of thin oxide layers on TiO_2 .

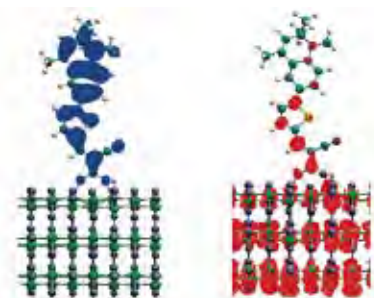


Fig. 2. HOMO (red) and LUMO (blue) of C2 chromophore adsorbed on anatase TiO_2 (101).

(3) Development of novel methods.

Despite its success, DFT is not suitable for all applications, and we are continuing to develop novel approaches to extend the functionality of DFT for: large systems; energy levels; and charge transfer. It is hard to address large system sizes with standard implementations of DFT (which have a computer effort which increases with the cube of the number of atoms); we are using the Conquest linear scaling code (which has a computer effort that increases linearly with the number of atoms, and has been applied to systems containing millions of atoms) as a basis for this work. This code is the result of an on-going collaboration between NIMS and UCL. We have already implemented the constrained DFT technique for studying charge transfer excitations with the code, and are testing a new implementation of time-dependent DFT within the code as a route to reliable energy level calculations for large systems.

References

- 1) U. Terranova, D.R. Bowler, *J. Phys. Chem. C* **114**, 6491 (2010).
- 2) C. O'Rourke, D.R. Bowler, *J. Phys. Chem C* **114**, 20240 (2010).
- 3) C. O'Rourke, U. Terranova, Y. Tateyama, D.R. Bowler, *in preparation* (2011).
- 4) U. Terranova, D. R. Bowler, *J. Mater. Chem.*, in press (2010).

Construction of Interphases with Atomic/Molecular Order for Efficient Conversion of Energy/Materials

MANA Principal Investigator Kohei UOSAKI

(Field Coordinator)

MANA Scientist
 MANA Research Associate
 Graduate Student
 Visiting Scientist

Hidenori Noguchi, Satoshi Tominaka
 Qin Xu, Sedden Beyhan
 Y. Sun, S. Tong, Y. Okawa, Y. Zhang, G. Elumalai
 Aleksandra Pacula



1. Outline of Research

One of the most challenging problems for chemists/material scientists is construction of efficient energy/materials conversion systems. In this study, we would like to establish techniques to construct interfacial phases for highly efficient energy/materials conversion, mainly at solid/liquid interfaces, by arranging metal, semiconductor and organic molecules with atomic/molecular resolution. Furthermore, the detailed *in situ* analyses by STM, non-linear spectroscopy, and x-ray techniques of the structure and functions of the interfaces as well as theoretical study are carried out so that structure-function relations should be established and rational design and construction of the desired interfacial phases become possible. Specifically, we have carried out 1. construction of catalytic interfaces by arranging atoms on metal surfaces in ordered manner., 2. construction of photoenergy conversion interfaces by forming ordered molecular layers on metal and semiconductor surfaces, and 3. experimental and theoretical investigations of structure and electron transfer processes at solid/liquid interfaces.

2. Research Activities

(1) *Construction of catalytic interfaces by atomically ordered modification of metal surfaces and microfabrication techniques.*

Development of highly efficient multi-functional electrocatalysts attracted considerable attention because of their important applications for interfacial energy conversion. Catalytic activities depend on the composition and structure of the catalysts. For example, the atomic ratio giving maximum catalytic activity for electrochemical methanol oxidation reaction, which is one of the most important reactions in fuel cell, is suggested to be Pt₅₀Ru₅₀. It is, however, not

easy to prepare the catalysts with precise atomic arrangement. Usually two metal complexes are mixed together and decomposed thermally to obtain alloy. In this case, bulk ratio can be controlled but not nano-scale arrangement at the surface where reactions take place. Here, we employed a new method, in which multi-nuclear metal complex is adsorbed on a substrate and then decomposed thermally so that atomically arranged nano-alloys can be formed. We have already demonstrated that Pt-Ru complexes are adsorbed on a gold(111) electrode surface in ordered manner and subsequent decomposition of the adsorbed species by heating followed by electrochemical treatment resulted in highly dispersed PtRu particles on the surface with remarkably high electrocatalytic activity for methanol oxidation.¹⁾



Fig. 1. Scheme for rational design of catalytic electrodes for advanced fuel cell systems by using microfabrication techniques.

This year we have extended this method for Pt-Ni systems. Despite their low noble metal contents, the Pt-Ni catalysts showed much higher activity for methanol oxidation.

Rational design of catalytic electrodes for advanced fuel cell systems by using microfabrication techniques (*e.g.*, lithography) are also investigated by arranging materials from atomic scale to macroscopic scale followed by modification of the surface of nanostructured conductive materials by chemical/electrochemical techniques as shown schematically in Fig. 1.

(2) *Photoenergy Conversion at Metal and Semiconductor Surfaces Modified with Ordered Molecular Layer.*

It is very important to produce hydrogen from water and form useful compounds by reducing CO₂ using solar energy.

Up-hill electron transfer is the basis of these processes. We have already achieved the visible light induced up-hill electron transfer at porphyrine-ferrocene thiol modified gold electrode with high quantum efficiency but low absorbance of porphyrine in near IR region makes the overall efficiency low. The performance of the system was substantially enhanced by the addition of gold nano particles, which acted as plasmonic photon-antennas as shown in Fig. 2.²⁾

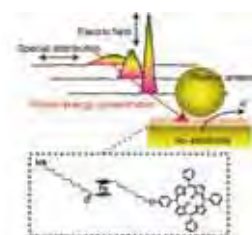


Fig. 2. Scheme for plasmonic enhancement of visible light induced up-hill electron transfer at gold electrode modified with porphyrine-ferrocene coupling molecule.

In situ XAFS measurements were performed to determine the structure of Pt complexes at various potentials and ligand exchange steps were clarified and structure of the catalyst when reaction took place was determined.

(3) *Experimental and Theoretical Investigations of Structure and Electron Transfer Processes at Solid/Liquid Interfaces.*

To construct interfacial phases for highly efficient energy/materials conversion, it is essential to have information on the structure and electron transfer dynamics at solid/liquid interfaces. This year we studied molecular structure of polymer brush on the solid surface in contact with various environments (dry nitrogen, water vapor, liquid water, and aqueous electrolyte solution) and it is demonstrated that molecular structures of both polymer brush and environments, *i.e.*, water, interactively change (Fig. 3).³⁾



Fig. 3. Environment dependent molecular structure of polymer brush on solid surface.

References

- 1) H. Uehara, Y. Okawa, Y. Sasaki and K. Uosaki, *Chem. Lett.* **38**, 148 (2009).
- 2) K. Ikeda, K. Takahashi, T. Masuda, and K. Uosaki, *Angew. Chem. Int. Ed.*, WEB published (2010) (Highlighted in the frontispiece in a February, 2011 issue).
- 3) K. Uosaki, H. Noguchi, R. Yamamoto, and S. Nihonyanagi, *J. Amer. Chem. Soc.* **132**, 17271 (2010).

Dye Sensitized Solar Cells

MANA Principal Investigator

MANA Scientist

MANA Research Associate

Liyuan HAN

Ashraful Islam, Masatoshi Yanagida,
Norifusa Satoh
Surya Prakash Singh, Shufang Zhang,
Saim Emin



1. Outline of Research

We aim to develop new and promising technologies for dye-sensitized solar cells, as alternatives to traditional silicon solar cells (DSCs). The main focus of our research here will be (Fig. 1)

- (1) understanding of key parameters determining the operation efficiency of the devices, such as electron transport properties and charge recombination process at the interfaces
- (2) development of new device structures
- (3) novel material synthesis based on understanding of the device mechanism.

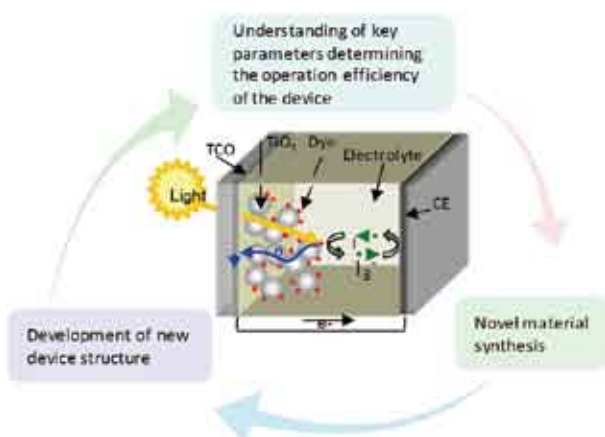


Fig. 1. Research and development feedback cycle.

2. Research Activities

(1) Tuning the HOMO energy level of Ru complexes.

The electrochemical properties of dye are one of the most important factors that influence the solar cell performance. In order to achieve efficient solar cell performance, the oxidation potential of dye (or HOMO) should be sufficiently positive; so that the neutral sensitizer can be regenerated via electron donation from the redox electrolyte. Five heteroleptic ruthenium complexes with different β -diketonato ligands have been synthesized (Fig. 2). These complexes exhibit a broad metal-to-ligand charge transfer absorption band across the whole visible range and into near 950 nm. The low-energy absorption bands and the E ($\text{Ru}^{3+/2+}$) oxidation potentials in these complexes could be tuned to about 15 nm and 110 mV, respectively, by choosing appropriate β -diketonate ligands. Under standard AM 1.5, the dye 1 yielded an overall conversion efficiency of 6.2%. A systematic tuning of HOMO energy level shows that an efficient sensitizer should possess a redox potential value of $> +0.53$ V vs. SCE.

(2) Scattering effect of rutile TiO_2 nanorods.

In general, large size of particles are added to TiO_2 film

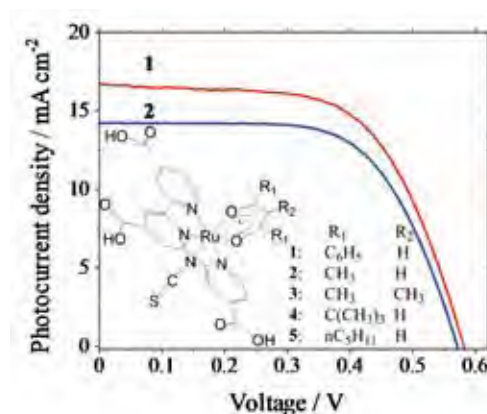


Fig. 2. Photocurrent voltage characteristics of DSCs sensitized with the complexes 1 and 2 at AM 1.5 illuminations (light intensities: 100 mW cm^{-2}). Inset shows the molecular structures of complexes 1-5.

to increase light scattering effect, which causes an enhancement of light-harvesting efficiency in DSCs. However, these large particles will lower dye uptake on TiO_2 film due to reduction of internal surface areas of the photoanode films. Here, rutile TiO_2 nanorods were in-situ synthesized in anatase TiO_2 nanocrystals (Fig. 3) because rutile TiO_2 of high refractive index is a good scattering material. The cell, with this mixing-phase TiO_2 shows higher IPCE at long wavelength (>600 nm) due to light scattering effect. Finally, conversion efficiency is improved because of enhanced short-circuit photocurrent.

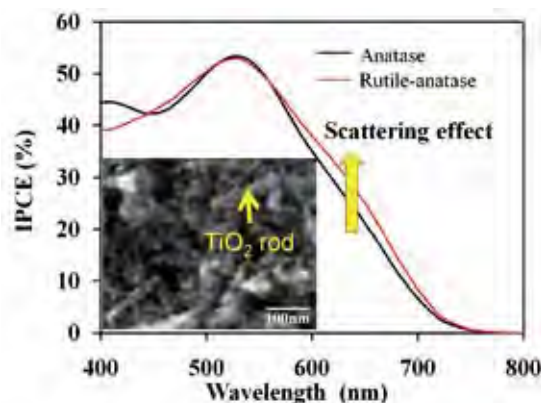


Fig. 3. IPCE spectra of the DSCs based on anatase and rutile-anatase TiO_2 film. Inset: FE-SEM image of rutile-anatase film.

References

- 1) S. Gao, A. Islam, Y. Numata, L. Han, *Appl. Phys. Exp.* **3**, 062301 (2010).
- 2) A. Islam, L.P. Singh, M. Yanagida., L. Han, *Int. J. Photoenergy*, in press (2010).
- 3) W.Q. Peng, M. Yanagida, L. Han, *J. Nonlinear Optical Phys. Mater.*, in press (2010).

Solid State Batteries

MANA Principal Investigator

MANA Scientist
MANA Research Associate

Kazunori TAKADA

Tsuyoshi Ohnishi
Taeri Kwon



1. Outline of Research

Lithium batteries have been powering portable electronics including cellular phones and note PC's for 20 years. In addition, now they are expected to play new roles for the realization of a low-carbon society as power sources in electric vehicles and energy storage device in smart grids. However, the safety issue arising from their combustible organic electrolytes remains unsolved.

Solid electrolytes will make a breakthrough due to their non-flammability. In addition, single-ion conduction in solid electrolytes will effectively suppress the side reaction deteriorating battery performance. These features will pave the way to next-generation batteries. Our goal is to realize all-solid-state lithium batteries through the researches on ionic conduction in solids.

2. Research Activities

(1) Nanoionics at oxide cathode and sulfide solid electrolyte interface.

Ionic conductors often show anomalous ionic conduction at their surface or interface, which is categorized into "nanoionics". Nanoionics takes place in space-charge layers originated from different electrochemical potentials of the mobile ions at the hetero-interfaces. Since high electromotive force of lithium batteries comes from large difference of the electrochemical potential between the electrodes, nanoionics will be prominent in lithium systems.

Our previous study revealed that space-charge layer formed on the electrolyte side at LiCoO₂/sulfide solid electrolyte interface is lithium-depleted and thus highly-resistive to be rate-determining, which can be eliminated by interposition of oxide solid electrolyte.¹⁻³⁾ In order to verify this scenario, interfacial phenomena on LiMn₂O₄ surface were investigated.

Interposition of LiNbO₃ also decreased the interfacial resistance at the LiMn₂O₄ electrode by two orders of magnitude, as shown in Fig. 1. In addition, change in the electrode properties was very similar to that observed for LiCoO₂. These results strongly suggest the validity of the scenario: the interfacial phenomena are universal among the interfaces between 4 V cathodes and sulfide electrolytes.

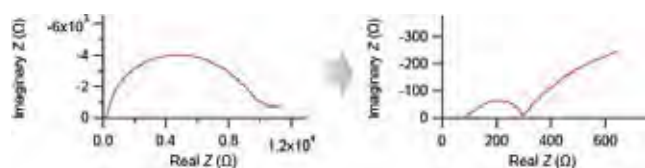


Fig. 1. Change in impedance of LiMn₂O₄ electrode by the interposition of LiNbO₃.

(2) Epitaxial growth of lithium battery materials.

Although the importance of nanoionics has been recognized, studies on interfacial ionic conduction are still in the pioneering stage. Studies on ion-conducting ceramics have been done mainly using polycrystalline samples. Since there are many non-uniform interfaces including grain boundaries in the polycrystalline samples, it is quite difficult to clarify the interfacial phenomena. In order to know what happens at the interface, we need well-defined interface, which can be obtained between single-crystal ionic conductors. Therefore, we are studying epitaxial growth of battery materials.

In 2010, we studied epitaxial growth of LiCoO₂, which has been used as cathode material in lithium-ion batteries, by pulsed-laser deposition. We investigated the deposition condition including ablation condition, substrate temperature, and oxygen pressure and found out that the film quality strongly depends on the deposition condition, for instance, as shown in Fig. 2.⁴⁾ LiCoO₂ film obtained under the optimized condition has high purity, high crystallinity, and atomically-flat surface.

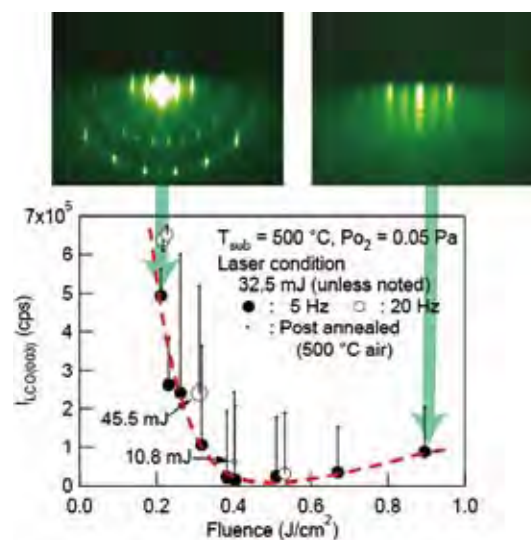


Fig. 2. Relationship between the quality of the LiCoO₂ films and the laser fluence.

References

- 1) N. Ohta, K. Takada, L. Zhang, R. Ma, M. Osada, T. Sasaki, *Adv. Mater.* **18**, 2226 (2006).
- 2) N. Ohta, K. Takada, I. Sakaguchi, L. Zhang, R. Ma, K. Fukuda, M. Osada, T. Sasaki, *Electrochem. Commun.* **9**, 1486 (2007).
- 3) K. Takada, N. Ohta, L. Zhang, K. Fukuda, I. Sakaguchi, R. Ma, M. Osada, T. Sasaki, *Solid State Ionics* **179**, 1333 (2008).
- 4) T. Ohnishi, B. T. Hang, X. Xu, M. Osada, K. Takada, *J. Mater. Res.* **25**, 1886 (2010).

Nanostructured Materials for Solid Oxide Fuel Cells and Sustainable Development

MANA Principal Investigator

MANA Scientist
MANA Research Associate

Enrico TRAVERSA

Emiliana Fabbri, Tamaki Naganuma, Daniele Pergolesi
Lei Bi, Corrado Mandoli, Ziqi Sun, Marco Fronzi,
Rohit Khanna, Shobit Omar



1. Outline of Research

World population raise and the need for improving the quality of life of a still large percentage of human beings are the driving forces for searching alternative, sustainable energy production systems. The main goal of the MANA research project is the fabrication of μ -SOFC devices¹⁾ based on oxide proton conducting electrolytes,²⁾ through the understanding of nanostructured materials performance as single component or in assemblies. Pulsed laser deposition (PLD) is used for fabricating tailored oxide thin films for SOFCs. The focus is on chemically stable high temperature proton conductors (HTPCs), such as Y-doped barium zirconate (BZY). Electrode materials are studied to improve the performance of fuel cells, based on developing mixed proton-electronic conductors.³⁾

In a global view of exploiting nanomaterials for a sustainable development, interdisciplinary research is also pursued in the biomedical field. Population aging affects sustainable development, since healthcare treatments are needed to improve elder people quality of life. For this aim, nanomaterials are investigated for therapies.

2. Research Activities

Our research activities can be summarized as follows:

- Thin film electrolytes for μ -SOFCs⁴⁻⁶⁾ and ionic conducting superlattices⁷⁻⁸⁾, deposited by PLD.
- Development of chemically stable materials for HTPC electrolytes (Fig. 1).⁹⁻¹³⁾
- Development of new cathode materials with low area specific resistance at low temperatures.¹⁴⁻¹⁵⁾
- Design of highly porous 3D scaffolds for soft tissue engineering.¹⁶⁻¹⁸⁾
- Potential therapeutic use of ceria nanoparticles.¹⁹⁾

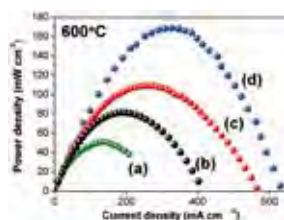


Fig. 1. Comparison between the power density outputs obtained at 600°C for BZY20-based SOFCs: using a novel sinteractive anode¹¹⁾ (a), using Pr-co-doped BZY20 electrolyte¹⁰⁾ (b), fabricating dense BZY20 thin membranes by PLD⁹⁾ (c), and using the ionic-diffusion method¹²⁾ (d).

(1) High Proton Conduction in Grain Boundary Free BZY Films Grown by PLD.⁴⁾

Grain-boundary free thin films of BZY ($\text{BaZr}_{0.8}\text{Y}_{0.2}\text{O}_{3-\delta}$), deposited on MgO single crystal substrates, showed the largest proton conductivity ever reported for any oxide material at 350°C, 0.01 S cm^{-1} (Fig. 2). The excellent crystalline order of BZY films allowed for the first time the experimental measurement of the large BZY bulk conducting properties above 300°C, expected in the absence of blocking grain boundaries.

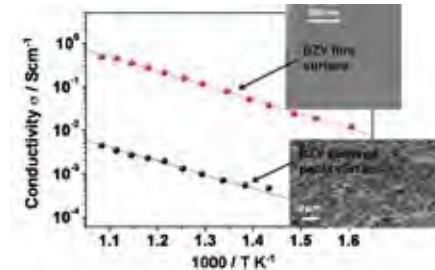


Fig. 2. Proton conductivity of the BZY20 film and sintered pellet. The insets show the SEM micrographs of the surface of the BZY20 film (top) and of the BZY20 pellet (bottom).

(2) Cooperation of Biological and Mechanical Signals in Cardiac Progenitor Cell (CPC) Differentiation.¹⁸⁾

3D cardiac tissue-specific scaffolds made of PLA with an ordered array of square pores reproduced anisotropic cardiac-like stiffness (Fig. 3). Adult murine CPC differentiation into cardiac phenotype was induced within few days by the cooperation of biological and mechanical stimuli, which emulates *in vitro* the cardiac niche.

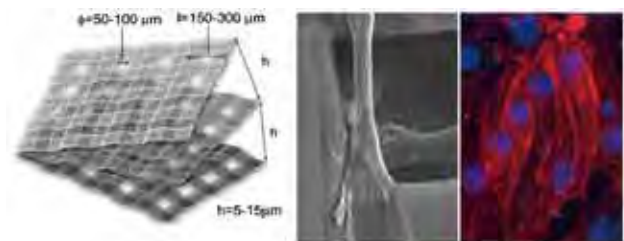


Fig. 3. Exploded view of the 3D biodegradable scaffold made of PLA (left). SEM micrograph of a CPC stretched bridging over the pore window (center). An immuno-fluorescence microscope image showing cell nuclei (blue) and cytoskeletal sarcomeres (red) of fully differentiated CPCs over the 3D scaffold (right).

References

- E. Traversa, *Interface* **18**, 49 (2009).
- E. Fabbri, D. Pergolesi, E. Traversa, *Chem. Soc. Rev.* **39**, 4355 (2010).
- E. Fabbri, D. Pergolesi, E. Traversa, *Sci. Technol. Adv. Mater.* **11**, 044301 (2010).
- D. Pergolesi et al., *Nature Mater.* **9**, 846 (2010).
- E. Fabbri et al., *Energy Environ. Sci.* **3**, 618 (2010).
- D. Pergolesi et al., *Electrochem. Comm.* **12**, 977 (2010).
- S. Sanna et al., *Small* **6**, 1863 (2010).
- E. Fabbri, D. Pergolesi, E. Traversa, *Sci. Technol. Adv. Mater.* **11**, 054503 (2010).
- E. Fabbri et al., *Solid State Ionics* **181**, 1043 (2010).
- E. Fabbri et al., *Adv. Funct. Mater.* **21**, 158 (2011).
- L. Bi et al., *Energy Environ. Sci.*, (DOI: 10.1039/C0EE00387E).
- L. Bi et al., *Energy Environ. Sci.*, (DOI: 10.1039/C0EE00353K).
- Z. Sun et al., *PCCP*, (DOI: 10.1039/C0CP01470B).
- E. Magnone, M. Miyayama, E. Traversa, *J. Electrochem. Soc.* **157**, B357 (2010); *J. Electroceram.* **24**, 122 (2010).
- C. Abate et al., *J. Am. Ceram. Soc.* **93**, 1970 (2010).
- C. Mandoli et al., *Macromol. Biosci.* **10**, 127 (2010).
- S. Soliman et al., *Acta Biomater.* **6**, 1227 (2010).
- S. Pagliari et al., *Adv. Mater.*, (DOI: 10.1002/adma.201003479).
- C. Mandoli et al., *Adv. Funct. Mater.* **20**, 1617 (2010).

Reticular Materials

MANA Principal Investigator

MANA Researcher
MANA Research Associate

Omar M. YAGHI

Kentarō Tashiro
Pothenappan Vairaprakash, Hisanori Ueki,
Alejandro M. Fracaroli

1. Outline of Research

The synthesis of mononuclear metal complexes by design is a well-established process. In sharp contrast, however, a protocol for the synthesis of complexes containing multiple homo- or hetero-metals, in a designed fashion, remains largely absent so far, where it is inevitable to get a mixture of products with respect to the number, nuclearity, or sequence of metal centers. In this project, we are aiming to develop a conceptually new synthetic methodology to create metal complex arrays with controlled number, nuclearity, or sequence of metal centers (Fig. 1). This methodology will open a new era of metal complex-based materials science by producing multimetallic systems that are inaccessible via traditional synthetic methodologies. Especially, the controlled sequence of metal centers in the arrays, like those in proteins and nucleic acids, will be the most attractive characteristics of this type of materials. Moreover, since our methodology is potentially extendable to automated, parallel processes, high-throughput preparation of the libraries of metal complex arrays will be expected. By taking advantage of such features, we will, in the next step, challenge to create catalysts having extraordinary high and unique activity, selectivity, and tunability, which should make a great contribution to realize our future sustainable life.

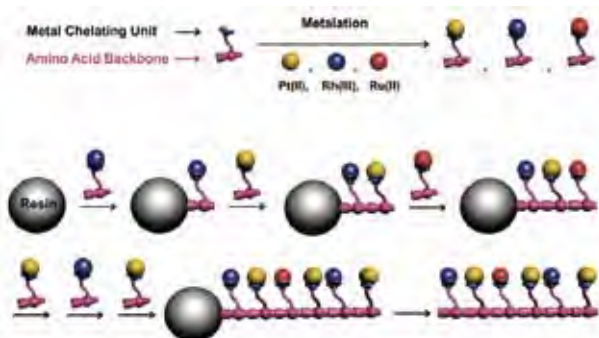


Fig. 1. Solid-phase synthesis of metal-organic complex arrays.

2. Research Activities

(1) Synthesis of a Series of Metal-Organic Complex Arrays via Merrifield Solid-Phase Peptide Synthesis.¹⁾

Merrifield solid-phase peptide synthesis is a well-established synthetic technique for polypeptides, where the order in which the amino acids are added determines their sequence in the product. By taking advantage of the consecutive nature of this procedure, we have successfully produced heterometallic dyad, triad, tetrad, pentad, and hexad complexes (Fig. 2).

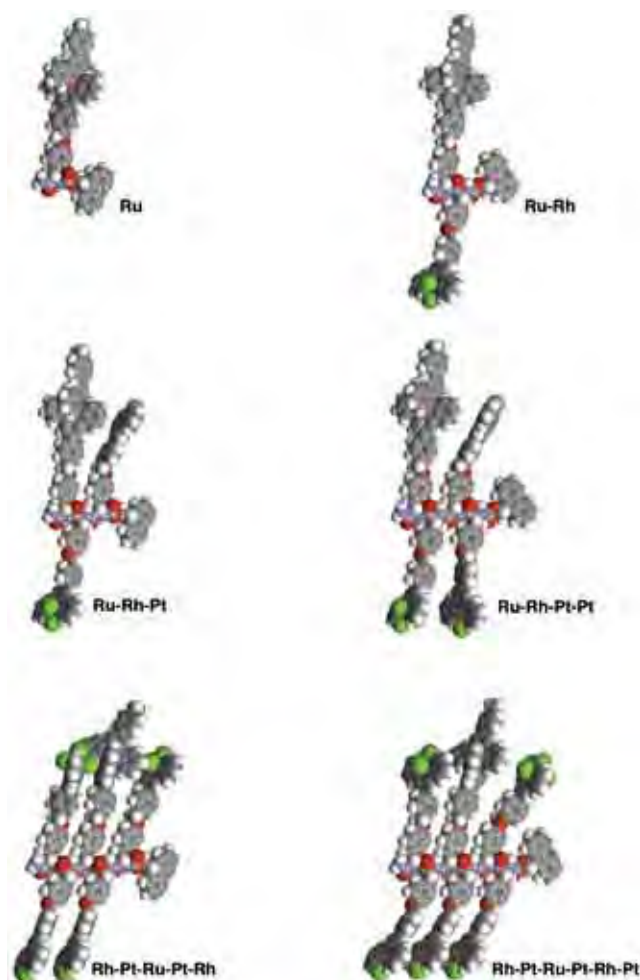


Fig. 2. Molecular structures of metal-organic complex arrays.

(2) Demonstration of Sequence Control.¹⁾

It was critical to confirm that no metal exchange took place during the full reaction workup procedures. Any metal exchange would give unexpected sequences with disproportionate relative metal-to-metal content. We confirmed the absence of metal exchange activity in the metal complex monomers on the basis of the fact that ¹H NMR spectra of mixtures containing one of the monomers and another terpyridine ligand that were kept standing for 2 days at 25 °C showed no resonances to the demetalated ligand. We also confirmed that no other sequences with unexpected metal content were detected by mass spectroscopy of the products as-cleaved from the polymeric resins.

Reference

1) P. Vairaprakash, H. Ueki, K. Tashiro, O.M. Yaghi, *JACS*, published on the WEB <http://pubs.acs.org/doi/pdf/10.1021/ja1097644>.

Nanoarchitectonics of Hybrid Artificial Photosynthetic System

MANA Principal Investigator

MANA Research Associate
Graduate Student

Jinhua YE

Y. Bi, H. Tong, M. Amina,
X. Chen, J. Cao, B. Yue, M. Zhang, P. Li



1. Outline of Research

Fundamental research and development of artificial photosynthesis technology comprising of nano-structured metal/inorganic/organic semiconductor hybrid system will be conducted. Special attention will be paid to the design of new nano semiconductor materials harvesting major part of solar light, understanding of interactions between photon, carrier, molecules, and manipulation of these interactions for realization of higher photon efficiency by nanoarchitectonics. A breakthrough in the efficiency of solar-chemical energy conversion is expected.

In order to accomplish this purpose, we set following four sub-themes and are conducting the materials exploration research effectively by organically coordinating these sub-themes (Fig. 1):

1) Design and fabrication of new semiconductors which can utilize solar energy sufficiently by energy band structure engineering, with the help of theoretical calculation basing on the first principle theory. Engineering of band gap as well as CB, VB potentials will be carried out simultaneously to meet the potential requirement of photosynthetic reaction.

2) Nanoarchitectonics of the photosynthesis system will be conducted, by not only fabrication of nano particles using various soft chemical method, but also assembling of nano-metal/nano-oxide hybridized system to achieve efficient transportation and separation of electron-hole charge carriers.

3) Evaluation of photon efficiency in various reactions will be performed using a solar-simulator and various gas chromatography.

4) Photosynthetic mechanism will be investigated experimentally and theoretically, to establish guidelines for development of higher efficient system.

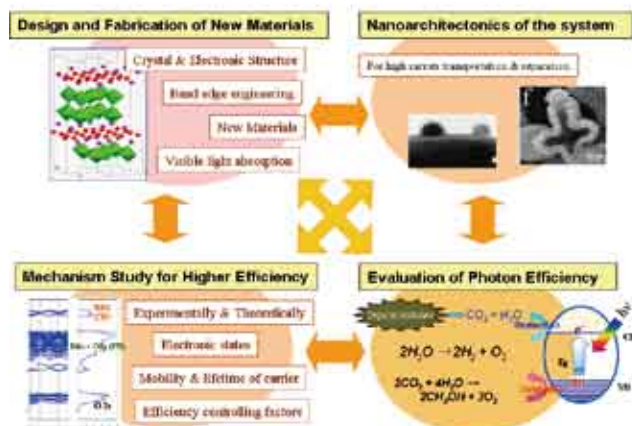


Fig. 1. Four sub-themes and their organic coordination for conducting effective materials exploration research.

2. Research Activities

(1) A photo-active material Ag_3PO_4 with world-highest efficiency.¹⁾

The new material was developed by incorporating p block element into a simple AgO oxide with narrow band gap. The new photocatalyst showed extremely high quantum yield (~90% at 420 nm) towards water oxidation as well as organic contaminates decomposition under visible light. This study not only supplies a new strategy for developing visible-light-driven photocatalysts, but also shows a great step towards the realization of an artificial photosynthetic system.

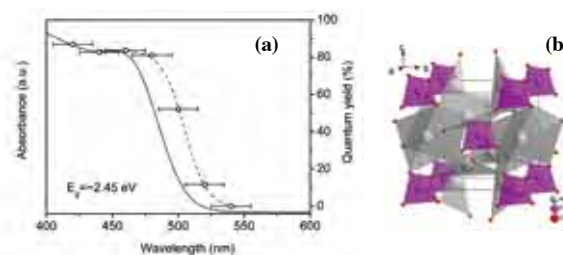


Fig. 2. (a) UV-vis diffuse reflectance spectrum and apparent quantum yields and (b) Crystal structure of Ag_3PO_4 .

(2) New photocatalysts converting CO_2 into CH_4 fuel.^{2,3)}

We have developed a room-temperature synthesis of mesoporous $ZnGa_2O_4$ via a cation exchange reaction between $Zn(CH_3COO)_2$ and “reactive-template” $NaGaO_2$ -based hydrate. Such prepared mesoporous $ZnGa_2O_4$ showed enhanced photoactivity for converting CO_2 into CH_4 fuel in contrast to the sample prepared by solid state route, since large specific surface area of the mesoporous photocatalyst are beneficial to CO_2 capture and conversion.

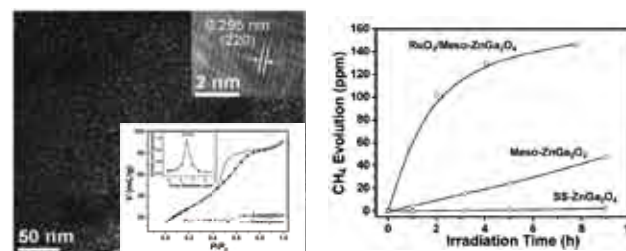


Fig. 3. (left) Mesoporous structure of $ZnGa_2O_4$; (right) Photocatalytic conversion of CO_2 to CH_4 over various $ZnGa_2O_4$ samples.

References

- 1) Zhiguo Yi, Jinhua Ye, Naoki Kikugawa, Tetsuya Kako, Shuxin Ouyang, et al., *Nature Mater.* **9**, 559 (2010).
- 2) S.C. Yan, S.X. Ouyang, J. Gao, M. Yang, J.Y. Feng, X.X. Fan, L.J. Wan, Z.S. Li, J.H. Ye, et al., *Angew. Chemie* **49**, 6400 (2010).
- 3) Ning Zhang, Shuxin Ouyang, Peng Li, Yuanjian Zhang, Guangcheng Xi, Tetsuya Kako, and Jinhua Ye, *Chem. Commun.* DOI: 10.1039/C0CC04687F

Smart Nano-Biomaterials

MANA Principal Investigator Takao AOYAGI

(Field Coordinator)
MANA Scientist
Graduate Student

Mitsuhiro Ebara
Yohei Kotsuchibashi



1. Outline of Research

Our research group is interested in developing ‘smart’ biotechnologies using stimuli-responsive polymers that respond to small changes in external stimuli with large discontinuous changes in their physical properties. These ‘smart’ biomaterials are designed to act as an “on-off” switch for drug delivery technologies, gene therapy, affinity separations, chromatography, diagnostics etc.

Poly(N-isopropylacrylamide) is one of the typical thermo-responsive materials and much attention is attracting in nanobio-field. To obtain poly(N-isopropylacrylamide)-based functional materials, we newly designed functional monomers (see Fig. 1). The monomers are simple derivatives of N-isopropylacrylamide, which have specific functional groups on the isopropyl group. The simple reaction of acryloyl chloride and functional compounds such as amino-acid, amino-alcohol derived to the corresponding monomers. The resulting copolymers contain comonomer random sequences based on very similar copolymerization reactivity, as well as show both the good chemical reactivity and nice stimuli-response. Such series of functional monomers surely are very useful for smart biomaterials that can be applied to nano-bio field.

Moreover, we are very interested in the nanostructure design to create smart biomaterials. Nano fibers, nanoparticles, nano assembly, hydrogel and so on are our research target.



Fig. 1. Schematic representation of coil-globule transition of poly(N-isopropylacrylamide).

2. Research Activities

Here, we show the double thermo-responsive block copolymer aiming at effective targeted drug delivery.

To achieve this purpose, we synthesized the block copolymers applying an atom transfer radical polymerization (abbreviated as ATRP). The block copolymer is comprising two segments (blocks), which have two different lower critical solution temperature (abbreviated as LCST).

As seen in Fig. 2, in cold condition that is below first LCST, the block copolymer is completely soluble in aqueous milieu. Increasing the solution temperature, between first and second LCST, they form the micelle-like associates and are very useful to reserve drug molecules

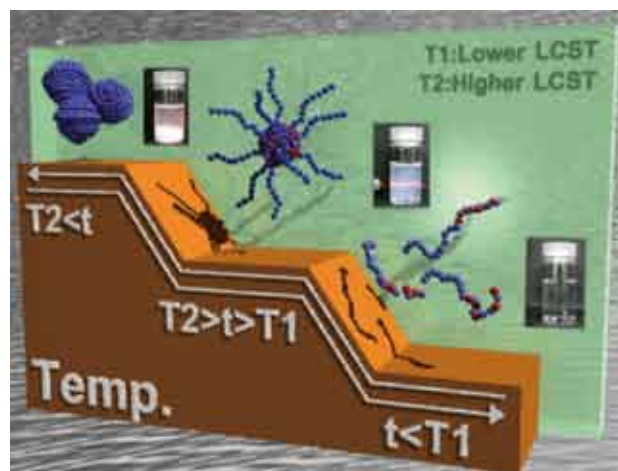


Fig. 2. Concept of association of double thermo-responsive block copolymer.

in the core phase. In hot condition that is above second LCST, the outer polymer chains that form shell structure also shrink and eventually they form the aggregates. The unstable structure would improve the drug release form the core phase. Actually, we prepared Poly(N-isopropylacrylamide)-b-(Poly(N-isopropylacrylamide-co-N-butoxymethylacrylamide) (abbreviated as PNbP(NcoB)) and the thermo-responsive behavior was shown in Fig. 3.

Consequently, the block copolymer is very useful component to fabricate practicable nano-sized drug carrier for targeted drug delivery. Combination with local heating would enhance the efficiency of anti-cancer drug by hyperthermia effect and local drug release by remote control from outside of body.

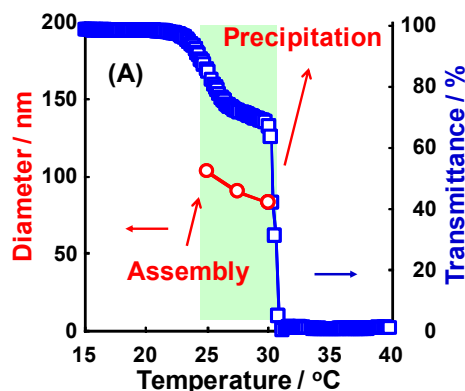


Fig. 3. Thermo-responsive behavior of PNbP(NcoB).

Reference

1) Y. Kotsuchibashi, M. Ebara, K. Yamamoto, T. Aoyagi, *J. Polym. Sci. Part A* **48**, 4393 (2010).

PEGylated Polymer Micelle-Based Nitric Oxide (NO) Photodonor with NO-Mediated Antitumor Activity

MANA Principal Investigator **Yukio NAGASAKI**

(Satellite at Univ. Tsukuba, Japan)

MANA Scientist
Graduate Student

Naoki Kanayama
Kazuhiro Yamaguchi



1. Outline of Research

The objective of our research is to create new biomaterials. Nitrogen oxide is known to play versatile roles *in vivo*. Excessive NO generation reported to cause antitumor effect *in vivo*. We started to design new polymer micelle based NO-photodonor for novel anticancer chemotherapy (Fig. 1). PEGylated polymer micelles containing 4-nitro-3-trifluoromethylphenyl units within the core moiety were prepared, and their photo-triggered nitric oxide (NO)-generating ability was confirmed by electron spin resonance (ESR) spin-trapping and the Griess method. These micelles were found to be able to deliver exogenous NO into tumor cells in a photo-controlled manner and showed an NO-mediated antitumor effect, indicating the usability of this molecular system in NO-based tumor therapy.

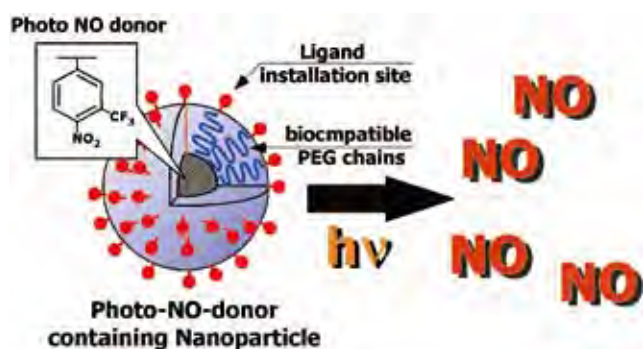


Fig. 1. Schematic illustration of polymeric micelle based NO-photodonor for novel anti-tumor chemotherapy.

2. Research Activities

Photo-triggered NO generation from the micelles was first tested by electron spin resonance (ESR) spin-trapping using *N*-methyl-D-glucamine dithiocarbamate complex ($(\text{MGD})_2\text{-Fe}^{2+}$), which reacts with NO to give a stable paramagnetic complex, $(\text{MGD})_2\text{-Fe}^{2+}\text{-NO}$. A freshly prepared $(\text{MGD})_2\text{-Fe}^{2+}$ complex solution and the NO-micelles were mixed in a quartz cell (molar ratio: $[(\text{MGD})_2\text{-Fe}^{2+}]/[\text{NTP unit}] = 20$), after which the mixed solution was irradiated for 1 h. Before irradiation, the mixed solution showed no significant peak in the ESR spectrum, while the appearance of characteristic peaks corresponding to the formation of the paramagnetic $(\text{MGD})_2\text{-Fe}^{2+}\text{-NO}$ complex was observed after irradiation. This indicates the photo-triggered NO generation from the NO-micelles. Though NO is rather hydrophobic character, it might be released from the NO-micelles through the PEG outer layer due to the high mobility of gaseous NO.

In order to assess the photo-induced NO-mediated antitumor effect of the ND micelles, *in vitro* examination

was performed using HeLa cells. Fig. 2a shows the change in the viability of HeLa cells as a function of the concentration of NO-micelles. Without UV light irradiation, the NO-micelles showed a relatively lower cytotoxicity, and the 50% inhibitory concentration (IC_{50}) was found to be 4.9 mg mL^{-1} . This might be due to the existence of the biocompatible PEG outer layer at the surface of the NO-micelles. Upon UV light irradiation, the cytotoxicity of the NO-micelles was enhanced with the increase in irradiation time, and a significant decrease in the IC_{50} value of the ND micelles was confirmed (after 3-min irradiation (6.12 J cm^{-2}) $\text{IC}_{50} = 1.9 \text{ mg mL}^{-1}$, after 10-min irradiation (20.4 J cm^{-2}) $\text{IC}_{50} = 0.2 \text{ mg mL}^{-1}$). It should be noted that the fluence of the UV light employed in this experiment did not affect the viability of HeLa cells in the absence of NO-micelles (Fig. 2b), indicating that the photo-induced enhancement of the cytotoxicity of the NO-micelles was caused by the photoproducts, NO and polymer-bonded oxyl radicals. Oxyl radical and its degradation products are known to exhibit no significant cytotoxicity, which strongly emphasize that the liberated NO works mainly to an antitumor effect in a photo-controlled manner.

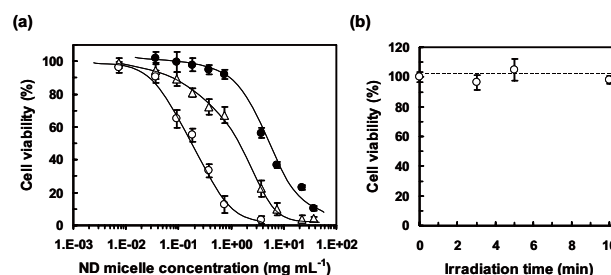


Fig. 2. (a) Viability of HeLa cells treated with NO-micelles at various concentrations with (open symbol) or without (filled circle) UV light irradiation. The plotted data are averages of five experiments \pm SD. (b) Viability of HeLa cells without NO-micelle treatment after UV light irradiation. The plotted data are averages of five experiments \pm SD.

In conclusion, we demonstrated the photo-controlled delivery of exogenous NO into target cells using a PEGylated polymer micelle containing NO photogenerative units within the core moiety. The amount of generated exogenous NO was confirmed to be sufficiently high to induce an antitumor effect, indicating the usability of this molecular system for NO-based tumor therapy. Finally, we wish to emphasize that the main objective of this study was to verify the effectiveness of a PEGylated polymer micelle-based NO photodonor system for tumor treatment. Further studies which address this issue, among others, are underway and the results will be reported elsewhere.

Laser-Based Inelastic Photoemission Spectroscopy

MANA Independent Scientist **Ryuichi ARAFUNE**



1. Outline of Research

My main objective is to explore and elucidate some aspects of the interaction between light and matter that take place uniquely at the solid surfaces. Currently, we concentrate on developing laser-photoemission spectroscopy (PES) into a novel technique to probe surface dynamics. Vibrational dynamics of adsorbate-substrate modes of adsorbed atoms and molecules can yield direct information on the nature of the bonding with the surface and on the energy exchange between the adsorbate and the substrate. Such modes appear at low-energy region (<100 meV). Unfortunately, no time-resolved surface vibrational technique that is applicable to low-energy vibrational modes has been developed thus far. Thus, a novel technique that can access such low energy vibrational modes is highly demanded.

Recently, we found that the photoemission spectra excited by the laser light contained the vibrationally induced inelastic components.¹⁾ This result indicates that the laser-excited and low-energy photoelectron strongly interacts with vibrational elementary excitations. We believe that this inelastic interaction has potentiality for measuring the dynamics of the electron-vibration interaction. The aim of this research project is the development of a novel PES and measurement of the vibrational dynamics (including the charge transport property) at solid surfaces. By measuring low energy photoelectron spectra of surfaces excited by the pulse laser light whose energy is tuned slightly higher than the work function of the solid surface, we will elucidate some aspects of the dynamic interactions between low-energy electrons and surface elementary excitations. This technique enables us to investigate vibrational and electronic dynamics of adsorbate on solid surfaces in the time range of picoseconds to femtoseconds.

2. Research Activities

(1) Mechanism of inelastic photoemission process.

It is prerequisite to elucidate the mechanism of the inelastic photoemission when one applies this technique to reveal surface vibrational dynamics. By using laser PES, we have investigated inelastic interaction between phonon modes (including vibrational modes of adsorbates) and photoelectron emitted from the solid surfaces. The laser PES spectra of the clean and oxidized Cu(110) as well as that of the oxidized Cu(001) contained the step structure arising from the phonon excitation, whereas the spectrum of the Cu(001) was determined by just using the electronic density of states and the Fermi-Dirac distribution (Fig. 1). The selective excitation of the phonon modes suggests that some selection rules operate in the inelastic photoemission spectroscopy. By analyzing the spectra, two propensity rules were obtained. One requires the wave vector matching between the phonon mode and the electron in the photoexcited state on the surface. Additionally, the polarization of the atomic motion within the surface or adsorbate, which interacts inelastically during LPE, must lie parallel to the surface plane. These results imply that the inelastic interaction during laser photoemission process arises dominantly from the resonance scattering and not from the dipole one.

(2) Two-photon photoemission.

One of the next directions of the application of this technique is monitoring surface relaxation processes after photoexcitation through the vibration states by means of the pump-probe method. In the pump-probe experiments, it is important to expose the sample to the pump and probe light pulses simultaneously. The precision of the overlapping two pulses determines the temporal resolution. Non-linear effect is useful for checking simultaneity because of high sensitivity to temporal overlapping between two pulses. Accordingly, to gain expertise on nonlinear effect in the laser photoemission experiments and further to explore dynamic phenomena at the solid surface, we have started a new line of research, which is two-photon photoemission, from the latter half of this year. At present, we have only preliminary data for the Cu(110) surface. They suggest unoccupied states which have not been detected by inverse photoemission spectroscopy are available at this surface.

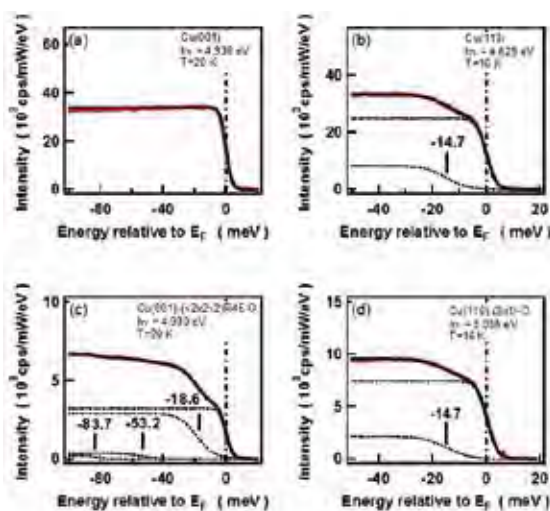


Fig. 1. Laser-PES of clean and oxidized Cu(110) and Cu(001) surfaces.

Reference

- 1) R. Arafune *et al.*, *Phys. Rev. Lett.* **95**, 207601 (2005).

Search for New Ferroelectric, Magnetic and Multiferroic Materials using High-Pressure Technique

MANA Independent Scientist Alexei A. BELIK



1. Outline of Research

In multiferroic systems, two or all three of (anti)ferroelectricity, (anti)ferromagnetism, and ferroelasticity are observed in the same phase. These systems may have wide technological applications because they allow control of electric properties by magnetic field and control of magnetic properties by electric field (Fig. 1). The application would include, for example, multiple-state memory elements. Multiferroic materials have been studied in the past, but those studies did not attract wide attention most probably due to the lack of materials with strong magnetoelectric coupling and high ordering temperatures. Multiferroics have experienced revival interest and return to the forefront of condensed matter and materials research in the recent years because of the advanced preparation and characterization techniques. However in the field of multiferroic materials, two major problems still remain: (1) preparation of materials with multiferroic properties at and above room temperature (RT) and (2) preparation of materials with strong coupling between different order parameters.

Materials with a perovskite-type structure are of great interest in many fields of science and technology. Their applications range from the use as catalysts or sensors to superconductors, ferromagnetic, or ferroelectric materials. A new interest appeared recently for perovskite RCrO_3 and RMnO_3 as multiferroic materials.

We aim to develop new room-temperature multiferroic materials based on the perovskite-type structure using advanced high-pressure synthetic technique. We expect to find and develop new environmentally friendly lead-free materials with ferroelectric and multiferroic properties which will have superior properties compared with the known materials. The most attractive application of these materials is in non-volatile ferroelectric random access memory (FeRAM) elements.

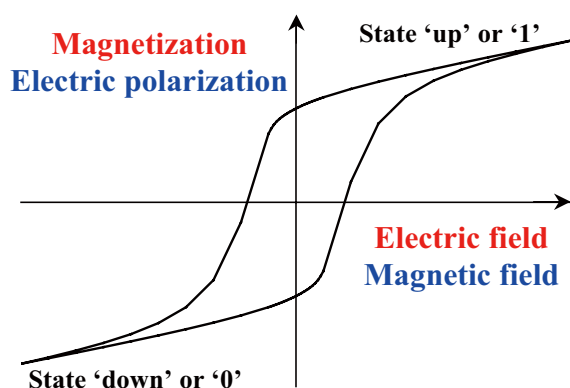


Fig. 1. Ferroelectric/ferromagnetic hysteresis loop: the basis of many memory elements.

2. Research Activities

(1) *Development of new near-room-temperature multiferroics and In-containing perovskites.*^{1,2)}

Using high pressure, we could prepared new perovskite materials $(\text{In}_{1-x}\text{M}_x)\text{MO}_3$ ($\text{M} = \text{Mn}$ and $\text{Mn}_{0.5}\text{Fe}_{0.5}$). They turned to be multiferroics possessing spontaneous polarization and magnetism near room temperature. $(\text{In}_{1-x}\text{Mn}_x)\text{MnO}_3$ is quite unusual because it contains Mn^{2+} ions at the A perovskite site, and ordered Mn^{3+} and Mn^{4+} ions at the B perovskite site.

(2) *Investigation of effects of the oxygen content on structural and physical properties of multiferroic BiMnO_3 .*³⁾

Ferroelectric properties of BiMnO_3 are still controversial. In these studies, we tried to understand effects of the oxygen content on structural and magnetic properties of $\text{BiMO}_{3+\delta}$. In $\text{BiMnO}_{3+\delta}$, the change of δ results in changes from ferromagnetic insulators to a spin-glass insulator; crystal structures change from $C2/c(\text{I})$ to $C2/c(\text{II})$ to $Pnma(\text{II})$.

(3) *Discovery of a new semiconducting ferromagnet $\text{Bi}_3\text{Mn}_3\text{O}_{11.6}$ with the highest T_c .*⁴⁾

We investigated effects of the oxygen content on $\text{Bi}_3\text{Mn}_3\text{O}_{11+\delta}$ that can be prepared at high pressure. These phases show interesting magnetic properties. In particular, we found that $\text{Bi}_3\text{Mn}_3\text{O}_{11.6}$ shows the highest ferromagnetic transition temperature for semiconducting ferromagnet materials (Fig. 2).

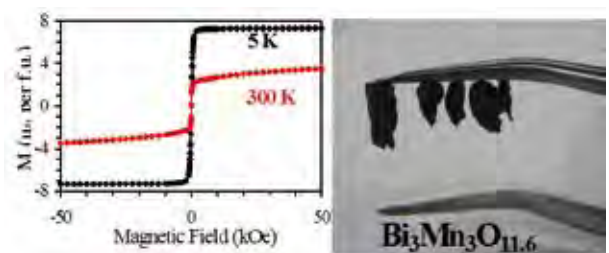


Fig. 2. Isothermal magnetization curves for $\text{Bi}_3\text{Mn}_3\text{O}_{11.6}$ at 5 and 300 K, and pieces of the sample attached to magnetized tweezers at room temperature.

References

- 1) A.A. Belik, T. Furubayashi, Y. Matsushita, M. Tanaka, S. Hishita, E. Takayama-Muromachi, *Angew. Chem. Int. Ed.* **48**, 6117 (2009).
- 2) A.A. Belik, Y. Matsushita, M. Tanaka, E. Takayama-Muromachi, *Angew. Chem. Int. Ed.* **49**, 7723 (2010).
- 3) A.A. Belik, K. Kodama, N. Igawa, S. Shamoto, K. Kosuda, E. Takayama-Muromachi, *J. Am. Chem. Soc.* **132**, 8137 (2010).
- 4) A.A. Belik, E. Takayama-Muromachi, *J. Am. Chem. Soc.* **132**, 12426 (2010).

Next-Generation Semiconductor Nanomaterials and Nanodevices

MANA Independent Scientist Naoki FUKATA



1. Outline of Research

Technical progress in silicon integrated circuits (Si VLSI) has, up to the present time, been driven by the miniaturization, or scaling, of gates, oxide layers, p-n junctions, substrates, and other elements in metal-oxide semiconductor field-effect transistors (MOSFETs), which are the building blocks of VLSI. Advances in performance and integration through conventional scaling of device geometries are, however, now reaching their practical limits in planar MOSFETs. To overcome the limiting factors in planar MOSFETs, vertical structural arrangements using semiconductor nanowires have been suggested as the basis for next-generation semiconductor devices.

In order to realize the next-generation vertical-type MOSFETs, it is indispensable to develop characterization methods and to investigate the site, distribution, bonding states, and electrical activity of dopant impurities in NWs. Recently, I could experimentally succeed in detecting the

dopant impurities (B and P) and clarify their bonding and electrical states in SiNWs and GeNWs with diameters less than 20 nm by micro-Raman scattering and electron spin resonance methods. These results are noteworthy because these are the first experimental results for SiNWs and GeNWs. Now I stand at the forefront in area of study about the detection and the characterization of dopant impurities in SiNWs.

2. Research Activities

(1) Effect of doping for growth of GeNWs.

The growth of high quality semiconductor nanowires is considered to be a key point for the study of next-generation vertical-type MOSFETs. In order to grow defect-free GeNWs with uniform diameter, I applied the UHV-CVD method this time (Fig. 1). I also performed in-situ doping during the growth of GeNWs. The diameter of P-doped GeNWs does not significantly depend on the PH_3 gas ratio, resulting in a uniform diameter. On the other hand, the shape of the B-doped GeNWs strongly depends on the ratio of B_2H_6 gas to GeH_4 gas during the growth. The shape changes with increasing B_2H_6 gas and finally shows cone-like structures for the case of B_2H_6 gas of 2.2 sccm

(2) Three step B doping.

The B-doped GeNWs showed an increasingly tapered structure with increasing B concentration. To avoid tapering and gain a uniform diameter along the growth direction of the GeNWs, a three step process was found to be useful, namely growth of GeNWs followed by B deposition and then annealing (Fig. 2).

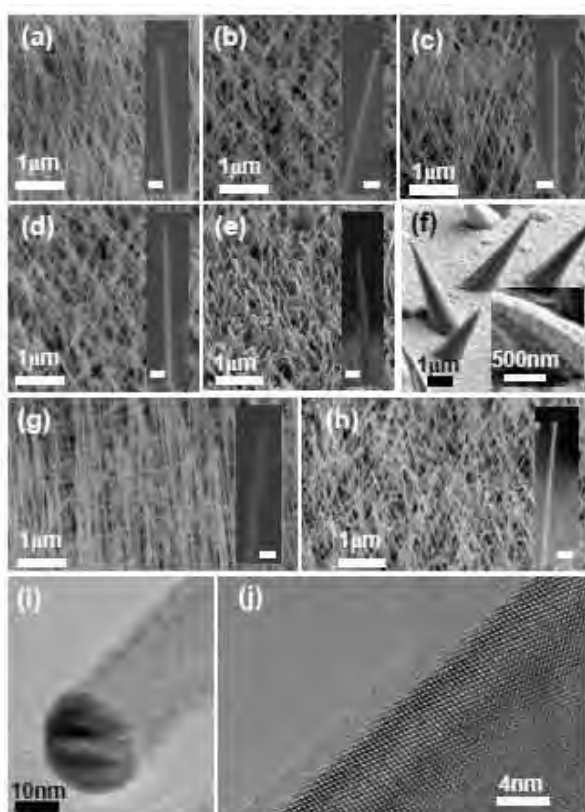


Fig. 1. SEM images of GeNWs synthesized by CVD with gas mixtures with ratios of GeH_4 to B_2H_6 of (a) 10:0, (b) 10:0.2, (c) 10:0.4, (d) 10:0.7, (e) 10:1.0, and (f) 10:2.2. The insets show the magnification of single NWs. The scale bar is 20 nm. SEM images of GeNWs synthesized by CVD with gas mixtures with ratios of GeH_4 to PH_3 of (g) 10:1.0 and (h) 10:7.0. The insets show the magnification of single NWs and the scale bars are 30 nm. (i) TEM image of GeNWs synthesized by CVD with gas mixtures with a ratio of GeH_4 to B_2H_6 of 10:0. (j) High resolution TEM image of (i).

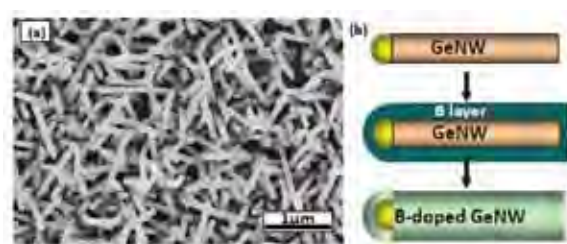


Fig. 2. (a) SEM images of B-doped rod-type GeNWs before annealing. (b) TEM images of B-doped rod-type GeNWs (e) Illustration of the formation process of B-doped rod-type GeNWs with uniform diameters.

References

- 1) N. Fukata et al., *Appl. Phys. Lett.* **90**, 153117 (2007).
- 2) N. Fukata et al., *Appl. Phys. A* **93**, 589 (2008).
- 3) N. Fukata et al., *Appl. Phys. Lett.* **93**, 203106 (2008).
- 4) N. Fukata, *Adv. Mater.* **21**, 2829 (2009).
- 5) N. Fukata et al., *ACS Nano* **4**, 3807 (2010).

Fluorescent Metallo-Supramolecular Polymers

MANA Independent Scientist Masayoshi HIGUCHI



1. Outline of Research

Fluorescent metallo-supramolecular polymers are of great interest, because the properties such as solubility or viscosity are controllable by changing the ligands and metal-ion species. Especially, metallo-supramolecular polyelectrolytes (MEPE) based on bis-terpyridine (btpy) or the derivatives have well recognized their importance in tuning of optoelectronic properties after linking with conjugated molecules. The optoelectronic properties, which largely depend on light emission efficiency of fluorescent MEPE, can be tuned by choice of the metal ions and modification of the ligands. Using the different metal ions as template to assemble, the organic building blocks into polymer chains through coordination to chelating terpyridyl units is an appealing strategy for construction of photoluminescent materials. We planned to synthesize new ditopic bis-terpyridine (btpy) ligands containing triethylene glycol (TEG) chains at the ortho-position of peripheral pyridine ring and obtain fluorescent Fe(II) metallo-supramolecular polyelectrolytes via complexation of Fe(II) ions with the new ligands.

2. Research Activities

We have designed and synthesized a new tpy ligand (L1, Fig. 1) containing a TEG chain at the ortho-position of the peripheral pyridine ring of 6-bromo-4'-(4-bromophenyl)-[2,2';6',2''] terpyridine (1) in good chemical yield via chemoselective nucleophilic substitution. Only one peripheral pyridine ring of tpy was substituted to prevent steric crowding in the coordination sphere. The synthon of L1 opens the door for synthesis of new btpy ligands, L2 and L4, using one pot Suzuki-type dimerization of mono-terpyridines (Fig. 1). For comparative study of MEPEs properties, L3 without TEG chains is also synthesized using above methodology from 4'-(4-Bromo-phenyl)-[2,2';6',2''] terpyridine (2). All the ligands, L1-L4, were purified by alumina column chromatography followed by preparative GPC and were characterized by NMR and mass spectroscopy techniques.

Novel fluorescent Fe(II)-MEPEs were synthesized via complexation of Fe(II) ions with new btpys containing flexible TEG chains at the ortho-position of peripheral pyridine rings. Metal-ion induced self-assembly of the btpys was carried out by refluxing an equimolar amount of the ligand and Fe(OAc)₂ in acetic acid under argon atmosphere, followed by slow evaporation of the solvent and drying in vacuo. The color of solution turns purple during complexation, indicating the formation of corresponding Fe(II)-MEPEs (Fig. 2). The Fe(II) ion is known as quencher of fluorescence, but FeL2-MEPE shows higher retention of quantum yield as compared to the unsubstituted analogues (FeL3-MEPE). We investigated the substituent effects of

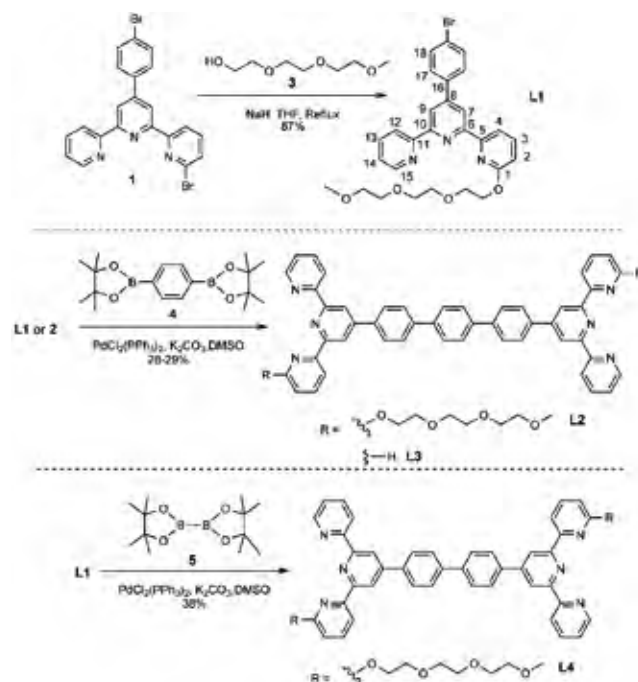


Fig. 1. Synthetic scheme of organic ligands L1-4.

TEG chains into metallo-supramolecular polymers towards fluorescent and electrochemical properties in detail. The introduction of TEG chains to the ligand resulted in enhancing the fluorescence of the corresponding polymers: FeL2-MEPE with the TEG chains retains nearly three times higher fluorescence quantum yield than FeL3-MEPE without the TEG chains. As a proof principle, we have studied their photophysical and electrochemical properties taking the account for the effect of substituent at the peripheral pyridine unit and the length of spacer. This study highlights that controlled design of ligand may help to modulate the optoelectronic properties of a given chromospheres through metallo-supramolecular polymerization.

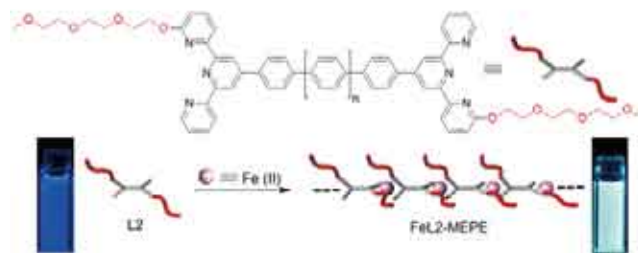


Fig. 2. Fluorescent Metallo-Supramolecular Polymers.

Reference

- 1) R.R. Pal, M. Higuchi, et al., *Polym. J.* **42**, 336 (2010).

Graphene-Based Quantum-Dot Devices

MANA Independent Scientist Satoshi MORIYAMA



1. Outline of Research

The recent discovery of graphene has opened a door to new vistas of low-dimensional physics. Their electronic properties are expected to differ from the well-studied 2-dimensional electron gas in a semiconductor heterostructure. The low-energy physics of graphene is described theoretically by $(2+1)$ -dimensional Dirac fermions, where ‘2-dimensions’ corresponds to a graphite sheet and ‘1-dimension’ denotes time. The corresponding energy dispersion becomes the so-called Dirac cone, which leads to rich physics inherited from quantum electrodynamics.

Our research objective is the realization of quantum wires and quantum dots in graphene-based materials by using the nano-fabrication process, toward the novel graphene-based quantum devices. It will be expected that the fabricated quantum wires or quantum dots become integrated quantum circuits because of its 2-dimensional sheet structure. Furthermore, their low atomic weight and the low nuclear spin concentration, arising from the only 1.1% natural abundance of ^{13}C are expected for having weak spin-orbit interactions and hyperfine interactions. Therefore, graphene-based quantum devices are promising candidates for spin-based quantum information processing and spintronic devices.

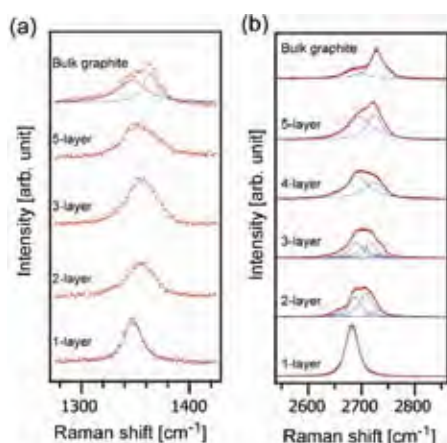


Fig. 1. Raman spectra of different varieties of multilayer graphite and of reference bulk graphite. (a) D -band spectra; (b) $2D$ -band spectra. Spectra are shifted for clarity.

2. Research Activities

(1) Fabrication of quantum-dot devices in graphene.¹⁾

We fabricated quantum-dot devices in graphene-based two-dimensional materials and measured their electrical transport properties. Graphene samples are prepared by micro-mechanical cleavage of graphite crystals and deposited on the surface of a silicon substrate with a 290 nm thickness of oxidized silicon. Optical microscope contrast and

Raman spectroscopy measurements can be identified the single-, double-, triple-, and few-layer graphene flakes on the substrate. We determined the fine details of graphene layers on a SiO_2/Si substrate from their Raman fingerprint and fabricated double-quantum-dot devices with the identified graphene flakes. Based on previous studies of bulk graphite, we explain the Raman bands. The G band originates from the doubly degenerate zone-centre E_{2g} mode, which involves a phonon with the highest energy at the Γ point in the Brillouin zone. The $D/2D$ bands are caused by double resonance with one or two in-plane transverse optical phonons close to the K point in the Brillouin zone. These bands reflect the electronic structure near the two nodes of the Dirac-cone energy dispersion [described as $(2+1)$ -dimensional Dirac fermions] as well as phonon dispersion close to the K point. In Fig. 1(a), the D band has a maximum intensity at the section boundaries between flake and substrate, and we use this fact to examine D -band data. In Fig. 1(b), variations in the $2D$ band are clearly evident. For single-layer graphene, the $2D$ band can be fitted with a single Lorentzian peak.

Graphene sheets can be carved out to form nanostructures such as quantum wires and quantum dots. We applied a nanofabrication process to the identified graphene flakes to create a single-dot structure and double-dot device structure comprising two lateral quantum dots coupled in series. The electrical transport measurements through a single-dot structure indicated single-electron transistor characteristics at low temperatures. For a double dot structure, we have confirmed coupled quantum dot formation. In Fig. 2, the experimental charge stability diagrams revealed variable interdot tunnel coupling that changes continuously and non-monotonically as a function of gate voltage.

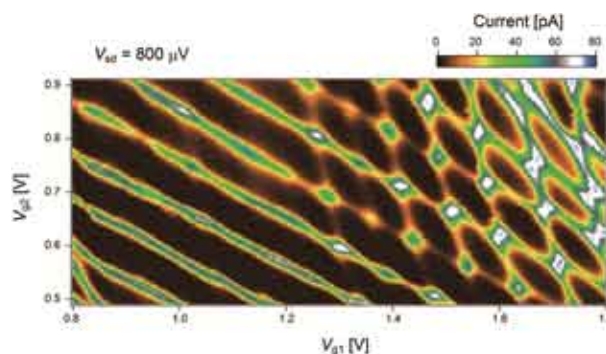


Fig. 2. Experimental charge stability diagrams for coupled quantum dots with variable interdot coupling regime.

Reference

- 1) S. Moriyama, E. Watanabe, D. Tsuya, S. Uji, M. Shimizu, K. Ishibashi, *Sci. Technol. Adv. Mat.* **11**, 054601 (2010).

Controlling the Electromagnetic Waves on the Nano-Scale and Atomic-Scale

MANA Independent Scientist
MANA Research Associate

Tadaaki NAGAO

Gui Han, Chung Vu Hoang, Makiko Oyama, Rana Masud



1. Outline of Research

The technology for amplifying, confining, and scattering the light in nanoscale objects is strongly desired as a key technology for future optical communication and sensing. By hybridizing the plasma oscillation with the electromagnetic field near the metal surface we can manipulate the light at a much shorter wavelength than that in free space. Such hybridized waves with contracted wavelength are called plasmon polaritons.

When the size of the object shrinks beyond the micrometer scale and when it reaches down to the nanometer or sub-nanometer scale, novel effects that originate from its smallness and its shape come into play. Atom-scale size effects become especially pronounced in metallic objects, since the Fermi wavelengths of typical metals are in the Ångström range. Plasmon polaritons in metal nanostructures show maximum tunability by changing the shape, the size, and thus the dimensionality of the objects. Such feature can be utilized for tailoring optical properties for future nano-photonics/optics devices for information technology as well as high-sensitivity sensors and efficient catalytic materials.

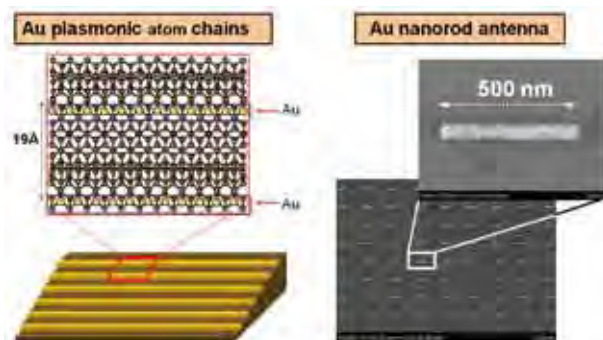


Fig. 1. (Left) Atomic-scale structure of a self-assembled one-dimensional atom chain (schematic diagram). (Right) Nanoscale one-dimensional nanoantenna of gold prepared by electron lithography (SEM photo).

2. Research Activities

By utilizing bottom-up nanofabrication techniques such as ultrahigh-vacuum MBE growth on template crystal surfaces, we have produced 1D, 2D, and 3D patterned “atomic-scale low- dimensional” metallic nanostructures with precise controlling of its crystallinity and sizes (Fig. 1). By “molding” the plasmons into size/shape controlled small objects, we aim to explore and freely design the dielectric and optical properties of nanostructures for future photonic applications. For the genuine low-dimensional systems such as atom chains, and atom sheets, nearly no fundamental knowledge on plasmon has been available and

we experimentally explored these systems in detail.

Also, shape-controlled quasi-2D metal-nanoisland array (such as grown by MBE or by the wet-chemistry route) are of special technological importance but not yet studied systematically in a quantitative manner. Their plasmon resonances are related to strong nearfield enhancement, which enables surface enhanced IR absorption (SEIRA), and we aim at developing these SEIRA-active device structures for chemo/biosensing applications. Since plasmonic interaction of well-defined specially shaped 3D gold nanostructures with vibration modes may give even higher SEIRA, we also study top-down lithographic structures in order to reach a maximum SEIRA effect.

In our project, we target

- 1) Mesoscale plasmonic structures for infrared chemo/biosensors with attomol sensitivity and quantitative analysis.
- 2) Nanoscale plasmonic structures for antenna resonances in mid-infrared spectral range.
- 3) Atom-scale metallic structures for exploiting plasmonic excitation, and propagation, confinement, and cavity effects in ultimately tiny systems (Fig. 2).

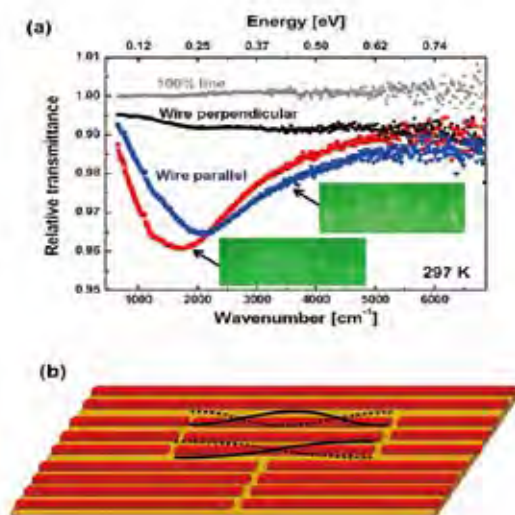


Fig. 2. (a) IR transmittance with electrical field polarized parallel (red squares and blue triangles) and perpendicular (black circles) to the In atom wires. (b) Schematic illustration of the plasmons in atomic wires. The atom wires are segmented by domain boundaries and 1D plasmons are confined to form standing-wave antenna resonance modes (Dotted and solid curves).

References

- 1) T. Nagao et al., *Phys. Rev. Lett.* **97**, 116802 (2006).
- 2) T. Nagao et al., *Sci. Technol. Adv. Mater.* **11**, 054506 (2011).
- 3) D. Enders et al., *Jpn. J. Appl. Phys.* **49**, L1222 (2007).
- 4) D. Enders et al., *Phys. Chem. Chem. Phys.*, in press (2011).

Development of Photoresponsive Biointerfaces

MANA Independent Scientist Jun NAKANISHI



1. Outline of Research

Biointerfaces are interfaces between biomolecules and materials. They play pivotal roles in biomedical devices such as materials for drug delivery, tissue engineering, and bioanalysis. The major purpose of the present study is to develop chemically functionalized biointerfaces with photochemically active compounds and apply them for analyzing and engineering cellular functions (Fig. 1).

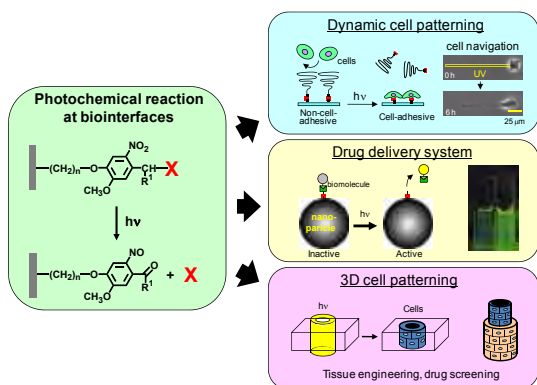


Fig. 1. Photoresponsive biointerfaces developing in this study.

2. Research Activities

(1) Dynamic control of cell adhesion on amino-terminated surfaces.¹⁾

Dynamic control of cell adhesion on substrates is a useful technology in tissue engineering and basic biology. We developed a method for the control of cell adhesion on amino-bearing surfaces by reversible conjugation of an anti-fouling polymer, poly(ethylene glycol) (PEG), via a newly developed photocleavable linker (1, Fig 2A). This molecule has alkyne and succinimidyl carbonate at each end, which were connected by photocleavable 2-nitrobenzyl ester. Under this molecular design, the molecule crosslinked azides and amines, whose linkage cleaved upon application of near-UV light. By using aminosilanised glass and silicon as model substrates, we studied their reversible surface modification with PEG-azide based on contact angle measurements, ellipsometry, and AFM morphological observations. Protein adsorption and cell adhesion dramatically changed

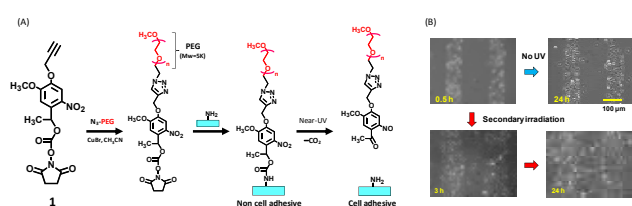


Fig. 2. (A) Reversible conjugation of PEG to amino-bearing surfaces via photocleavable linker (1). (B) Cell photopatterning and induction of migration by the secondary irradiation.

by PEGylation and the following irradiation, which can be used for cellular patterning (Fig. 2B). Also, the capability of the substrate to change cell adhesiveness by photoirradiation during cell cultivation was demonstrated by inducing cell migration. We believe this method will be useful for dynamic patterning of cells on protein-based scaffolds.

(2) Precise patterning of photoactivatable glass coverslip for fluorescence observation of shape-controlled cells.²⁾

Shape of the cells is a key determinant of cellular fates and activities. We developed a method for controlling cellular shape on a chemically modified glass coverslip with micropatterned cell adhesiveness. The glass surface was chemically modified with an alkylsiloxane monolayer having a caged carboxyl group, where single-cell-size hydrophilic islands with hydrophobic background were created by irradiating the substrate in contact with a photomask to produce the carboxyl group (Fig. 3A). Thus created surface hydrophilicity pattern was converted to a negative pattern of a protein repellent amphiphilic polymer, Pluronic F108, according to its preferential adsorption to hydrophobic surfaces (Fig. 3B). The following addition of a cell-adhesive protein, fibronectin, resulted in its selective adsorption to the irradiated regions. In this way, cell-adhesive islands were produced reproductively, and the cells formed a given shape on the islands. As examples of the cell shape control, we seeded HeLa cells and NIH3T3 cells to an array of triangular spots and fluorescently imaged the dynamic motions of cell protrusions extended from the periphery of the cells (Fig. 3C,D). The present method is useful for studying molecular mechanism of cell polarity formation.

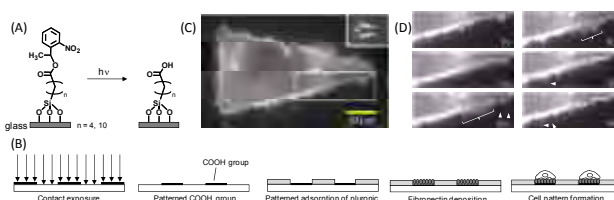


Fig. 3. (A) Photocleavage reaction of silane layers. (B) Surface patterning procedure used in the present study. (C) Geometrical confinement of NIH3T3 cells in a triangular shape and (D) dynamic motion of cell protrusions extended from its contour.

References

- 1) S. Kaneko, H. Nakayama, Y. Yoshino, D. Fushimi, K. Yamaguchi, Y. Horiike and J. Nakanishi, *Phys. Chem. Chem. Phys.*, in press.
- 2) J. Nakanishi, Y. Kikuchi, Y. Tsujimura, H. Nakayama, S. Kaneko, T. Shimizu, K. Yamaguchi, H. Yokota, Y. Yoshida, T. Takarada, M. Maeda, Y. Horiike, *Supramol. Chem.* **22**, 396 (2010).

Computational Physical Chemistry

MANA Independent Scientist Yoshitaka TATEYAMA



1. Outline of Research

We are challenging to make novel theoretical frameworks for physicochemical phenomena such as electron transfer, proton transfer & photoexcitation (Fig. 1), since their quantitative calculations are still less established than the conventional techniques for ground state properties.

Our main projects are as follows; (1) development and/or establishment of theories and computational methods for problems in physical chemistry based on the "density functional theory (DFT) and ab-initio calculation techniques", and (2) understanding microscopic mechanisms of elementary reactions in physical chemistry problems by applying these computational techniques. Of particular interest are surface/interface chemistry, electrochemistry and photochemistry in these years.



Fig. 1. Research targets in the computational physical chemistry (Tateyama independent scientist) group in MANA.

2. Research Activities

(1) *Interfacial water structures and hydrogen-bond networks of photocatalytic systems by first-principles molecular dynamics with TiO₂ slabs soaked in bulk water.*¹⁾

First-principles molecular dynamics (FPMD) using supercells with "bulk" water between the TiO₂ anatase (101) and (001) surfaces were carried out for the first time. We showed explicit atomistic structures of strong and weak hydrogen bonds on the TiO₂/water interfaces, which had been suggested experimentally so far (Fig. 2). The results also give insights into the H₂O or OH coverage on the interfaces

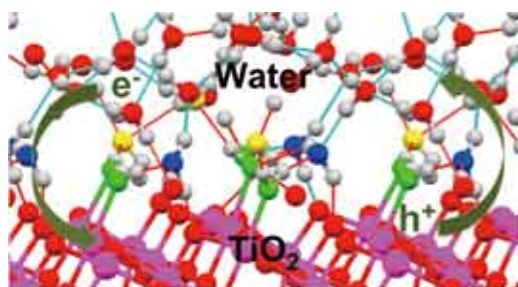


Fig. 2. Snapshot in the equilibrium trajectory of TiO₂ anatase/water interface obtained by our FPMD simulations. Explicit structures of strong and weak hydrogen bonds are found in this interfacial region.

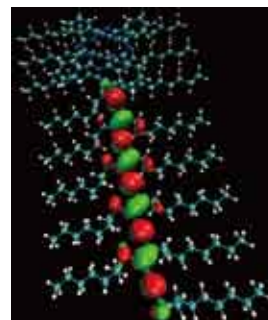


Fig. 3. HOMO distribution of polydiacetylene with adsorbed phthalocyanine on a surface, calculated by the first-principles wavelet-basis method.

and their hydrophobicity-hydrophilicity, which is important to understand the photocatalytic mechanisms microscopically.

(2) *First-principles large-scale calculation studies on structures and electronic states of surface and solid/solution interface systems.*^{2,3)}

We have investigated electronic states of equilibrium diamond(111)/water interfaces to understand the interface reaction dependence on the interface structure and the mechanism of surface conductivity²⁾. We have also examined the chain polymerisation of diacetylene compounds on a surface as well as the effect of phthalocyanine adsorption on the polymerisation, and given possible structure models, which are consistent with the STM observations in experiments (Fig. 3).
(3) *Development of new formulation of non-adiabatic coupling in the framework of TDDFT-LR scheme.*⁴⁾

Non-adiabatic coupling (NAC) is indispensable for the excited-state dynamics simulation. We have developed a new formulation to calculate NAC using derivative operator in the framework of TDDFT-LR scheme, and demonstrated its accuracy and the universality (Fig. 4).

$$\begin{aligned} \langle \Psi_0 | \frac{\partial}{\partial R_\alpha} | \Psi_I \rangle &= \omega_I^{-1} \langle \Psi_0 | \frac{\partial \hat{H}}{\partial R_\alpha} | \Psi_I \rangle = \omega_I^{-1/2} \mathbf{h}_\alpha^I \mathbf{S}^{-1/2} \mathbf{F}_I \\ \langle \Psi_0 | \frac{\partial}{\partial R_\beta} | \Psi_I \rangle &= \omega_I^{1/2} \mathbf{d}_\beta^I \mathbf{S}^{1/2} \mathbf{F}_I \end{aligned}$$

Fig. 4. A new universal formulation of non-adiabatic coupling (NAC) necessary for the excited-states dynamics simulation within the TDDFT-LR framework.

References

- 1) M. Sumita, C. Hu, and Y. Tateyama, *J. Phys. Chem. C* **114**, 18529 (2010).
- 2) T. Watanabe et al., *Diamond & Related Materials* **19**, 772 (2010).
- 3) Y. Okawa et al., submitted.
- 4) C. Hu, O. Sugino, H. Hirai, Y. Tateyama, *Phys. Rev. A* **82**, 062508 (2010).

Photoluminescence and Raman Study on Boron Doped Diamond

MANA Independent Scientist Shunsuke TSUDA



1. Outline of Research

Diamond is one of the most expected materials, especially for a post-silicon device. Large band gap and very high stability are huge advantages for the purpose.

Furthermore, diamond shows superconductivity after sufficient carrier doping. At present, it is well accepted that the superconducting transition temperature (T_c) is governed by carrier density. Most popular evaluation method of carrier density is Hall measurement. However, at high doping samples, carrier density obtained from Hall measurements exceeded the boron density. This anomalous behavior can be attributed to multi-band effect. In other words, Hall measurement is not appropriate for evaluating the carrier density of highly boron doped diamond.

Unfortunately, the T_c is, at highest, ~ 10 K. To achieve higher T_c , further carrier density is required. NMR study indicates that inactive carriers exist in highly doped samples. Therefore, by optimizing the growth condition, higher T_c may realize. For the purpose, we should find another simple method to evaluate the carrier density.

As a candidate for another evaluation method, we tried two methods: photoluminescence and Raman scattering

2. Research Activities

(1) Photoluminescence study.

We performed photoluminescence measurements on boron doped diamond at room temperature. The samples were fabricated by using Microwave Plasma assisted Chemical Vapor Deposition method (MPCVD) on silicone substrate. The samples were polycrystalline. The excitation laser was focused onto the sample via objective lens of $\times 40$. The spot size was $\sim 10 \mu\text{m}$. The spectra were obtained by using two lasers; He-Au laser with 224 nm (2.0 $\mu\text{J}/\text{pulse}$, 20Hz) and He-Cd laser with 325 nm (15 mW, CW).

Fig. 1(a) shows photoluminescence spectra obtained by 224 nm excitation. This excitation energy is larger than the indirect band gap of diamond. For diamond substrate (type Ia), we obtained broad luminescence centered at ~ 510 nm. On the other hand, from MPCVD synthesized samples, we got no significant signal.

Fig. 1(b) shows photoluminescence spectra obtained by 325 nm excitation. In contrast to the result with 224 nm excitation, we found many fine structures on the spectra for MPCVD synthesized samples and diamond substrate. However, the peak positions did not depend on the carrier density.

These results indicate that most of the luminescence excited by 325 nm excitation is related to in-gap state such as defect and impurity.

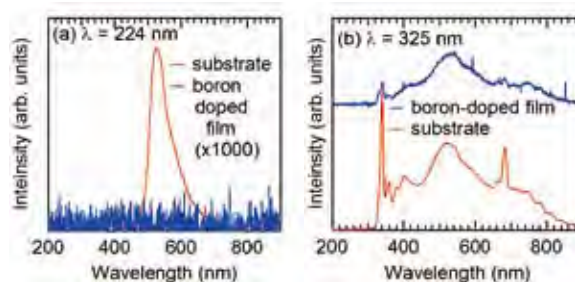


Fig. 1. Photoluminescence spectra of diamond substrate (type Ia) and boron-doped diamond film excited (a) by 224 nm and (b) 325 nm.

(2) Raman scattering study.

We performed Raman measurements on boron doped diamond at room temperature. The excitation laser was focused onto the sample via objective lens of $\times 40$. The spot size was $\sim 10 \mu\text{m}$. The spectra were obtained by using two lasers; 325 nm (15 mW, CW) and 514.5 nm (100mW, CW).

Diamond shows Fano-like resonance after sufficient boron doping into diamond. Fig. 2(a) shows representative Raman spectra obtained by green laser excitation. An edge like structure originated from optical phonon mode appears at $\sim 1330 \text{ cm}^{-1}$. Present results are consistent with former reports. Fig. 2(b) shows Raman spectra obtained by He-Cd laser excitation. We found two peaks at $\sim 1330 \text{ cm}^{-1}$ and $\sim 1600 \text{ cm}^{-1}$. The peak at lower Raman shift corresponds to optical phonon mode from sp^3 bond in diamond lattice. The other peak can be assigned to a vibration mode originated from sp^2 bond because G-band in graphite appears around this energy.

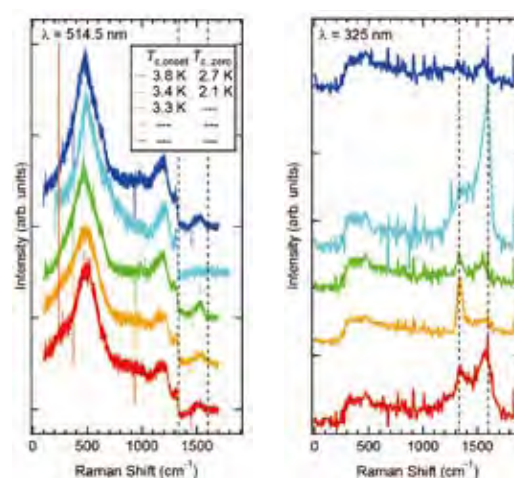


Fig. 2. Raman spectra of boron-doped diamond excited by (a) 514.5 nm and (b) 325 nm. Vertical broken lines at 1330 cm^{-1} and 1600 cm^{-1} seems to be corresponding to sp^3 and sp^2 bonding.

Aqueous Design, Electronic Structure and Size Dependence Effect of Metal Oxide Quantum-Confined Structures

MANA Independent Scientist Lionel VAYSSIERES



1. Outline of Research

We aim to contribute to the development of a new generation of clean metal oxide materials using nanoscale and quantum confinement phenomena to create multifunctional structures and devices for renewable energy, environment, and health by cost-effective large scale fabrication techniques. We are developing series of novel materials for solar hydrogen generation, photovoltaics, sensors, and surface controlled nanoparticles and quantum dots for nanotoxicology studies utilizing low-cost and large scale materials chemistry such as aqueous chemical growth to fabricate structures and devices based on quantum-confined metal oxide (hetero)-nanostructures.¹⁾

2. Research Activities

We have synthesized and characterized the electronic structure and basic structural, optical, and photoelectrochemical properties of novel visible light active iron oxide-based semiconductors consisting of vertically oriented quantum rod arrays. Doped and/or quantum dot sensitized bundle of iron oxide quantum rods which by intermediate band effects enable a full visible absorption profile while still being stable against photo-corrosion for efficient and low cost solar hydrogen generation by direct water splitting at neutral pH allowing therefore the use of the largest free natural resource on Earth, that is seawater, as unique electrolyte.²⁾

Another aspect of our research activities involved the controlled fabrication of quantum dots of tailored sizes without surfactant and thus the ability to control their surface acidity and properties.³⁾ Size effect in general on the physical properties and electronic structure of metals and semiconductors are well established in the literature. However, the effect of quantum dot size on the chemical properties of materials and, in particular, on the surface chemistry of hydrated metal oxides has scarcely been reported. Yet, such an effect could be of great relevance for a better fundamental understanding of structure-properties relationships and for nanotoxicology studies. We have investigated the effect of the size of quantum dots of $\gamma\text{-Fe}_2\text{O}_3$ on their aqueous surface chemistry. Indeed, the effect of size on the surface chemistry of metal oxides was demonstrated by the reversal of the surface acidity from acidic to neutral to basic by changing the size from 12 to 7.5 to 3.5 nm, respectively.⁴⁾

The latest developments include the synthesis of large quantities of pure TiO_2 anatase quantum dots without the use of surfactant. Thermodynamically and kinetically stable aqueous suspensions have been obtained at various concentration of Ti from which powders have been extracted by ultracentrifugation. Fig. 1 shows the HRTEM image and DLS analysis of a typical stable aqueous suspension of

anatase TiO_2 prepared in water at low temperature.

In depth analysis of the size dependence over two orders of magnitude (i.e. from 2 to 200nm in diameter) electronic structure performed at synchrotron radiation reveals a direct effect of the nanoparticle size on the orbital character of TiO_2 anatase quantum dots.⁵⁾

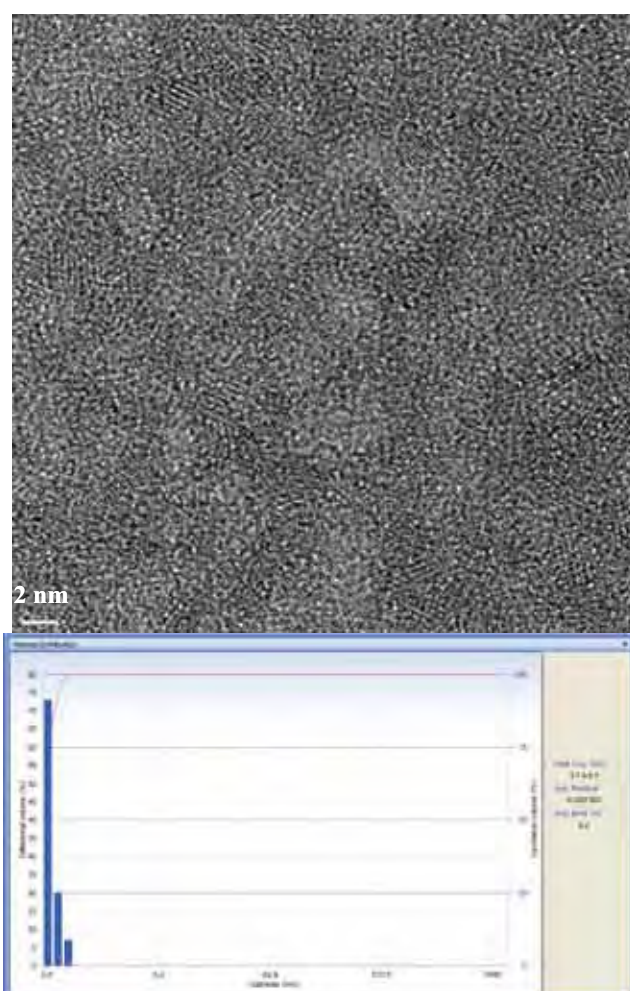


Fig. 1. High resolution transmission electron microscopy (top) and dynamic light scattering analysis (bottom) of a stable aqueous suspension of anatase TiO_2 consisting of ~1-2nm quantum dots.

References

- 1) L. Vayssieres, "Metal oxide rods and dots-based structures and devices: cost-effective fabrication and surface chemistry control", in *Business & Safety Issues in the Commercialization of Nanotechnology*, S.S. Mao, L. Merhari, J. van Schijndel, L. Tsakalakos, R. Hurt, H. Liu, and T.J. Webster editors (*Mater. Res. Soc. Symp. Proc.* 1209, Warrendale, PA, 2010), 1209-P01-07.
- 2) *On Solar Hydrogen & Nanotechnology*, L. Vayssieres editor (John Wiley & Sons, 2009).
- 3) L. Vayssieres, *Langmuir*, in press (2011).
- 4) L. Vayssieres, *J. Phys. Chem. C* **113**, 4733 (2009).
- 5) L. Vayssieres, C. Persson, J. Guo, *Phys. Rev. Lett.*, submitted.

Gold Nanoparticles in Nanoporous CN for Catalysis

MANA Independent Scientist Ajayan VINU



1. Outline of Research

Metal nanoparticles have attracted much attention in the fields of catalysis, separation, magnetism, optoelectronics, and microelectronics owing to their unique physical and chemical properties. Several methods are available for the fabrication of metal nanoparticles. Among the methods, the fabrication of the nanoparticles on the surface of porous support with a high surface area, especially, nanoporous matrix, with different pore diameter and structure is quite attractive as they offer well-ordered pores with controllable size, high surface area, and large pore volume. The ordered nanopores dictate the size and shape of the nanoparticles as they are formed in the confined matrix whereas the high surface area and large pore volume help the formation of high degree of homogeneously dispersed nanoparticles on the surface of the support. Although the size of the nanoparticle can be controlled by nanoporous support strategy, the stabilization and the reduction of the particles on the porous surface after their formation is quite challenging. Very recently, Vinu et al.¹⁾ reported the synthesis of nanoporous carbon nitride (MCN) with ordered pores and controlled textual parameters through a simple polymerization reaction between carbon tetrachloride and ethylene diamine by using SBA-15 as sacrificial template, which has inbuilt $-NH_2$, and $-NH$ groups on the nanoporous walls which can provide a platform for the generation of metal and metal oxide nanostructures.

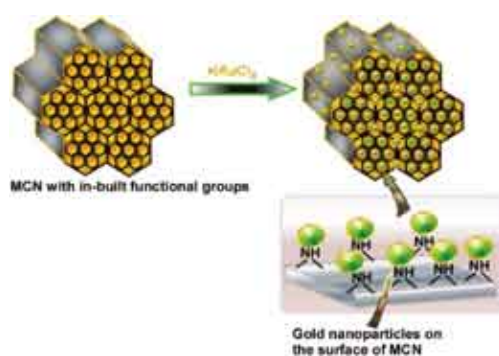


Fig. 1. The schematic representation of the encapsulation of gold nanoparticles over MCN with in-built functional groups without any external stabilizing agent.

Herein, we demonstrate for the first time the fabrication of highly dispersed Au nanoparticles with a size less than 7 nm on the surface of the MCN support which acts as stabilizing, size controlling, and reducing agent without the need for any external agent and the surface modification (Fig. 1). We also demonstrate that the Au nanoparticles embedded on MCN are highly active, selective and recyclable catalyst in the three component coupling reaction of benzaldehyde, piperidine, and phenyl acetylene for the synthesis of prop-

argylamine which is an intermediate for the construction of nitrogen containing biologically active molecules and for the synthesis of polyfunctional amino derivatives.²⁾

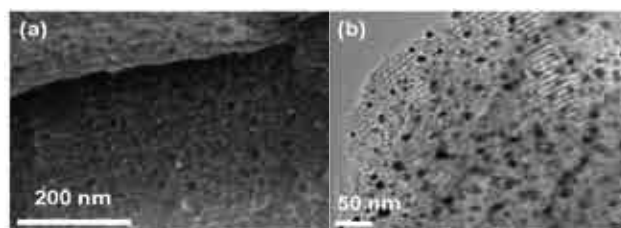


Fig. 2. (a) FE-HRSEM and (b) HRTEM images of Au nanoparticles encapsulated MCN.

2. Research Activities

HRTEM and HRSEM image of the Au nanoparticle encapsulated MCN is shown in Fig. 2. It can be seen from Fig. 2b that a regular arrangement of dark spherical spots which correspond to Au nanoparticles is clearly observed along the nanochannels of the support. Interestingly, a linear arrangement of mesochannels which are arranged in a regular interval is also clearly seen, suggesting that mesostructure of the support is stable even after the formation of Au nanoparticles. The average size of the Au nanoparticles obtained from the HRTEM image is found to be ca. 7 nm which is equal to the size of the pores of the support. The amount of Au present in the sample is 0.05 atomic percent which matches well with ICP analysis report. The catalytic efficiency of CN-Au-150 was tested in three component coupling of aldehyde, amine, and alkyne. Initially, benzaldehyde, piperidine and phenylacetylene were mixed with 20 mg of CN-Au-150 in toluene. The reaction was completed in 24h with a yield of the final product of almost 96%, as analyzed by gas chromatography. These results prompted us to study the substituent effects on the aromatic ring. Interestingly, electron deficient aromatic aldehydes like *p*-nitrobenzaldehyde also gave reasonable conversion under similar conditions. Even, halo substituted benzaldehyde e.g. *p*-chlorobenzaldehyde also furnished the desired product in good yield. It should be noted that no conversion was found in the absence of catalyst or using only pure MCN catalyst under identical conditions. These results clearly indicate the importance of the encapsulation of the Au nanoparticles inside the mesochannels of the MCN stabilizer.

References

- 1) A. Vinu, *Adv. Funct. Mater.* **18**, 816 (2008).
- 2) K.K.R. Datta, B.V. Subba Reddy, K. Ariga, A. Vinu, *Angew. Chem. Intl. Ed.* **49**, 5961 (2010).

Theory Design and Physical Properties Forecast of Nano-Carbon Systems

MANA Independent Scientist Katsunori WAKABAYASHI



1. Outline of Research

Our research target is to theoretically reveal the peculiar electronic, magnetic, transport and optical properties in nano-carbon materials such as graphene, nano-graphene, graphene nanoribbons, nanotubes using theoretical and/or computation method. Recently graphene, a single-layer of graphite, has attracted much attention both from the fundamental and applied sciences, since the electronic states are described by the massless Dirac Fermion in sharp contrast with the conventional two-dimensional electron gas on the semiconductor devices. Such unconventional electronic states are the sources of the peculiar electronic properties of graphene, which are characterized as the half-integer quantum Hall effect, the absence of backward scattering, Klein tunneling and ultrahigh mobility of electrons.

The successive miniaturization of the graphene electronic devices inevitably demands the clarification of edge effects on the electronic structures, electronic transport and magnetic properties of nanometer-sized graphene. The presence of edges in graphene has strong implications for the low-energy spectrum of the π -electrons. There are two basic shapes of edges, armchair and zigzag, which determine the properties of graphene ribbons. It was shown that ribbons with zigzag edges (zigzag ribbon) possess localized edge states with energies close to the Fermi level. These edge states correspond to the non-bonding configurations. In contrast, edge states are completely absent for ribbons with armchair edges. Recent experiments support the evidence of edge localized states. Also, it has been recently reported by several overseas groups that graphene nanoribbons can experimentally be produced by using lithography techniques and chemical techniques.

On the background mentioned above, the main purpose of our research is to clarify the peculiar features in electronic, magnetic and transport properties of nano- and meso-scopic systems based on carbon materials. Also, we aim to design and explore theoretically the new functionalities as the next-generation devices based on the peculiar electronic properties.

2. Research Activities

(1) Perfect Conducting Channel.¹⁻⁴⁾

Numerical calculations have been performed to elucidate unconventional electronic transport properties in disordered zigzag nanoribbons. The energy band structure of zigzag nanoribbons has two valleys that are well separated in momentum space, related to the two Dirac points of the graphene spectrum. The partial flat bands due to edge states make the imbalance between left- and right-going modes in each valley, i.e. appearance of a single chiral mode. This

feature gives rise to a perfectly conducting channel in the disordered system, i.e. the average of conductance $\langle g \rangle$ converges exponentially to 1 conductance quantum per spin with increasing system length, provided impurity scattering does not connect the two valleys, as is the case for long-range impurity potentials. We have also identified that these peculiar transport properties are related to the time-reversal symmetry breaking for pseudospin in graphene due to the presence of zigzag edge boundary.

(2) Development of Analytic Method.⁵⁻⁶⁾

The development of analytic method for massless Dirac Fermion systems is necessary not only for improvement of computational code but also for the intuitive understanding of quantum phenomena in the system. Recently we have succeeded to derive the full spectrum and corresponding wavefunction of graphene nanoribbons within the tight-binding model using wave-mechanics approach and transfer matrix approach. It is found that the state of pseudospin in graphene is sensitive to the orientation of graphene edge. The armchair edge conserves the state of pseudospin, while the zigzag edge does not. Also, we have developed the quasi-classical theory of Dirac Fermion systems with edge boundary on the basis of the gauge field theory which will serve for the further theoretical expedition.

(3) Identifying the Orientation of Edge of Graphene Using G Band Raman Spectra.⁷⁻⁸⁾

The electron-phonon matrix elements relevant to the Raman intensity and Kohn anomaly of the G band are calculated by taking into account the effect of the edge of graphene. The analysis of the pseudospin reveals that the longitudinal optical phonon mode undergoes a strong Kohn anomaly for both the armchair and zigzag edges, and that only the longitudinal (transverse) optical phonon mode is a Raman active mode near the armchair (zigzag) edge. The Raman intensity is enhanced when the polarization of the incident laser light is parallel (perpendicular) to the armchair (zigzag) edge. This asymmetry between the armchair and zigzag edges is useful in identifying the orientation of the edge of graphene.

References

- 1) K. Wakabayashi, Y. Takane, M. Yamamoto, M. Sigrist, *New J. Phys.* **11**, 095016 (2009).
- 2) K. Wakabayashi, Y. Takane, M. Yamamoto, M. Sigrist, *CARBON (Elsevier)* **47**, 124 (2009).
- 3) M. Yamamoto et al., *Phys. Rev. B* **79**, 125421 (2009).
- 4) K. Sasaki, K. Wakabayashi, T. Enoki, *New J. Phys.* **12**, 083023 (2010).
- 5) K. Wakabayashi, K. Sasaki, T. Nakanishi, T. Enoki, *Sci. Technol. Adv. Mat.* **11**, 054504 (2010).
- 6) K. Sasaki, K. Wakabayashi, T. Enoki, *J. Phys. Soc. Jpn.*, submitted.
- 7) K. Sasaki, K. Wakabayashi, *Phys. Rev. B* **80**, 155450 (2010).
- 8) K. Sasaki, R. Saito, K. Wakabayashi, T. Enoki, *J. Phys. Soc. Jpn.* **79**, 044603 (2010).

Rational Design of Mesoporous Metals

MANA Independent Scientist Yusuke YAMAUCHI



1. Outline of Research

Because of their scientific and practical significance, research on mesoporous materials, conducted mainly by using surfactant assemblies as templates, has been increasing rapidly. The specific features of regular pore arrangement, uniform mesopore size, and high surface area make these materials very promising for various applications. Especially, mesoporous metals with high electroconductivity have attracted particular interest for their very wide range of applications in such items as batteries, fuel cells, solar cells, chemical sensors, field emitters, and photonic devices. Although several mesoporous metals have been prepared in the past, the mesostructures of these metals are less ordered than those reported for inorganic oxides such as silica. Therefore, the rational design of highly ordered mesoporous metals with controlled compositions and morphologies for practical applications is a most attractive and challenging objective.

2. Research Activities

In 1997, Attard *et al.* proposed direct templating from lyotropic liquid crystals (LLCs) made of non-ionic surfactants at high concentrations. This direct templating approach created a novel avenue to the production of mesoporous metals as well as related nanomaterials. As a soft template, LLCs are more versatile and therefore more advantageous than the hard templates. In principle, the direct templating technique is applicable to a wide variety of metals which are generally known to be deposited by using electrochemical processes in the absence of LLCs because the process involves a simple replication of well-ordered LLCs by electrochemical processes. Therefore, we have reported many mesoporous metals by the chemical or electrochemical reduction of metal salts dissolved in aqueous domains of LLC. In addition to the controllability of various nanostructures (*e.g.*, lamellar, 2D hexagonal ($P6mm$), and 3D cubic ($Ia-3d$) structures) under chosen reaction bath compositions, it is possible to produce nanoparticles and nanotubes simply by changing the compositions (Fig. 1).

Moreover, mesoporous alloys with various compositions can be also designed by controlling the compositions. The most important advantage is that this method allows us to realize microfabrication of mesoporous metals and alloys via the solvent evaporation process, which is not achievable by the hard-templating approach. The fabrication of mesoporous metals on a micrometer scale should lead to the production of more advanced functional nanoscale devices and miniaturized sensors, and microelectronic devices.



Fig. 1. Formation process of Mesoporous Materials.

References

- 1) Liang Wang, Yusuke Yamauchi, *Chemistry-An Asian Journal* **5**, 2493 (2010).
- 2) Hamed Ataee-Esfahani, Liang Wang, Yoshihiro Nemoto, Yusuke Yamauchi, *Chemistry of Materials* **22**, 6310 (2010).
- 3) Hamid Oveisi, Norihiro Suzuki, Ali Beitollahi, Yusuke Yamauchi, *Journal of Sol-Gel Science and Technology* **56**, 212 (2010).
- 4) Tatsuo Kimura, Yusuke Yamauchi, Nobuyoshi Miyamoto, *Chemistry-A European Journal* **16**, 12069 (2010).
- 5) Liang Wang, Yusuke Yamauchi, *Journal of the American Chemical Society* **132**, 13636 (2010).
- 6) Yoji Doi, Azusa Takai, Sho Makino, Radhakrishnan Logudurai, Norihiro Suzuki, Wataru Sugimoto, Yusuke Yamauchi, Kazuyuki Kuroda, *Chemistry Letters* **39**, 777 (2010).
- 7) Yoji Doi, Azusa Takai, Yasuhiro Sakamoto, Osamu Terasaki, Yusuke Yamauchi, Kazuyuki Kuroda, *Chemical Communications* **46**, 6365 (2010).
- 8) Hamid Oveisi, Simin Rahighi, Xiangfen Jiang, Yoshihiro Nemoto, Ali Beitollahi, Soichi Wakatsuki, Yusuke Yamauchi, *Chemistry-An Asian Journal* **5**, 1978 (2010).
- 9) Hamid Oveisi, Ali Beitollahi, Masataka Imura, Chia-Wen Wu, Yusuke Yamauchi, *Microporous and Mesoporous Materials* **134**, 150 (2010).
- 10) Shosuke Kiba, Yoshinori Okawauchi, Norihiro Suzuki, Yusuke Yamauchi, *Chemistry-An Asian Journal* **5**, 2100 (2010).
- 11) Liang Wang, Chunping Hu, Yoshihiro Nemoto, Yoshitaka Tateyama, Yusuke Yamauchi, *Crystal Growth & Design* **10**, 3454 (2010).
- 12) Norihiro Suzuki, Tatsuo Kimura, Yusuke Yamauchi, *Journal of Materials Chemistry* **20**, 5294 (2010).
- 13) Tatsuo Kimura, Norihiro Suzuki, Prashant Gupta, Yusuke Yamauchi, *Dalton Transactions* **39**, 5139 (2010).
- 14) Hamid Oveisi, Norihiro Suzuki, Yoshihiro Nemoto, Pavuluri Srinivasu, Ali Beitollahi, Yusuke Yamauchi, *Thin Solid Films* **518**, 6714 (2010).
- 15) Liang Wang, Hongjing Wang, Yoshihiro Nemoto, Yusuke Yamauchi, *Chemistry of Materials* **22**, 2835 (2010).
- 16) Hamed Ataee-Esfahani, Liang Wang, Yusuke Yamauchi, *Chemical Communications* **46**, 3684 (2010).
- 17) Azusa Takai, Yusuke Yamauchi, Kazuyuki Kuroda, *Journal of the American Chemical Society* **132**, 208 (2010).
- 18) Wu Weng, Tetsuya Higuchi, Masao Suzuki, Toshimi Fukuoka, Takeshi Shimomura, Masatoshi Ono, Logudurai Radhakrishnan, Hongjing Wang, Norihiro Suzuki, Hamid Oveisi, Yusuke Yamauchi, *Angewandte Chemie International Edition* **49**, 3956 (2010).

Precise Structural Control of Polymer Materials toward Novel Biomaterials

MANA Independent Scientist Chiaki YOSHIKAWA



1. Outline of Research

Recently living radical polymerization (LRP) has been successfully applied to graft polymerization and grafted well-defined polymers on inorganic/organic substrates with an extremely high graft density. Such densely grafted polymers have been classified into the “concentrated” polymer brush, giving characteristic structure and properties¹⁾: For example, in a good solvent, these brushes are highly extended, nearly to their full length, providing strong resistance against compression, super lubrication, and size exclusion with a limit set for a very low molecular weight. Focusing on the unique structure and properties of the concentrated brushes, we are aiming to create, by utilizing the advantages of surface-initiated LRP (SI-LRP), novel biomaterials that would precisely control biofunctions and biological responses (biocompatibility). This year, (1) in order to develop a concentrated brush based novel biointerface, we have systematically investigated cell adhesion behavior on the concentrated brushes of various hydrophilic polymers and (2) in order to develop a novel nanofiber based biomaterial, we have fabricated shortened electrospun fiber modified with concentrated brush.

2. Research Activities

(1) Precise control of surface structure: A Novel Biointerface with concentrated brush.²⁾

As one of the most interesting potential applications of polymer brushes, attention has been directed toward biointerfaces to tune interactions of solid surfaces with biologically important molecules such as proteins and cells. Thus, recently, we systematically investigated protein adsorption on concentrated poly(2-hydroxyethyl methacrylate) (PHEMA) brushes.^{3,4)} The concentrated PHEMA brushes showed excellent protein repellency because of its unique size-exclusion effect. This notable result encouraged us to investigate the interaction between cells and concentrated brushes, since non-specific adsorption of proteins often triggers cell adhesion. Thus we examined cell adhesions on concentrated polymer brushes with different polymers. In this research, we examined hydrophilic polymers such as PHEMA, poly(2-hydroxyethyl acrylate) (PHEA), and poly(poly(ethylene glycol) methyl ether methacrylate) (PPEGMA). The concentrated polymer brushes of all the three, regardless of differences in chemical structure and hydrophilicity, almost completely suppressed the adhesion of L929 fibroblast cell in contrast to the corresponding semi-dilute polymer brushes. The further investigation with using other hydrophilic polymers and cells is now underway.

(2) Precise control of bulk structure: A Novel Shortened Electrospun fiber modified with concentrated brush.^{5,6)}

Electrospinning technique currently has attracted much interests for their potential applications in biomaterials such as tissue engineering scaffolds and wound cover materials, biosensors because this technique can fabricate non woven mat and sponge form composed of continuous long fibers of various polymers with diameters ranging from a several tens nm to a few μm , yielding large surface area, tuneable chemical property, and controllable mechanical property. However, in spite of such advantages, the electrospun fibers are still far from real applications because of poor control of shape and surface functionality. Thus, in this work, in order to broaden possible applications of electrospun nanofiber based biomaterials, we aimed to fabricate an electrospun polymer fiber with a rod-like short length and a concentrated polymer brush (Fig. 1).

First, we prepared hydrophilic concentrated polymer brush on the hydrophobic electrospun fibers by SI-LRP. Then we mechanically cut the fibers by a homogenizer. With increasing cutting time, the fiber length became shorter and more regulated. The obtained shortened fibers exhibited excellent water dispersibility due to the hydrophilic brush layer. Finally, we carried out cell adhesion test with the shortened fibers.⁷⁾ We confirmed that the short length of the fibers and the concentrated brush significantly affected on the cell adhesion behaviours. These results indicate that the shortened fiber with concentrated brush would be a new substrate for cells.

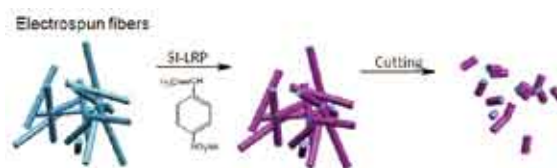


Fig. 1. Schematic illustration of fabrication of a shortened fiber with a concentrated polymer brush.

References

- 1) Y. Tsujii, K. Ohno, S. Yamamoto, A. Goto, T. Fukuda, *Adv. Polym. Sci.* **197**, 1 (2006).
- 2) C. Yoshikawa, Y. Hashimoto, S. Hattori, T. Honda, K. Zhang, D. Terada, A. Kishida, Y. Tsujii, H. Kobayashi, *Chem. Lett.* **39**, 142 (2010).
- 3) C. Yoshikawa, A. Goto, Y. Tsujii, T. Fukuda, T. Kimura, K. Yamamoto, A. Kishida, *Macromolecules* **39**, 2284 (2006).
- 4) C. Yoshikawa, A. Goto, Y. Tsujii, N. Ishizuka, K. Nakanishi, T. Fukuda, *J. Polym. Sci. Part A* **45**, 4795 (2007).
- 5) Japanese Patent 2010-197279.
- 6) C. Yoshikawa, K. Zhang, E. Zawadzak, H. Kobayashi, *Sci. Technol. Adv. Mat.*, accepted for publication.
- 7) E. Zawadzak, C. Yoshikawa, H. Kobayashi et al., in preparation.

Enhanced Photocurrent and Stability from Microscale ZnS Nanobelts-based Ultraviolet (UV)-Light Sensors

ICYS-MANA Researcher Xiaosheng FANG



1. Outline of Research

As one of the most appropriate objects for dimensionality- and size-dependent tuning of functional properties, wide band-gap semiconductor nanostructures made of ZnO, ZnS and diamond have attracted particular attention in the past few years. For example, these materials have been assembled into nanometer-scale ‘visible-light-blind’ or ‘solar-blind’ ultraviolet (UV)-light sensors with high sensitivity and selectivity.¹⁾ Although there has been a significant progress in fabrication and performance optimization of one-dimensional nanostructure-based photodetectors, it is still a challenge to develop an effective and low-cost device with high performance characteristics, such as high photocurrent/dark-current ratio, photocurrent stability and fast time response.

With a wide band-gap of 3.72 and 3.77 eV for cubic zinc blend (ZB) and hexagonal wurtzite (WZ) forms, a diverse range of possible structures and morphologies, and superior chemical and thermal stabilities, ZnS provides a novel prospective alternative for UV detectors that would be particularly useful within the UV-A band. Very recently, we have demonstrated an effective approach to fabricate individual ZnS nanobelt and multiple ZnS nanobelts-based UV-light sensors.²⁾ Although high sensitivity and selectivity of the sensors were indeed demonstrated, the current intensities and stabilities were far from satisfaction.

Although the top-down approach has exceedingly been successful in microelectronics, the technique is complicated, time-consuming and expensive. The most efficient way to improve the ZnS photocurrent intensity is the utilization of a large-area single crystal thin film. This, however, relies strongly on the growth technique and is costly. In fact, no UV-light sensors using ZnS single crystal thin films have been reported to date. An alternative approach is the direct integration of one-dimensional nanostructures into a thin-film-like microchip. Therefore we were inclined to develop the simplest, low cost method to assemble ZnS nanostructures into UV-light sensors and to fabricate stable devices possessing a high photocurrent.

2. Research Activities

We report an efficient and low-cost method to achieve high-performance ‘visible-blind’ microscale ZnS nanobelts-based ultraviolet (UV)-light sensors without using a lithography technique, by increasing the nanobelt surface areas exposed to light.³⁾ The fabrication of microscale CVD-grown ZnS nanobelts-based UV-light sensors was accomplished using Au microwire meshes as masks. 5 nm Au layer-coated quartz glasses instead of silicon wafers were used as deposition substrates. After growing the ZnS nanobelts by a simple CVD method, the quartz glass substrate

coated with a layer of ZnS nanobelts was transported to an electric gun deposition system (ULVAC UEP-3000-2C), the Cr/Au (10 nm/100 nm) electrodes were deposited using 100 μm and 50 μm Au wires as a mask. The size and electrode distance can be controlled by adjusting micrometer size Au wires in a standard optical microscope.

SEM image reveals that a typical belt length is several hundred micrometers (Fig. 1). Some of them may even reach a millimeter in length. The typical width and thickness of the belts are $\sim 5 \mu\text{m}$ and $\sim 100 \text{ nm}$, respectively. Most of the nanobelts are lying on the substrate providing a good physical contact. The devices not only exhibit about 750 times enhancement of a photocurrent compared to individual nanobelt-based sensors and an ultrafast time response, but also very good reproducibility and stability over 10 cycles of 320 nm light-on and light-off states during 1000 seconds at an applied voltage of 20 V are observed (inserted in the Figure). The photocurrent stability and time response to UV-light do not change significantly when a channel distance is altered from 2 μm to 100 μm or the sensor environment changes from air to vacuum and different measurement temperature (60 and 150 $^{\circ}\text{C}$). The photoelectrical behaviors can be recovered well after returning the measurements conditions to air and RT again. The low cost and high performance of the resultant ZnS nanobelt photodetectors guarantee their highest potential for visible-blind UV-light sensors working in the UV-A band.

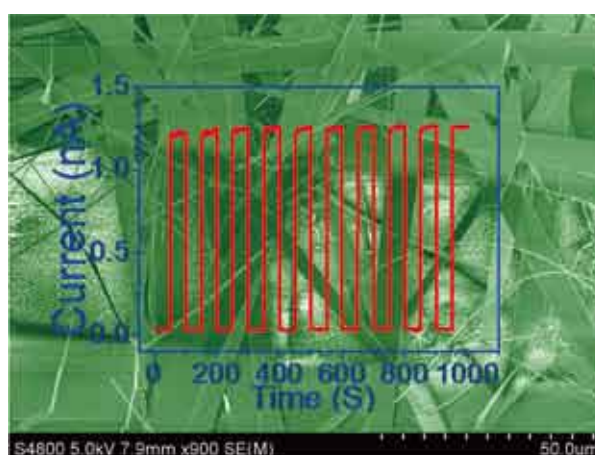


Fig. 1. Enhanced photocurrent and stability from microscale ZnS nanobelts-based UV-light sensors.

References

- 1) X.S. Fang, Y. Bando, U.K. Gautam, T.Y. Zhai, H.B. Zeng, X.J. Xu, M.Y. Liao, D. Golberg, *Crit. Rev. Solid State Mater. Sci.* **34**, 190 (2009).
- 2) X.S. Fang, Y. Bando, M.Y. Liao, U.K. Gautam, C.Y. Zhi, B. Dierre, B.D. Liu, T.Y. Zhai, T. Sekiguchi, Y. Koide, D. Golberg, *Adv. Mater.* **21**, 2034 (2009).
- 3) X.S. Fang, Y. Bando, M.Y. Liao, T.Y. Zhai, U.K. Gautam, L. Li, Y. Koide, D. Golberg, *Adv. Funct. Mater.* **20**, 500 (2010).

Natural Selection of Unipolarity in Zinc Oxide Nanorod Assemblies and Collective Luminescence

ICYS-MANA Researcher Ujjal K. GAUTAM



1. Outline of Research

Crystal assemblies are omnipresent and are useful for many devices. For example, the thin film technology strives on assembling layers of crystalline materials one on top of the other. Nature too has shown phenomenal control over biomineralization processes to produce exquisite looking crystal assemblies. When assembling into larger systems, the constituent crystals orient themselves with respect to each other following certain specific criteria. For example, the macroscopic shape of a skeletal plate of sea urchin is dictated by the crystallographic axis of calcite. Such assemblies lead to emergence of properties that are not directly related to the information encoded on each individual component, but are dependent on how these units are organized. Investigation of crystal-assemblies is crucial not only for understanding and mimicking the Nature's way of crystal-growth, but also for organization of materials for many applications, especially in small size domains, wherein the manipulation of individual components is an emerging challenge.

2. Research Activities

A specially interesting situation may arise when a constituent in an assembly contains an element of asymmetry in its crystal structure. Wurtzite zinc oxide (ZnO) is one such system, where sequential stacking of Zn- and O-atomic layers, one on top of the other, along the crystallographic *c* axis gives rise to intrinsic polarity within the crystal with partial positive and negative charges along Zn- and O-terminated ends, respectively (Fig. 1). In all assemblies and hierarchical structures of ZnO, a growth direction along this polar axis is usually maintained. What would be interesting to know is whether Nature goes a step further in assembling these systems, i.e., making the crystallographic axis as well as the polar direction relevant. This would lead to the existence of an additional symmetry, such as organization of dipoles inside the assembly, as shown schematically in Fig. 1 C, for instance.

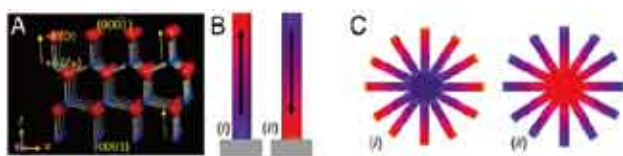


Fig. 1. (A) Crystal structure of wurtzite ZnO. Arrows indicate the polar direction of Zn-O bonds. (B) (i and ii) Schematic showing the orientation of polarity in two ZnO rods grown along the +*c* and -*c* crystallographic axis, respectively. (C) Schematic representation of two possible assemblies of ZnO rods. Besides a possibility of being randomly oriented, all rods in an assembly may also orient along (i) the negative or (ii) positive polar direction, making the two identical looking assemblies intrinsically different.

We have shown that in solvothermally grown ZnO flower-like assemblies (Fig. 2), every nanorods emanate from a central core with an identical polarity, either only positive or only negative. The positively polar assemblies have sharp pencil like branches while that for negatively polar branches are smooth in nature.

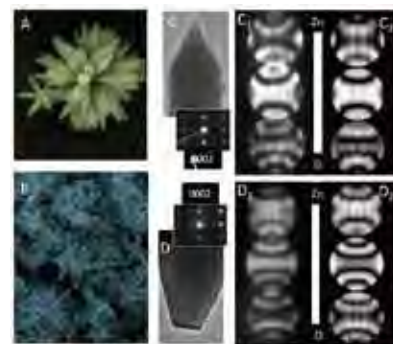


Fig. 2. (A,B) SEM images of the ZnO assemblies. (C and D) TEM images of positively and negatively polar branches respectively and their corresponding CBED patterns (subscripts 1 and 2 are experimental and simulated patterns).

This new kind of assembly is important for developing novel properties. The same property can never be attained by a single piece of material, or by assembling rods randomly, without considering their polarity. This is distinct in the optical emission of the nanoflowers. For instance, only a positive polar nanoflower emits stronger UV radiation from its tips though both types are obtained in the same reaction (Fig. 3). Such polarity control could be a general natural phenomenon and can occur in assemblies of others materials, too, such as those reported for ferroelectric, ferromagnetic, piezoelectric materials, etc., having an element of asymmetry

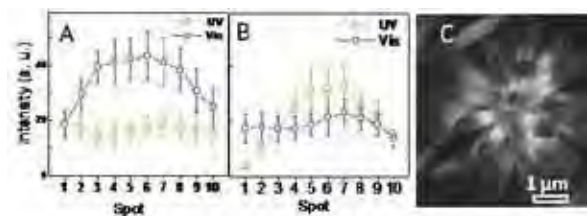


Fig. 3. Assuming 1 as the tip and 10 as the base of each rod in the two unipolar assemblies, the plots in A and B shows how, in a statistical sense, the UV and the visible luminescence varies in a collective manner within a positively polar and a negatively polar assembly respectively. (C) A cathodoluminescence image for an UV wavelength from a negative polar assembly.

Reference

1) U.K. Gautam, M. Imura, C. Sekhar Rout, Y. Bando, X. Fang, B. Dierre, L. Sakharov, A. Govindaraj, T. Sekiguchi, D. Golberg, C. N. R. Rao, *Proc. Natl. Acad. Sci.* **107**, 13588 (2010).

Magnetic-Field-Guided Self Assembly

ICYS-MANA Researcher

Fatin HAJJAJ



1. Outline of Research

One of the great challenges in the physics and chemistry of nanomaterials is the development of efficient methods for the fabrication and manipulation of ordered structures. Structured nanomaterials and stimuli-responsive soft materials formed by molecular self-assembly have attracted much attention recently owing to potential applications as high-tech smart materials. Liquid crystals are one such soft material that combines ordered and dynamic states. The incorporation of photo-, electro-, magneto-, and ion-functional moieties into liquid crystals leads to dynamic functional materials, the function of which can be tuned by stimuli-induced structural changes. The majority of research in this field has been focused on controlling the molecular organization of liquid crystals by the application of contact-dependent stimuli such as electrical fields, mechanical forces, temperature variations, and chemical change. However, these stimuli are harmful and with time tend to degrade the materials by the induction of mechanical stress, electrostatic charges, and unwanted redox reaction. Among all potential external stimuli, a magnetic field has the benefits of contactless control (remote triggering), instant-nonharmful action, and easy integration into electronic devices, though it has only been used limitedly in manipulating self-assembly processes due to the complication of the forces that are involved.

The aim of this study is to design supramolecular assemblies with enhanced material properties by a magnetically-guided self-assembly of the building blocks. To this end, novel magneto-responsive liquid crystals have already been constructed (Fig. 1).

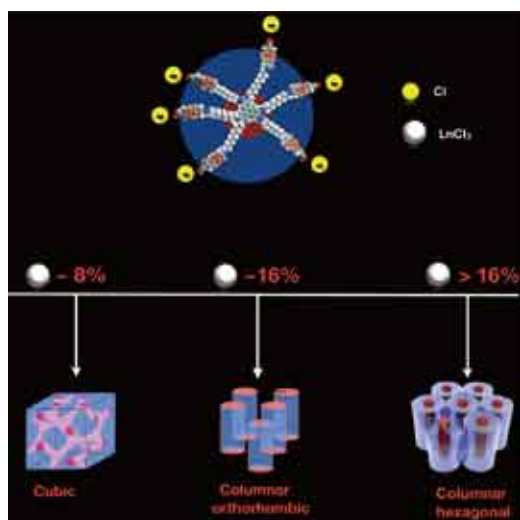


Fig. 1. Schematic illustration of TP-Cl liquid crystal self-assembly processes which can be controlled by the amount of LnCl₃.

Preliminary results showed that the columnar orthorhombic structure can be made to reassemble into 3D-cubic structure under the influence of magnetic fields. This order-order transition is irreversible and can only be erased by heating the magnetic-field-induced structures above its clearing points. Of central interest in this system are the facts that this transition is accompanied by a spectacular change of material properties (magnetic and optical) and also that the material properties can be tuned to a great extent by synthetic chemistry methods.

2. Research Activities

The synthesis of stable lanthanide-containing discotic liquid crystals (LCs) had been established. Depending on the ratio of added Ln³⁺ it is possible to engineer molecular assemblies with cubic, columnar orthorhombic, and columnar hexagonal structures at room temperature (Fig. 1). The thermal stability and mesophase behavior were confirmed by X-ray diffraction (Spring-8), polarized light optical microscopy (POM), and differential scanning calorimetry (DSC). Based on SQUID results, the samples show paramagnetic response from Ln³⁺ over a broad temperature range. In situ POM observations of the LCs phase growth on thin films indicate that the magnetic response of Ln³⁺ can make the material to undergo homeotropic alignment under a 5T magnetic field (Fig. 2). Permanent structural changes in the materials can be induced by cooling their isotropic melts ~450K in the presence of a 5T magnetic field (Fig. 3). Such irreversible magnetic-field-induced phase transition is very promising for nonvolatile memory applications.



Fig. 2. Time-dependent magneto-optical response of the materials at 420K under 5T. The optical images were taken with crossed-polarizers condition of the magneto-optical microscope.



Fig. 3. POM images of bulk materials at 300 K before (orthorhombic) and after (cubic) exposure to 5T.

Reference

- 1) F. Hajjaj, A. Yamaguchi, Y. Yamamoto, T. Fukushima, T. Aida, in preparation.

Single-Electron Tunneling through Molecular Quantum Dots in a Metal-Insulator-Semiconductor Structure

ICYS-MANA Researcher **Ryoma HAYAKAWA**



1. Outline of Research

Single-electron memories (SEM) that adopt Si and Ge nano-dots as floating gates hold promise for future Si-based memory devices.^{1,2)} The reason is that operating principle of SEM is based on the Coulomb blockade effect, which makes it possible to inject the carriers into the dots on the “single electron level”. Moreover, the device allows the multi-level memory operation and ultra-low power consumption, which are key challenges in future nano- electronics. In this study, we have proposed to use organic molecules as the floating gates (Fig. 1). Organic molecules have many advantages as quantum dots over their inorganic counterparts, including the following. 1) The molecules themselves have a uniform size at nanometer scale which is advantageous for quantum dot. 2) Energy-levels of the molecules are tunable by attaching functional groups such as electron-withdrawing (-donating) groups. 3) Molecules response to light irradiation to change their electronic properties, as exemplified by a photo-isomerization. From these points of view, organic molecules can be recognized as excellent quantum dots. We believe that the success of this study can provide one of the prototype devices for “More than Moore” to surpass the limit of conventional Si-technology.

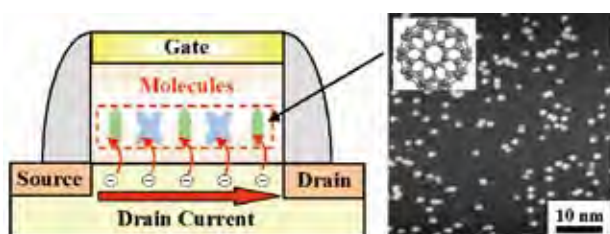


Fig. 1. Schematic illustration of single-electron memory with organic molecules as floating gates and STM image of C₆₀ molecules.

2. Research Activities

(1) Single-electron tunneling (SET) via organic molecules in a metal-insulator semiconductor (MIS) structure.

A double tunnel junction consisting of an Au/Al₂O₃ / molecule/SiO₂/Si multilayer, which is a basic component in SEM devices, was prepared to confirm whether organic molecules work as quantum dots in the device. Here, C₆₀ and copper phthalocyanine (CuPc) molecules were used as quantum dots because these molecules are well known as n-type and p-type semiconductors; their energy levels are markedly different.

We successfully demonstrate clear Coulomb staircases driven by C₆₀ and CuPc molecules in the respective samples (Figs. 2(a) and 2(b)). On the other hand, no such Coulomb staircases were visible in the samples without molecules. The result clearly indicates that each organic molecule works as single quantum dot in insulator layers.

Furthermore, it is noteworthy that intervals between neighboring staircases are non-uniform, in contrast to those

of ordinary SET for inorganic quantum dots. The threshold voltages of SET coincided with molecular orbitals of each single molecule^{3,4)}, demonstrating that resonant tunneling via molecular orbitals is responsible for observed SET. This finding suggests a path to control the SET according to molecular orbitals and leads to development of multi-functional SEM devices such as multi-level memory by combination of heterogeneous molecules and photo memory utilizing photo-isomerization.

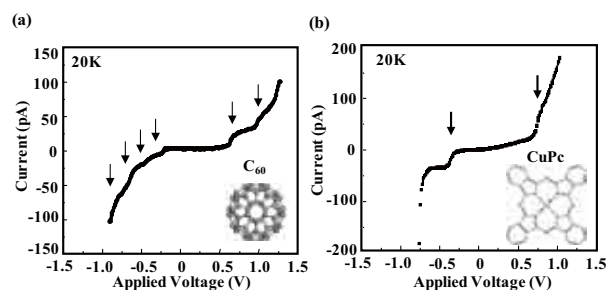


Fig. 2. *I-V* curves of the MIS structures with (a) C₆₀ and (b) CuPc molecules as quantum dots.

(2) Near room-temperature observation of single-electron tunneling.

The temperature dependence of *I-V* characteristics was examined in the sample with C₆₀ molecules to confirm the maximum temperature of the SET operation. *I-V* curves obtained at different temperatures are shown in Fig. 3. No change was observed up to 100 K. Although a further increase in temperature made the *I-V* curve unclear, the staircases still remained even at 260 K, close to room temperature. Further improvement of the tunneling layers would achieve stable operation at room temperature.

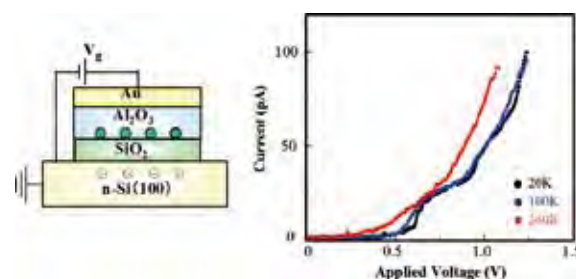


Fig. 3. Temperature dependence of *I-V* curves in sample with C₆₀.

References

- 1) S.Tiwari, F. Rana, H. Hanafi, H. Haratstein, E.F. Crabbe, K. Chan, *Appl. Phys. Lett.* **68**, 1377 (1996).
- 2) C. Pace, F. Crupi, S. Lombardo, C. Gerardi, G. Cocorullo, *Appl. Phys. Lett.* **87**, 182106 (2005).
- 3) C. Joachim, J.K. Gimzewski, R.R. Schlittler, C. Chavy, *Phys. Rev. Lett.* **74**, 2102 (1995).
- 4) J.E. Downes, C. McGuinness, P.A. Glans, T. Learmonth, D. Fu, P. Sheridan, K.E. Smith, *Chem. Phys. Lett.* **390**, 203 (2004).

Development of Diamond Field Effect Transistors by AlN/Diamond Heterostructure

ICYS-MANA Researcher Masataka IMURA



1. Outline of Research

The target materials are group III-nitride and diamond semiconductors, and the research interest is their combination. In this study, I demonstrate an AlN/diamond hetero- junction field effect transistor (HFET).

Diamond semiconductor is a promising candidate for high-frequency and high-power field effect transistors (FETs) that operate under harsh environments. This is because diamonds have significant advantages, including a high thermal conductivity of 22 W/cm·K and etc. However, because of the large-activation energies of dopants (for a phosphorus donor, 0.57 eV, and for a boron acceptor, 0.37 eV), it is difficult to obtain the high carrier density in diamonds at room temperature. Therefore, conductivity control is essential for the operation of high-frequency and high-power FETs.

A combination of other semiconductors and diamond using a heterostructure is one of the possible and challenging strategies for producing such electronic devices. In this study, AlN and diamond are used for the HFET, which is promising as a thermally stable, high-frequency, and high-power FET because of their good material properties. The purpose of this study is to develop an HFET prepared by the heterostructure between AlN and oxygen-terminated diamond.

2. Research Activities

(1) AlN Crystal growth and FET device fabrication.

Undoped AlN layers were grown on insulating (111) IIa-diamond substrates with an impurity concentration less than 1 ppm in a hydrogen flow using metalorganic vapor phase epitaxy (MOVPE). Thermal cleaning of the substrate was performed at 1240 °C in a mixed hydrogen and ammonia (NH₃) atmosphere for 5 min, and then the AlN layer was grown. Trimethylaluminum (TMAI) and NH₃ were used as the Al and N sources, respectively. Crystallographic characterization showed that the c-axis-oriented hexagonal AlN layers with a two-domain structure were obtained on the (111) diamond substrate. The details of the analysis are described in our previous report. Then, the FET device was fabricated by conventional lithography, etching, lift-off, and e-gun metal deposition.

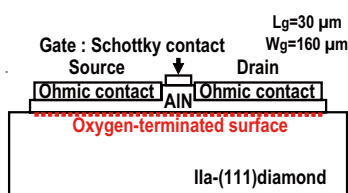


Fig. 1. Schematic of AlN/oxygen-terminated diamond HFETs.

Fig. 1 shows schematic cross-section of the AlN/ oxygen-terminated diamond HFETs, where the gate length (L_g), gate width (W_g), and source-drain distance are 30 μm , 160 μm , and 40 μm , respectively.

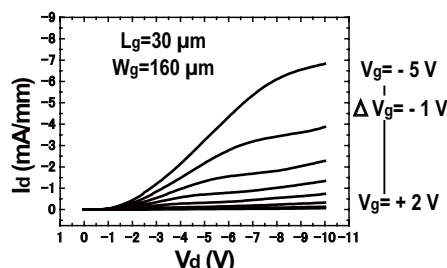


Fig. 2. Id-Vd property.

(2) Transistor property.

Fig. 2 shows the transistor characteristics of I_d - V_d , where I_d , V_d , and V_g , are the drain current normalized by W_g , drain voltage, and gate voltage, respectively. The absolute negative I_d value increases by increasing the absolute negative V_g value. The AlN/diamond HEFT is confirmed as the p-channel action FET with hole carrier. The FET is a normally on mode, and the threshold voltage ($V_{t^{\text{IV}}}$) is determined to be 2.9 ± 0.1 V. Note that the maximum drain current ($I_{d\text{MAX}}$) is obtained in the range from -6.8 to -1 mA/mm at $V_g < -2$ V under L_g as large as 30 μm . The extrinsic transconductance (g_m) was calculated to be from 0.05 to 0.2 mS/mm at $-2 < V_g < 0$ and $-10 < V_d < -4$ V.

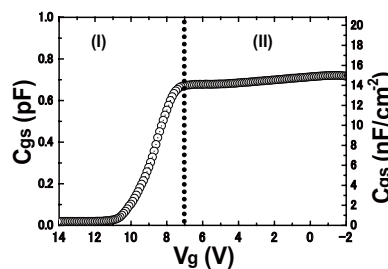


Fig. 3. C_{gs} - V_g property.

(3) Capacitance-voltage property.

Fig. 3 shows the C_{gs} - V_g curve, where C_{gs} is the gate-source capacitance and the measurement frequency is 1 MHz. The curve clearly indicates that the device works as the p-type semiconductor, which is consistent with the transistor properties. There are two typical regions clearly observed by the V_g values: (I) hole depletion and (II) hole accumulation regions shown in Fig. 3. The constant capacitance of 0.678 pF is obtained at $V_g = 5$ V in region II. The peak hole density is $8.6 \times 10^{18} \text{ cm}^{-3}$, and the sheet hole density integrated by depth from 0 to 7 nm is evaluated to be $1.2 \times 10^{11} \text{ cm}^{-2}$ by C_{gs} - V_g curve.

Orientation Controlled Film Growth by Nanosheet Seed Layer Method

ICYS-MANA Researcher

Tatsuo SHIBATA



1. Outline of Research

Thin film fabrication is one of the most important key-technologies which underpin today's information-intensive society. Thin films of various functional ceramics are used in an ever-increasing number of applications such as semiconductor, conductor, dielectrics, ferroelectrics, piezoelectrics, magnetism and optics. It is well known that the crystallographic structure and microstructure of functional ceramics are strongly correlated to their properties. Thus, the development of film fabrication techniques is of crucial importance from fundamental and industrial viewpoints. Up to now, a wide variety of film deposition processes has been investigated to attain well-controlled film growth of various ceramics. Among these techniques, substrates always play an important role. The surface structure of substrates strongly affects on the film growth process. For example, single crystals are known to be ideal substrates due to their well-defined surface structures. On the other hand, commonly used substrates, such as glass, metals and plastics, generally lack such feasible surfaces, and thus, more progress in thin film technology has been desired to achieve high-quality film fabrication on these substrates.

Recently, a new series of unique nano-scaled crystals named "nanosheet" has attracted much attentions due to their high two-dimensionality. The nanosheets are obtained by delaminating layered host compounds into elementary single layers via soft-chemical procedures. Focusing on the typical 2D-structure of the nanosheets, I found that the nanosheets had a great potential to lead and control the growth process of various crystals. In this research, I developed a novel nano-interface engineering technique to control the film deposition utilizing the nanosheets as a seed. The concept is as follows: modify the substrate surface by attaching the nanosheets like nano-scale wallpaper to tailor their surface patterns freely (Fig. 1).

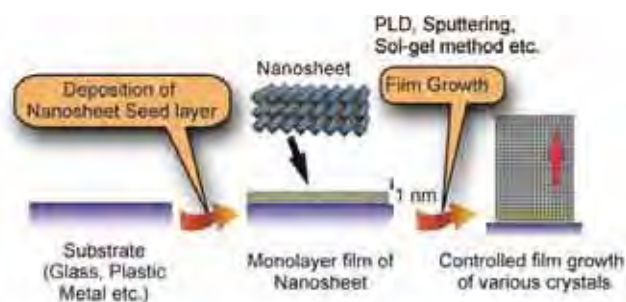


Fig. 1. Schematic explanation of nanosheet seed layer method.

2. Research Activities

(1) Micro-epitaxial film growth of c-axis oriented anatase-TiO₂ on glass substrates.

The recent discovery of the highly conductive nature of Nb-doped anatase showed its potential for an alternative TCO film. However, since anatase has a large crystallographic anisotropy, precise control of the film orientation is strongly required in order to achieve satisfactory performance. In this research, I succeeded in achieving high quality c-axis orientated film growth of anatase TiO₂ on glass substrate with 2D-perovskite nanosheet (Ca₂Nb₃O₁₀) employing their structural similarity between anatase (001) and the nanosheet. Cross-sectional TEM observation indicated that the anatase film was directly grown from the nanosheet surface keeping epitaxial relationship in the microscopic level. Through the collaboration with Prof. Hasegawa (The Univ. of Tokyo), we successfully attained the film resistivity of $4.0 \times 10^{-4} \Omega\text{cm}$ for Nb-doped anatase on glass substrate with the nanosheet seed layer, which is almost identical to that on the epitaxial film of $3.4 \times 10^{-4} \Omega\text{cm}$.

(2) Orientation controlled deposition of high-quality perovskite oxide thin films.

Perovskite structure is one of the most fundamental key-structure of functional ceramics. Thus, the orientation control of perovskite oxide and its analogues is quite important to design their properties. Here, SrTiO₃ (100) films were fabricated by PLD on glass substrates with the nanosheets having 2D-perovskite structure (Ca₂Nb₃O₁₀ and Ca₂NaNb₄O₁₃). The obtained films showed a clear correlation between the nanosheet size and the film quality. With increasing the nanosheet size, the intensity of XRD peaks increased and the FWHM of the θ -rocking curves decreased, indicating improvement of the film quality, particularly in the orientation degree (Fig. 2).

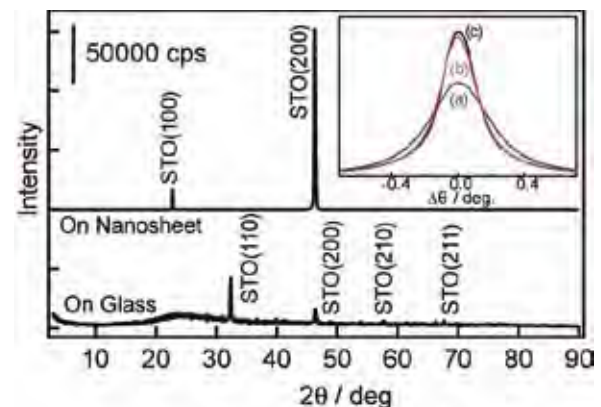


Fig. 2. XRD patterns for SrTiO₃ films on glass substrate with and without 2D-perovskite nanosheet seed layer. (Inset) θ -rocking curves of STO(200) for the films on different-sized nanosheets. (a) $L = 200\text{-}300\text{ nm}$, (b) $2\text{-}5\text{ }\mu\text{m}$, and (c) $10\text{-}15\text{ }\mu\text{m}$.

Synthesis and Characterization of C_{60} Microcrystal at Liquid-Liquid Interface: Effects of Mixing Solvents

ICYS-MANA Researcher Lok Kumar SHRESTHA



1. Outline of Research

Studies on self-assembled nanostructures of fullerene (C_{60}) continue to attract attention due to its unique structure and optical and electrical properties. Self-assembled one-dimensional (1-D) or 2-D structure of C_{60} has become a promising material in versatile applications in semiconductors and optoelectrical devices. To improve the utility of C_{60} , a various synthetic approaches have recently been explored to develop 1-D or 2-D C_{60} structures; rods with different axial ratios, tubes, flowers, or hexagon morphologies. A slow evaporation method has been explored for producing C_{60} nanorods that emit highly enhanced photoluminescence originating from a change in the electronic level during C_{60} self-assembly. Similarly, a vapor-solid process to produce disk-type C_{60} structures has used in optical devices due to their photoconductivity. Miyazawa and co-workers developed a liquid-liquid interfacial precipitation (LLIP) method to produce C_{60} nanowhiskers and nanotubes for use in nanoelectronics.¹⁾ They have also extended this method to produce porous nanowhiskers and hexagonal nanosheets by altering organic solvents used during synthesis.

It has been shown that solvent properties play an important role in the structure of C_{60} crystals. 1-D nanostructure has been achieved by LLIP method with the mixtures of isopropyl alcohol (IPA) and benzene or toluene; whereas, mixtures of polygon and hexagonal sheets from tertiary butyl alcohol (TBA)/benzene, and IPA/carbon tetrachloride (CCl_4) systems, respectively.²⁾ Nevertheless, regardless of the progress in controlling the size and morphology of C_{60} nano/microstructures, a systematic approach is still needed to facilitate the morphologically controlled synthesis of C_{60} crystals. Generally LLIP method utilizes two pure liquids (solvents and anti-solvents) for the synthesis of C_{60} nonocrystals. However, attention was not paid on the mixed solvents systems so far. It would be interesting to investigate the effects of mixing solvents and/or anti-solvents on the structure and properties of C_{60} crystals. This concept may lead to a new direction for the free structure control of C_{60} crystal via LLIP method. As a matter of fact that despite the extensive efforts to produce C_{60} structures with various sizes, shapes, and structures, the actual mechanism of crystal formation is still unclear and is a matter of open discussion, the mixing solvents and anti-solvents strategy may show the way us to better understand the mechanisms of crystal formation and assembly.

2. Research Activities

(1) Synthesis and characterization of C_{60} microcrystal.

C_{60} crystals with different morphologies were prepared following LLIP method. Interfaces containing saturated solution of C_{60} in organic solvents (benzene and CCl_4 or their

mixtures) and alcohols (IPA and TBA or their mixtures) were formed. First of all, C_{60} crystals were synthesized at liquid-liquid interfaces of benzene and mixed anti-solvents (IPA and TBA were mixed at different mixing ratios; 1:9 to 1:0.11). Next, anti-solvent was fixed and mixing ratios of solvents (CCl_4 and benzene) were varied. About 1 mL of saturated solution of C_{60} in organic solvent was taken in a clean and dry 10 mL glass bottle and about 5 mL of anti-solvent was added to this solution slowly and the system was left undisturbed for about 20 min. Then the mixture was ultrasonicated at room temperature for 1 min and stored for 24 h at a temperature corresponding to synthesis temperature. The thus obtained C_{60} microcrystals were characterized by using electron microscopy (SEM and TEM), X-ray diffraction (XRD), and Raman spectrometry.

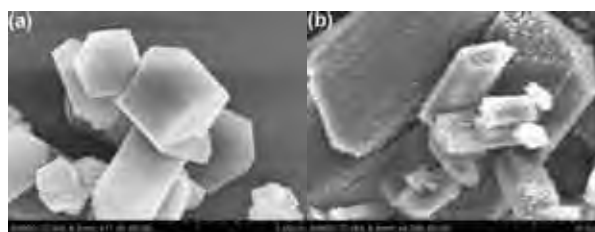


Fig. 1. SEM images of C_{60} microcrystal prepared in mixed IPA-TBA/benzene systems via LLIP method; (a) IPA-TBA = 1:9, and (b) 1:2.3.

It is interesting to note that shape, size, and structure of self-assembled C_{60} crystals obtained from mixed anti-solvents and solvents are very much different from those obtained from non mixed systems. Fig.1 shows SEM images of C_{60} microcrystal prepared in mixed IPA-TBA/benzene systems. As is seen in SEM images, giant microcrystals consisting of well defined nanocrystals are formed in the mixed IPA-TBA system. At 1:1 ratio of IPA and TBA, mixed morphologies of nanowhiskers and polygons are observed; whereas, above this ratio, nanocrystals are assembled and giant microcrystals are formed. On the other hand, in the mixed solvent systems, porous C_{60} hexagonal shaped microcrystals with controllable pore size distribution could be achieved. Though the mechanism of crystal growth is yet to know, the strategy of mixing solvents seems to be a facile route to the morphology and porosity control of C_{60} crystal. Therefore a detail investigation will be carried out in near future and particular attention will be paid to the real practical application of these self-assembled C_{60} structures.

References

- 1) K. Miyazawa, Y. Kuwasaki, A. Obayashi, M. Kuwabara, *J. Mater. Res.* **17**, 83 (2002).
- 2) M. Sathish, K. Miyazawa, J.P. Hill, K. Ariga, *J. Am. Chem. Soc.* **131**, 6372 (2009).

Fabrication of Novel Nanostructured Bioceramics

ICYS-MANA Researcher

Pavuluri SRINIVASU



1. Outline of Research

Research on the development of new biomaterials that promote bone tissue regeneration is receiving great interest by the biomedical scientific community. Recent advances in nanotechnology have allowed the design of materials with nanostructure similar to that of natural bone. These materials can promote new bone formation by inducing the formation of nanocrystalline apatites analogous to the mineral phase of natural bone onto their surfaces, i.e. they are bioactive. They also stimulate osteoblast proliferation and differentiation and, therefore, accelerate the healing processes. Silica-based ordered mesoporous materials are excellent candidates to be used as third generation bioceramics that enable the adsorption and local control release of biological active agents that promote bone regeneration. This local delivery capability together with the bioactive behavior of mesoporous silicas opens up promising expectations in the bioclinical field. This involves the growth of nanocrystalline carbonate hydroxyapatites similar to the biological ones onto the materials surfaces, that is, bioactive behavior. Moreover, these biomaterials should stimulate osteoblasts adhesion, proliferation, and differentiation to reduce the postoperative periods. Natural hard tissues in vertebrates are natural composite materials, composed of an organic matrix and an array of inorganic nanoapatites. The inorganic phase consists of nanocrystalline apatites with average length of 50 nm, width of 25 nm, and thickness of 2–5 nm.¹⁻³⁾ Thus, the present research is focused on development of nanostructured template synthesis of bioceramics and study of their properties.

2. Research Activities

(1) Nanostructured bioactive-glasses.

The synthesis involved the use of a nonionic triblock copolymer surfactant as structure-directing agent and the employment of tetraethyl orthosilicate (TEOS), triethyl phosphate (TEP), and calcium nitrate. The textural and structural properties of this new family of mesoporous glasses can be controlled by changing the CaO content of mesoporous glasses. A progressive evolution from 2D-hexagonal to 3D-bicontinuous cubic structure with an increase in the textural properties was observed when decreasing the CaO content. The possibility of tailoring both structural and textural features of mesoporous glasses is undoubtedly an attractive advance towards the development of biomaterials that is able to fulfill the essential requirements for specific biomedical applications.

The composition of $\text{SiO}_2\text{-CaO-P}_2\text{O}_5$ had been synthesized in aqueous solution, using two-step, self-assembly process, followed by hydrothermal treatment. The bioactive-glass thus obtained exhibited an ordered structure and high surface area. The textural parameter of bioactive glasses was controlled by changing the molar concentration of calcium.

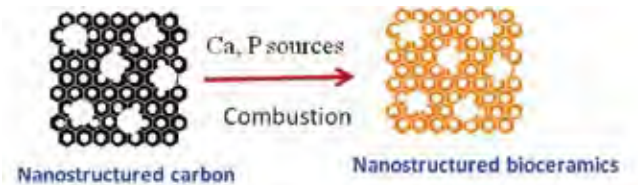


Fig. 1. Schematic image for fabrication of bioceramics.

(2) Nanostructured carbon templated synthesis of bioceramics.

To the nanostructured carbon calcium and phosphorous solutions were added with stirring further the solution was evaporated in air. Nanostructured bioceramics was obtained after combustion of the carbon template (Fig. 1). Electron microscopic images showed that the nano calcium phosphate bioceramics have disordered interconnected nanostructures with diameter of 20-30 nm (Fig. 2).

Furthermore, these images also confirm the nanostructured carbon can prevent the formation of bulk crystals and helps to fabricate nanocrystals. Selected area electron diffraction of the material confirms that the products are of nanocrystals of calcium phosphate bioceramics. EDS patterns suggests the non-stoichiometric calcium phosphates. Sorption measurement shows that the material has surface area more $30 \text{ m}^2\text{g}^{-1}$ with pore volume of $0.3 \text{ cm}^3\text{g}^{-1}$. The strong adsorption at 1056 and 566 cm^{-1} can be assigned to P-O stretching and bending mode of phosphate was confirmed by infrared spectroscopy.

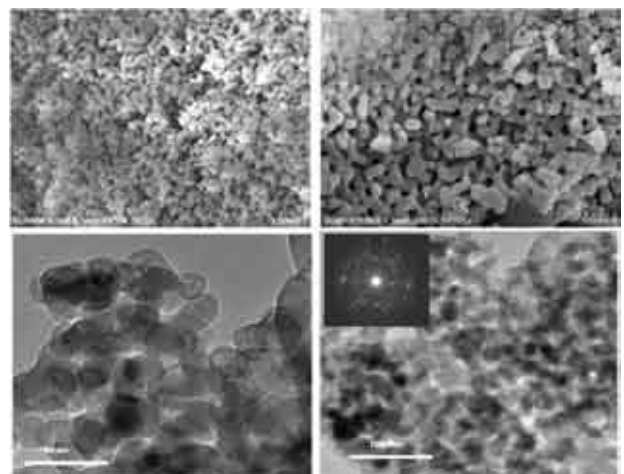


Fig. 2. Electron microscopy images of bioceramics.

References

- 1) K.-D. Kvhn, Bone Cements (Springer, Berlin, 2000).
- 2) K.S. Suslick, G.J. Price, *Ann. Rev. Mater. Sci.* **29**, 295 (1999).
- 3) I.W. Hamley, *Nanotechnology* **14**, 39 (2003).

High-Pressure Synthesis of New Layered Cobalt Oxyfluoride

ICYS-MANA Researcher

Yoshihiro TSUJIMOTO



1. Outline of Research

The development of transition metal oxides with perovskite-based structure has stimulated search for multi-anion systems such as oxynitrides and oxysulfide because incorporation of the two different anions in one structure offers further opportunity to effectively induce the chemical and physical properties which the pure oxides cannot possess. This is exemplified by the discoveries of colossal magnetoresistance in EuNbO_2N and photocatalytic activity in BaTaO_2N and $\text{Sm}_2\text{Ti}_2\text{O}_5\text{S}_2$.

In particular, interests in oxyfluoride also stem from a rich variety of order/disorder patterns between fluoride and oxide anions. Ruddlesden-Popper (RP) type layered perovskites were reported to exhibit several kinds of anion distribution pattern. For example, terminal apical sites in perovskite block layer are randomly or regularly occupied by O and F as seen in $\text{Sr}_2\text{FeO}_3\text{F}$ and $\text{Ba}_2\text{ScO}_3\text{F}$. For $\text{LaSrMnO}_4\text{F}$, fluorine is intercalated into only interstitial sites between the perovskite blocks. A more complicated example is the fluorine occupations of both the terminal apical sites and the interstitial sites as seen in $\text{Sr}_2\text{CuO}_2\text{F}_{2+\delta}$. Apparently oxyfluoride chemistry was significantly developed, but the kind of transition metals in the reported oxyfluorides is extremely limited. In fact, the majority of studies on oxyfluoride chemistry focused on the fluorination of strongly correlated systems such as copper and manganese oxides. To further deepen our understanding of the oxyfluoride chemistry, search for oxyfluorides with the other transition metals is necessary.

2. Research Activities

Co-based oxyfluorides have been less studied despite expectations that strong correlation between spin, charge and orbital degrees of freedom may be found similar to those in

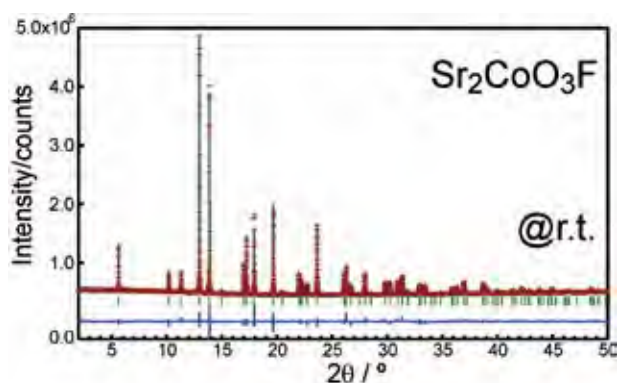


Fig. 1. Synchrotron XRD patterns of $\text{Sr}_2\text{CoO}_3\text{F}$.

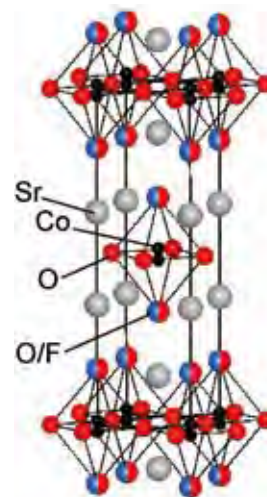


Fig. 2. Crystal structure of $\text{Sr}_2\text{CoO}_3\text{F}$. Occupancy factor of each Co site is 50%.

the copper and manganese oxides. In my study, the first layered cobalt oxyfluoride $\text{Sr}_2\text{CoO}_3\text{F}$ was successfully synthesized under pressure of 6 GPa and temperature of 1700 °C.

Fig. 1 shows the synchrotron XRD patterns collected at room temperature from the cobalt oxyfluoride on NIMS beamline at SPring-8 with $\lambda = 0.65298 \text{ \AA}$. On the basis of Rietveld structure analysis, the crystal structure was determined to be the tetragonal structure with the space group $I4/mmm$ ($a = 3.83318(1) \text{ \AA}$, $c = 13.30531(4) \text{ \AA}$).

Fig. 2 shows the crystal structure of $\text{Sr}_2\text{CoO}_3\text{F}$. A shifting of Co ions from the basal plane caused by preferential occupation of fluorine at the apical sites leads to distorted square-pyramidal coordination around the cobalt. The random distribution of oxygen and fluorine at the apical sites is extremely unusual in comparison with related oxyfluorides. O/F disorder is observed in $\text{Ba}_2\text{ScO}_3\text{F}$, but the scandium cation takes octahedral coordination without splitting of the Sc site. On the other hand, O/F order is realized in $\text{Sr}_2\text{FeO}_3\text{F}$ where Fe atom takes FeO_5 square pyramidal coordination. From these examples, we can expect that square pyramidal coordination is a requirement for anion ordering. However, $\text{Sr}_2\text{CoO}_3\text{F}$ exhibits coexistence of the anion disorder between O and F and the square pyramidal coordination around Co.

Reference

- 1) Y. Tsujimoto, J.J. Li, K. Yamaura, Y. Matsushita, Y. Katsuya, M. Tanaka, Y. Shirako, M. Akaogi, E. Takayama-Muromachi., *Chem. Commun.*, to be published.

Bottom-Up Synthetic Strategy to Highly Organized Multi-Functional System

ICYS-MANA Researcher

Hisanori UEKI



1. Outline of Research

Our biological system is multi-functional system, composed of central dogma (DNA, RNA, and protein) and multi-enzymatic system in the downstream. Each component of the system is independent, having their own roles and systems, but closely communicates with each other. Thus, multi-functional biological systems consist of many unit multi-functional systems, which has been developed through a long time period, and proper orientation of components/functions/unit systems and proper communications between them allow us to control easily, and mostly unconsciously, the complicated system all at once all the time for maintaining our life.

On the other hand, artificial multi-functional systems in molecular level are by far less developed compared with the above natural system. We can easily recognize that by the fact that total chemical synthesis of proteins is still dream of scientists despite their numerous time, efforts, and devotions.¹⁾ There are three main approaches for construction of multi-functionalized system in molecular level: (A) a system composed of multiple components with different functions without any physical contacts, (B) with physical/chemical contacts, and (C) multi-functions in a single molecule (Fig. 1). In the system A which is the most primitive system, each components/functions is drifting around freely in a media. This is suitable for a system with less or none communication between functions.²⁾ The efficiency of the system, in general, relies on given conditions (temperature, media, ratio, etc) and the compatibility among functions. In general, it is, however, not easy to realize the high efficiency due to the high degree of freedom of function parts. The system B is relatively developed in materials science as composite materials.³⁾ In this system, each components/functions are contacting each other, which allow them to communicate easily. Thus, the layout of all components play pivotal role on the efficiency, since some contacts activate but some contacts inhibit. Judicious choice of components and precise control of their array is the key to realize efficient systems. Recently, development in crystallization and self-assembly technique of small organic molecules opened the door for organic chemists to explore this area and produced many useful organic and inorganic hybrid materials. It is, however, very difficult to construct less symmetric structures because of the nature of

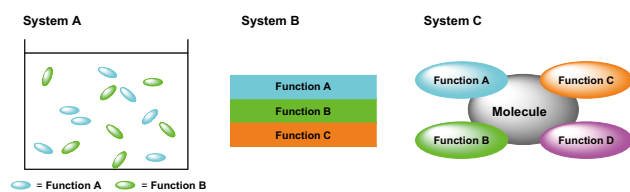


Fig. 1. Multi-functional chemical systems.

crystallization and self-assembly. Furthermore, relatively larger amounts of each component are crucial compared with system A or C. On the other hand, significant downsizing of a system is possible in the system C since all functions can be in a molecule. For the system C, molecular design, especially the control in orientations of each function moieties, plays pivotal role to realize efficient systems. Despite development in synthetic chemistry, this control is still difficult due to free rotations of each part of molecules, and therefore, this research field is quite less explored. This approach, however, has great flexibility in the molecular design including less symmetric structures, allowing us the bottom-up preparation of multi-functional molecules. Therefore, it possesses great potential for production of new materials.

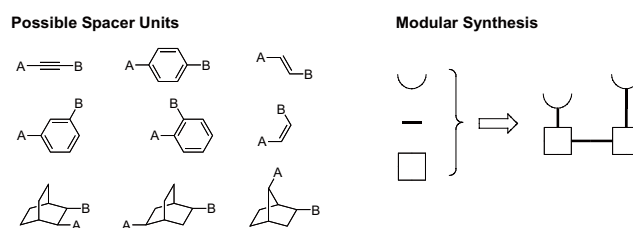


Fig. 2. Possible spacer units and modular synthesis.

2. Research Activities

(1) Design and synthesis of spacer units.

The present study is focusing on the development of bottom-up rational preparation of highly ordered multi-functionalized system. To reach the goal, as noted above, primal importance is laid on molecular design, especially spacer molecules which connect each function units. Spacer molecules should be relatively rigid to control the positions of function parts, and shape-persistent molecules meet this requirement. They are usually composed of π -conjugated molecules or multi-cyclic compounds (Fig. 2). Utilization of various coupling reactions allows us to obtain shape-persistent molecules with various shapes and properties.

(2) Construction of multi-functional system and its evaluation.

After preparation of various spacer unit molecules, they are assembled with function unit molecules for the construction of molecule with multi-functions. To have versatility in the shapes and properties of the final product, modular synthesis is adopted (Fig. 3). Then, the efficiency of the multi-functions is evaluated. It should be noted that the efficiency can be easily improved/modified under the current synthetic strategy.

References

- 1) S.B.H. Kent, *Chem. Soc. Rev.* **38**, 338 (2009).
- 2) H. Liu, T. Jiang, B. Han, S. Liang, Y. Zhou, *Science* **326**, 1250 (2009).
- 3) R.F. Gibson, *Compos. Struct.* **92**, 2793 (2010).

Direct Fabrication of Raman-Active Nanoparticles by Top-Down Physical Routes

ICYS-MANA Researcher

Jung-Sub WI



1. Outline of Research

Surface enhanced Raman scattering (SERS) based analysis has been considered problematic for practical applications due to the lack of a reproducible way to create homogeneous plasmonic nanostructures needed to overcome the inherently low Raman signals.^{1,2)} For my ICYS research, I propose a top-down technology based synthetic approach to produce highly reproducible Raman-active nanoparticles for use of in-vitro or in-vivo molecular imaging reagents. Direct-fabrication of synthetic nanoparticles by top-down physical routes, in which materials are vacuum deposited in a nano-patterned polymer template, allows exquisite control over material composition, multilayer structure, and particle size/shape which are hardly achievable with chemical synthesis of nanoparticles. This capability enables us to make artificially engineered nanoparticles with unique physical properties, such as the surface plasmonic field enhanced Raman-active nanoparticles.

2. Research Activities

(1) Design and synthesis of surface plasmonic field enhanced Raman-active nanoparticles.

Optimal design and fabrication of Raman-active nanoparticles have been conducted. In the in-vivo application of Raman-active nanoparticles, one of the major issues is the limited information depth originating from the light absorption in tissues and weak intensity of Raman signal. My research strategy for increasing the information depth is to boost the signal intensity through the incorporation of 'Raman hot spots; nanometer-scale dielectric slits between neighboring Au disks or cylinders' at the inside of individual nanoparticle. The overall dimensions of the nanoparticles have been considered to tune the plasmonic resonance frequency to the near-infrared window.

The direct-fabrication of Raman-active nanoparticles includes three main steps: preparation of polymer pocket arrays, vacuum deposition of target materials, and final release of nanoparticles. For the process set-up, several equipments and chemicals in MANA foundry have been utilized as follows. After spin coating the bi-layer resist stack of ZEP520a and polymethylglutarimide (PMGI), e-beam exposure was conducted with the ELIONIX system with a beam accelerating voltage of 50 keV. Then, e-beam resist (ZEP520a) and underlying polymer (PMGI) were sequentially developed to prepare the polymer pocket arrays. Next, Au and SiO₂ films were deposited using the SHIBAURA sputter system and the ULVAC evaporation system. Finally, the SERS characteristics of the prepared Au nanostructures were analyzed by scanning confocal Raman microscopy (WITEC alpha300s).

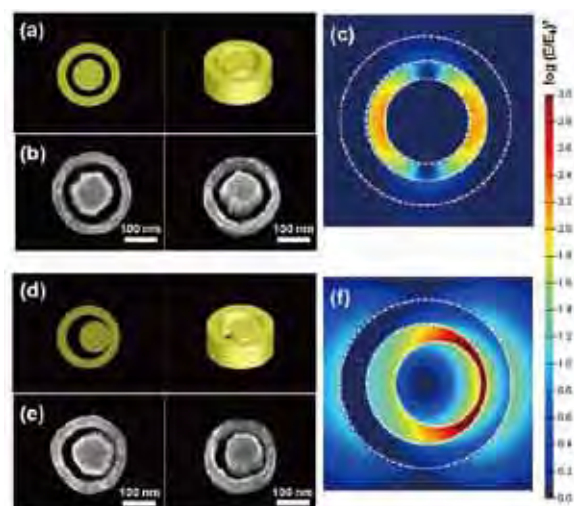


Fig. 1. (a,d) Schematic and (b,e) SEM images of Au disk/ring nanostructures with (a,b) on-axis and (d,e) off-axis symmetry. SEM images of the right side were obtained from a 30° tilted-view. (c,f) The squared magnitude of the local electric field amplitude of Au nanostructures with (c) on-axis and (f) off-axis disk. Electromagnetic simulation was performed using Lumerical three-dimensional finite-difference time-domain software. The Au nanostructures were placed in a uniform medium of air and illuminated from the top with a linearly-polarized plane wave. ($\lambda=780$ nm).

(2) Au Disk/Ring Nanostructures with On & Off symmetry.

Following the process flow described in the previous section, the Au disk/ring nanostructure was fabricated as shown in Figure 2. The outer ring and the inner disk were formed by the oblique-angle sputter deposition and the evaporation with the surface-normal angle, respectively. Therefore, the circular gap could be simply defined from the two successive deposition steps without the additional e-beam lithography and plasma etching. Through the tilting of the evaporation angle, the axial symmetry between the disk and the ring also could be controlled as demonstrated in Figure 2(e). The shift of the inner disk was precisely changed from 0 to 20 nm. Interestingly, the breaking of the symmetry induces a further increase of the electromagnetic field as shown in the simulation results of Figure 2(c) and 2(f). In the preliminary test with the Raman molecule of 3,3'-diethylthiatricarbocyanine iodide (DTTCI), the Au disk/ring nanostructure with the off-axis symmetry shows the 10-times increase of the Raman signal intensity as compared to the nanostructure with the on-axis symmetry. More effective ways to incorporate the Raman molecules into the prepared plasmonic nanostructures are now being investigated.

References

- 1) S. Nie, S.R. Emory, *Science* **275**, 1102 (1997).
- 2) Y. Fang, N.H. Seong, D.D. Dlott, *Science* **321**, 388 (2008).

Photovoltaic CIGS Thin-Films from Nanoparticle Powders using Aerosol Deposition

ICYS-MANA Researcher Jesse WILLIAMS



1. Outline of Research

$\text{Cu}(\text{In,Ga})\text{Se}_2$ is an attractive photovoltaic material because it has a band gap that is optimal for the solar spectrum (shown in Fig. 1), and unlike silicon, it has a direct band gap, which means it can efficiently absorb light using only a thin-film of material. Other appealing properties of CIGS are that they are non-toxic and stable. CIGS solar cells have demonstrated conversion efficiencies of about 20%.¹⁾ These solar cells were produced using vacuum deposition techniques, which offer good control over the deposition conditions. However, vacuum deposition techniques are not scaleable for large area deposition and limited to batch processing, and they are inherently costly. However, non-vacuum based techniques do not have such limitations, and, thus, they are a cheaper route for thin-film production.

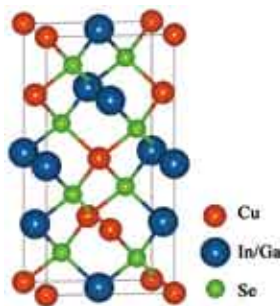


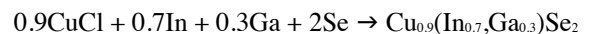
Fig. 1. The unit cell of CIGS, which is in chalcopyrite family.

Aerosol deposition is a non-vacuum deposition technique that produced dense films from nanoparticle precursors, and the resulting stoichiometry of the films is dictated by the stoichiometry of the nanoparticles. So far, aerosol deposition has been used to form dense films for piezoelectric, capacitors, and ferroelectrics.^{2,3)} We aim to produce high-quality fully dense CIGS films from nanoparticle precursors using the aerosol deposition method.

2. Research Activities

(1) Nanoparticle synthesis.

CIGS nanoparticles are synthesized using a thermal reflux method. Specifically the process involves heating the reactants in the solvent triethylene glycol to drive the reaction:



It is important to control the stoichiometry of the particles as well as their size because particle size is a key factor for aerosol deposition. The particles must be in the size range 500 nm – 1 μm , and it is possible to tailor particle size by controlling solution concentration, reaction time, and reaction temperature. Nanoparticles of the appropriate phase and size have been synthesized as shown below.

(2) Aerosol deposition.

Aerosol deposition uses a pressurized carrier gas to spray the nanoparticle at the substrate surface. The deposition chamber is kept at reduced pressures to maintain high particle velocity. The spray process first abrades the surface clean and then the film begins to deposit. Because the particles are at high velocities, they form a dense film through a process called room temperature impact consolidation. Using He gas, dense CIGS films can be deposited from the synthesized nano-powders, shown in Fig.2.

(3) Solar cell synthesis.

Now we are building a solar cell to investigate the photovoltaic properties of the aerosol deposited films. The solar cell structure is glass substrate / Mo back electrical contact / CIGS light absorber / i-ZnO buffer layer / ZnO:Al transparent conducting oxide. Currently, we are developing the ZnO transparent conducting oxide layer.

References

- 1) I. Repins et al., *Progress in Photovoltaics* **16**, 235 (2008).
- 2) J. Akedo, M. Lebedev. *Jap. J. Appl. Phys.* **38**, 5397 (1999).
- 3) D. Popovici et al., *Key Engineering Materials* **388**, 163 (2009).
- 4) J. Williams, N. Ohashi, D. Zhuo, Jap. Patent Appl. 2010-226230.

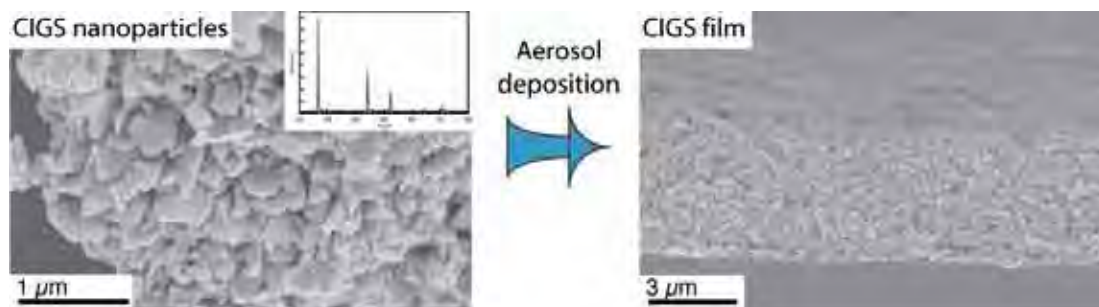


Fig. 2. Using the aerosol deposition technique, nano-powders are spray deposited to form dense thin films.

Nanomechanical Membrane-Type Surface Stress Sensor (MSS): Opening a New Era of Sensors

ICYS-MANA Researcher Genki YOSHIKAWA



1. Outline of Research

Nanomechanical cantilever sensors (Fig. 1) have been emerging as a key device for real-time and label-free detection of various analytes ranging from gaseous to biological molecules.^{1,2)} The major sensing principle is based on the analyte-induced surface stress, which makes a cantilever bend. This simple mechanics opened a myriad of possibilities for the use of atomic force microscopy (AFM) cantilever deflection technique beyond imaging. While most studies employ optical detection of the cantilever deflection, lever-integrated piezoresistive sensing does not require bulky and complex peripheries related with an optical read-out and can be used for the detection in any opaque liquid (e.g. blood) with large multidimensional arrays. In spite of these inherent advantages, piezoresistive cantilevers have not been widely in use for sensing applications. The reason is that, without effective mechanical amplification schemes, their sensitivity is far below that of optical methods.

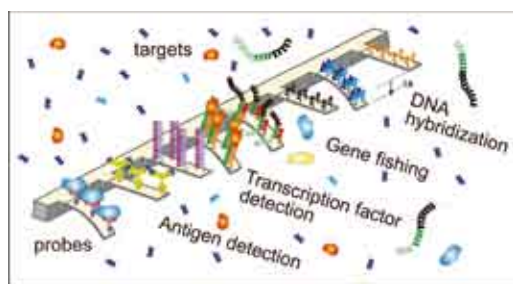


Fig. 1. Bio-functionalized cantilever array sensors.

2. Research Activities

(1) Optimization of piezoresistive cantilever sensors towards highly sensitive membrane-type surface stress sensors (MSS).

Comprehensive analytical consideration of strain amplification schemes for sensing applications based on the strategies of the constriction and double lever geometries³⁾ has led us to a highly sensitive membrane-type surface stress sensor (MSS; Fig. 2).^{4,5)} It is based on the piezoresistive read-out integrated in the sensor chip. The MSS is not a simple “cantilever”, rather it consists of an “adsorbate membrane” suspended by four piezoresistive “sensing beams”, composing a full Wheatstone bridge. The analyte-induced isotropic surface stress on the membrane is efficiently transduced onto the piezoresistive beams as an amplified uniaxial stress. Experimental evaluation of a first prototype MSS demonstrates a high sensitivity which is a factor of more than 20 higher than that obtained with a standard piezoresistive cantilever and comparable with that of optically read-out cantilevers (Fig. 3). The finite element analyses indicate that changing dimensions of the membrane and beams can further increase the sensitivity substantially. Given the various conveniences and advantages of the integrated piezoresistive read-out, this platform is expected to open a new era of sensors.

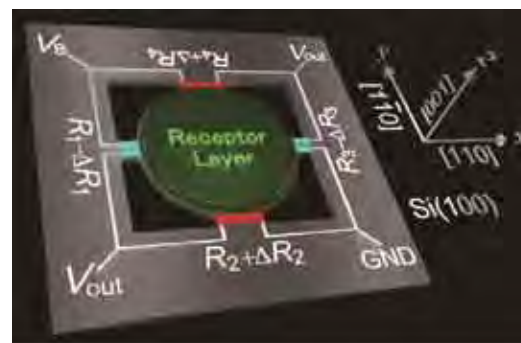


Fig. 2. Membrane-type Surface stress Sensor (MSS).

(2) Mechanical analysis and optimization of nanomechanical sensors coated with a solid receptor layer.⁶⁾

An analytical model for nanomechanical cantilever sensors coated with a solid receptor film is formulated, taking account of all relevant physical parameters of both cantilever and coating film. This model provides accurate values verified by an excellent agreement with those simulated by finite element analyses. It will help toward analyzing the static behavior of nanomechanical sensors in conjunction with physical properties of coating films as well as optimizing the films for higher sensitivity.

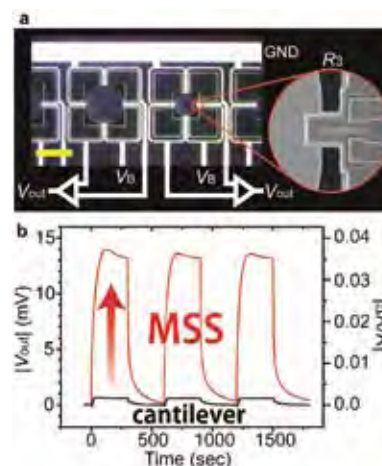


Fig. 3. (a) The fabricated MSS array chip with a schematics of a part of electrical connections. Yellow scale bar: 500 μm . (b) Experimentally obtained output signal (V_{out}) of MSS (red) and a standard piezoresistive cantilever (black).

References

- 1) J.W. Ndieyira et al., *Nature Nanotech.* **3**, 691 (2008).
- 2) G. Yoshikawa, H.P. Lang, T. Akiyama, L. Aeschmann, U. Stauffer, P. Vettiger, M. Aono, T. Sakurai, C. Gerber, *Nanotechnology* **20**, 015501 (2009).
- 3) G. Yoshikawa, H. Rohrer, *International Workshop on Nanomechanical Cantilever sensor*, Banff, (2010).
- 4) G. Yoshikawa, T. Akiyama, S. Gautsch, P. Vettiger, H. Rohrer, *Nano Lett.*, accepted for publication.
- 5) G. Yoshikawa, T. Akiyama, P. Vettiger, H. Rohrer, *patent pending*.
- 6) G. Yoshikawa, *submitted*.

One-Dimensional Inorganic Nanostructures for High-Performance Photodetectors

ICYS-MANA Researcher

Tianyou ZHAI



1. Outline of Research

One-dimensional (1D) inorganic nanostructures such as nanowires (NWs), nanobelts (NBs), and nanotubes (NTs) have stimulated numerous studies due to their importance in basic scientific research and potential technological applications. It is generally accepted that 1D inorganic nanostructures are ideal systems for exploring a large number of novel phenomena at the nanoscale and investigating the size and dimensionality dependence of functional properties. They are also expected to play important roles as both interconnects and key units in nanoscale electronic, optoelectronic, electrochemical, and electromechanical devices.

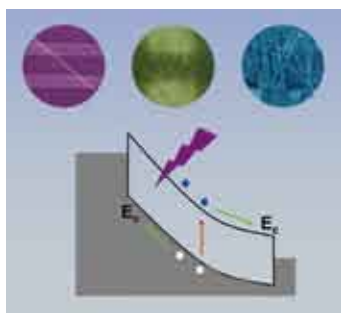


Fig. 1. Typical devices and mechanism of 1D nanostructure photodetectors.

Among many available nanoscale devices, the photodetectors are critical for applications as binary switches in imaging techniques and light-wave communications, as well as in future memory storage and optoelectronic circuits (Fig. 1). In view of their high surface-to-volume ratios and Debye length comparable to their small size, 1D inorganic nanostructures have already displayed superior sensitivity to light in diverse experiments. We aim to develop an effective approach to construct high-performance photodetectors based on 1D ZnS, ZnSe, CdS, In_2Se_3 , and Sb_2Se_3 nanostructures.¹⁻⁵⁾

2. Research Activities

(1) Sb_2Se_3 nanowires as Visible-Light photodetectors.

We fabricated high-quality single-crystalline Sb_2Se_3 NWs using a facile hydrothermal process through careful adjustment of the experimental parameters, and first investigated the single-NW photoconductive properties. The current across the structure dramatically increases by more than 10 times, from 4 pA (dark condition) to 58 pA (600-nm light illumination). Both rise and decay times are less than 0.3 s. The calculated responsivity (R_λ) and external quantum efficiency (EQE) for the Sb_2Se_3 NW irradiated by 600-nm light are ~ 8.0 A/W and ~ 1650 % respectively.

(2) In_2Se_3 and S-doped In_2Se_3 NWs as Visible-Light photodetectors.

We first reported on the fabrication of high-quality single-crystalline In_2Se_3 NW arrays and demonstrated the performances of an individual intrinsic and S-doped In_2Se_3 NW in a photoconductive device. The In_2Se_3 NW arrays were fabricated by thermal evaporation of In_2Se_3 powders at 900 °C using Au nanocrystals as catalysts. Under visible light illumination the current across the In_2Se_3 NW dramatically increased compared to the dark current (Fig. 2). By introducing In_2S_3 powders into the precursors, the In_2Se_3 NWs were on-demand doped by sulfur, and such doping did not affect the structural integrity. The doped NW shows enhanced conductivity from 5×10^{-5} S/cm (undoped) to 3.8×10^{-4} S/cm (doped), and increased ratios of photocurrent to dark current ($I_{\text{light}}/I_{\text{dark}}$), from 3.6 (undoped) to 9.4 (doped). The rise and fall times of doped In_2Se_3 NW device were measured to be around 9.6 μs and 9.0 μs , respectively, which were slightly longer than those in undoped In_2Se_3 NW device (2.3 μs and 1.6 μs). The R_λ and EQE for the doped case were as high as ~ 1331 A/W and $\sim 3.3 \times 10^5$ % respectively, for the incident wavelength of 500 nm at 3 V, which are higher than such values for the undoped material (~ 89 A/W and 2.2×10^4 %).

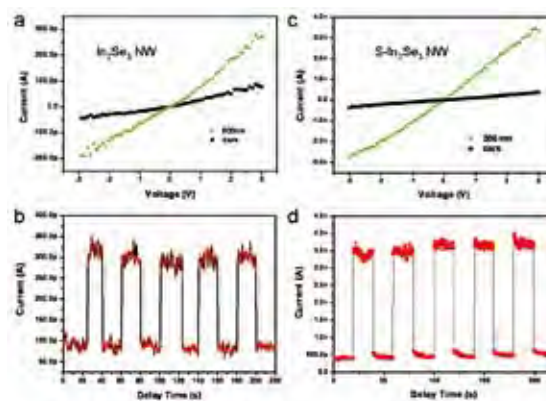


Fig. 2. Intrinsic and S-doped In_2Se_3 NWs as Visible-Light Photodetectors.

References

- 1) T.Y. Zhai, L. Li, X. Wang, X.S. Fang, Y. Bando, D. Golberg, *Adv. Funct. Mater.* **20**, 4233 (2010).
- 2) T.Y. Zhai, M.F. Ye, L. Li, X.S. Fang, M.Y. Liao, Y.F. Li, Y. Koide, Y. Bando, D. Golberg, *Adv. Mater.* **22**, 4530 (2010).
- 3) T.Y. Zhai, H.M. Liu, H.Q. Li, X.S. Fang, M.Y. Liao, Y. Koide, H.S. Zhou, Y. Bando, D. Golberg, *Adv. Mater.* **22**, 2547 (2010).
- 4) T.Y. Zhai, X.S. Fang, M.Y. Liao, X.J. Xu, B.D. Liu, Y. Koide, Y. Ma, J.N. Yao, Y. Bando, D. Golberg, *ACS Nano* **4**, 1596 (2010).
- 5) T.Y. Zhai, Y. Ma, L. Li, M.Y. Liao, X.S. Fang, Y. Koide, J.N. Yao, Y. Bando, D. Golberg, *J. Mater. Chem.* **20**, 6630 (2010).

Nano-Carbon Materials for Green Energy

ICYS-MANA Researcher

Yuanjian ZHANG



1. Outline of Research

Due to the rapid depletion of limited fossil energy sources and the increasingly worsening environmental pollution, the development of sustainable energy supply has attracted worldwide attentions. As the largest source of energy, solar light is readily available and renewable, thus has been regarded as an idea alternative. Among them, the devices, which use the photovoltaic effect to harness solar radiation have drawn many attentions. For example, silicon-based solar cells are now dominant and commercial available with satisfied efficiency. But they still suffer from high costs, thus a new generation of photovoltaic devices based on organic (polymers) and nanocrystalline semiconducting materials might offer a solution to make such devices cheaper.

Regarded as “doped” carbon-materials in which some carbon atoms are replaced by nitrogen atoms in a regular/irregular manner, carbon nitrides stand for a large family of related compounds (CN_x) in general.¹⁾ For example, a typical way to prepare bulk graphitic carbon nitride (g-C₃N₄) by thermal condensation of dicyandiamide is shown in Fig. 1.

Moreover, the slightly disordered precursor of g-C₃N₄ (for simplicity, we use g-C₃N₄ as the whole family of compounds) is found to be a typical semiconductor with band gap ranging up to 5 eV upon structural variations or adatoms by theoretic calculations. Therefore, it is promising to consider carbon nitrides as a candidate for applications in photoelectric conversion,²⁾ photocatalytic H₂ evolution from water³⁾ and degradation of organic pollutions.⁴⁾ In this case, carbon nitrides have several interesting features as follows. Firstly, it is facile for mass-preparation with a very competitive prices of order of several \$/Kg, which is always preferred. Secondly, because of intrinsic organic natures, it is easy to chemical functionalize/doping. Thirdly, contrary to

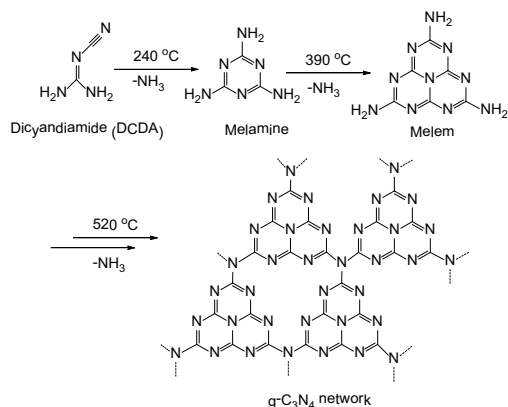


Fig. 1. Proposed pathway of condensation of dicyandiamide (DCDA) into g-C₃N₄.

many other organic semiconductors, carbon nitrides have a high thermal and chemical stability against oxidation, making handling them in air possible. Lastly, but not less important, both of carbon and nitrogen are among the most abundant elements in our planet, which is in accordance of the sustainable energy.²⁾ However, the overall efficiency of pristine bulk g-C₃N₄ is rather low, and has to be improved.

The present study is focused on a “structural doping” of g-C₃N₄, in which phosphorus heteroatoms were doped into g-C₃N₄ (Fig. 2). Besides being active layers in photoelectric conversion devices, such phosphorus-containing scaffolds and materials are also interesting for polymeric batteries, but also for catalysis and as catalytic supports.⁵⁾



Fig. 2. Proposed structure of phosphorus-doped polymeric carbon nitride (C: gray, N: blue, P: orange).

2. Research Activities

(1) Preparation of phosphorus-doped carbon nitride.


Phosphorus heteroatoms were doped into g-C₃N₄ via carbon-sites by polycondensation of the mixture of the carbon nitride precursors and phosphorus source (1-butyl-3-methylimidazolium hexafluorophosphate ionic liquid). SEM elemental mapping and chemical elemental analysis, FT-IR, XRD, XPS and solid state NMR results showed phosphorus was uniformly doped into bulk g-C₃N₄ by replacing some carbon atoms in the framework of the host g-C₃N₄.

(2) Physicochemical properties.

Most of the structural features of g-C₃N₄ were well retained after doping, but electronic features had been seriously altered, which provided not only a much better electrical (dark) conductivity up to 4 orders of magnitude but also an improvement in photocurrent generation by a factor of up to 5.

References

- 1) A. Thomas, A. Fischer, F. Goettmann, M. Antonietti, J.O. Müller, R. Schlögl, J.M. Carlsson, *J. Mater. Chem.* **18**, 4893 (2008).
- 2) Y.J. Zhang, M. Antonietti, *Chem.-Asian J.* **5**, 1307 (2010).
- 3) X.C. Wang, K. Maeda, A. Thomas, K. Takanebe, G. Xin, J.M. Carlsson, K. Domen, M. Antonietti, *Nature Mater.* **8**, 76 (2009).
- 4) S.C. Yan, Z.S. Li, Z.G. Zou, *Langmuir* **25**, 10397 (2009).
- 5) Y.J. Zhang, T. Mori, J.H. Ye, M. Antonietti, *J. Am. Chem. Soc.* **132**, 6294 (2010).



MANA is operating with the financial support of the World Premier International Research Center Initiative (WPI) of the Ministry of Education, Culture, Sports, Science and Technology (MEXT)

**International Center for Materials Nanoarchitectonics (MANA)
National Institute for Materials Science (NIMS)**

1-1 Namiki, Tsukuba, Ibaraki 305-0047, JAPAN
Phone: +81-29-860-4709, Fax +81-29-860-4706
E-mail: mana@nims.go.jp
URL: <http://www.nims.go.jp/mana/>